UNIVERSITY OF MINNESOTA
ST. ANTHONY FALLS HYDRAULIC LABORATORY
LORENZ G. STRAUB, Director

Technical Paper No. 18, Series B

# Hydraulics of Closed Conduit Spillways

## Parts II through VII
## Results of Tests on Several Forms of the Spillway

by

Fred W. Blaisdell, Hydraulic Engineer
USDA, ARS


March 1958

Study conducted by

UNITED STATES DEPARTMENT OF AGRICULTURE
AGRICULTURAL RESEARCH SERVICE
SOIL AND WATER CONSERVATION RESEARCH DIVISION

in cooperation with the

Minnesota Agricultural Experiment Station
and the
St. Anthony Falls Hydraulic Laboratory

Minneapolis, Minnesota

UNIVERSITY OF MINNESOTA
ST. ANTHONY FALLS HYDRAULIC LABORATORY
LORENZ G. STRAUB, Director

Technical Paper No. 18, Series B

# Hydraulics of Closed Conduit Spillways

## Parts II through VII
## Results of Tests on Several Forms of the Spillway

by

Fred W. Blaisdell, Hydraulic Engineer
USDA, ARS


March 1958

Study conducted by

UNITED STATES DEPARTMENT OF AGRICULTURE
AGRICULTURAL RESEARCH SERVICE
SOIL AND WATER CONSERVATION RESEARCH DIVISION

in cooperation with the

Minnesota Agricultural Experiment Station
and the
St. Anthony Falls Hydraulic Laboratory

Minneapolis, Minnesota

## ABSTRACT

The theory of the hydraulics of closed conduit spillways has been presented previously as Part I of this report series. Parts II to VI describe the laboratory tests, record the observed flow phenomena, and give the discharge and pressure coefficients necessary for the application of the theory. This information is given for five different forms of the closed conduit spillway, four of which are recommended. The drop inlet described in Part II is not recommended because of its poor hydraulic performance.

The large reduction in discharge caused by strong vortices is presented in Part VII.

# CONTENTS

# LIST OF FIGURES

# LIST OF TABLES

# HYDRAULICS OF CLOSED CONDUIT SPILLWAYS

## Results of Tests on Several Forms of the Spillway*

## FORWARD

The theory of and the symbols for the hydraulics of closed conduit spillways have been given in Part I** of this report series. Parts II to VI inclusive, which are included in this paper, give the results of laboratory tests on a number of different forms of the closed conduit spillway inlet; each spillway is described, the experimental setup and methods are explained, the characteristics of flow through the spillway are described, data that may be used for a determination of the flow through the spillway are presented, and coefficients for the determination of critical pressures within the spillway are summarized. When used in conjunction with the principles given in Part I, the information contained in this paper may be used to design closed conduit spillways having forms similar to those reported here. Part VII is devoted to a discussion of vortices and their effect on the discharge.

## Part II

## Circular Drop Inlet with Bell Crest and Elbow Barrel Entrance

## DESCRIPTION OF SPILLWAY

The first drop inlet spillways were made of 6-in. nominal diameter, vitrified clay tile, bell and spigot pipe. Both the drop inlet and the conduit were of the same size pipe. They were connected by a 90-degree vitrified clay tile elbow. The nominal slope of the conduit was 30 per cent. Actual slopes are given in Table II-1. The outlet discharged freely; that is, it was not submerged. (See Part I for the list of symbols.)

TABLE II-1

PROPORTIONS OF SPILLWAYS AND DISCHARGE COEFFICIENTS

| Series | D (ft) | $D_r/D$ | $D_{ro}/D$ | $\ell/D$ | S | Z/D | $Z_1/D$ | Inlet Crest | Conduit Entrance | Anti-Vortex Device | $C_o$ | $N_o$ | $C_s$ | $N_s$ | $K_e$ | $N_e$ |
|---|---|---|---|---|---|---|---|---|---|---|---|---|---|---|---|---|
| I | 0.496 | 1.00 rd. | 1.25 rd. | 19.84 | 0.308 | 14.20 | 8.56 | Converging bellmouth | Elbow | Tangent wall | -- | - | -- | - | 0.24 | 9 |
| II | 0.496 | 1.00 rd. | 1.40 rd. | 19.84 | 0.308 | 14.20 | 8.56 | Bell | Elbow | Tangent wall | -- | - | -- | - | 0.30 | 5 |
| III | 0.496 | 1.00 rd. | 1.40 rd. | 39.66 | 0.307 | 20.32 | 8.56 | Bell | Elbow | Tangent wall | -- | - | -- | - | 0.21 | 3 |
| IV | 0.496 | 1.00 rd. | 1.40 rd. | 59.40 | 0.310 | 26.52 | 8.56 | Bell | Elbow | Tangent wall | -- | - | -- | - | 0.30 | 2 |
| VIII | 0.496 | 1.00 rd. | 1.40 rd. | 59.42 | 0.319 | 22.00 | 3.99 | Bell | Elbow | Tangent wall | 8.42 | 6 | -- | - | -- | - |
| IX | 0.496 | 1.00 rd. | 1.40 rd. | 60.43 | 0.310 | 22.82 | 4.88 | Bell | Elbow | Tangent wall | -- | - | -- | - | 0.48 | 9 |
| L-1 | 0.333 | 1.00 rd. | 1.38 rd. | 34.01 | 0.293 | 15.22 | 5.70 | Bell | Elbow | Tangent wall | -- | - | 5.28 | 7 | 0.37 | 20 |
| L-2 | 0.333 | 1.00 rd. | 1.38 rd. | 34.00 | 0.293 | 14.47 | 4.97 | Bell | Elbow | Tangent wall | 6.58 | 12 | 5.31 | 12 | 0.43 | 17 |
| L-3 | 0.333 | 1.00 rd. | 1.38 rd. | 34.01 | 0.294 | 13.50 | 3.96 | Bell | Elbow | Tangent wall | 6.55 | 16 | 5.31 | 18 | 0.44 | 21 |

A second set of tests was conducted on a transparent drop inlet spillway. This was so flow conditions could be observed. The only differences between the tile and the transparent spillways were in the pipe diameter, which was 4 in. for the transparent pipe, and the elbow, which was constructed of segments of straight transparent pipe.

The drop inlets are shown in Fig. II-1; all drop inlet crests were the bell end of vitrified clay tile pipe, except for Series I. For Series I, the bell was filled with mortar to give the converging bellmouth entrance shown by King [I-31, Fig. 35]. The crest of the transparent drop inlet was square-edged, whereas the crest for the vitrified tile drop inlet was slightly rounded.

---

*Agricultural Research Service Report No. 41-505-50.

**Fred W. Blaisdell, Hydraulics of Closed Conduit Spillways--Part I. Theory and Its Application, St. Anthony Falls Hydraulic Laboratory Technical Paper No. 12-B, February 1958.

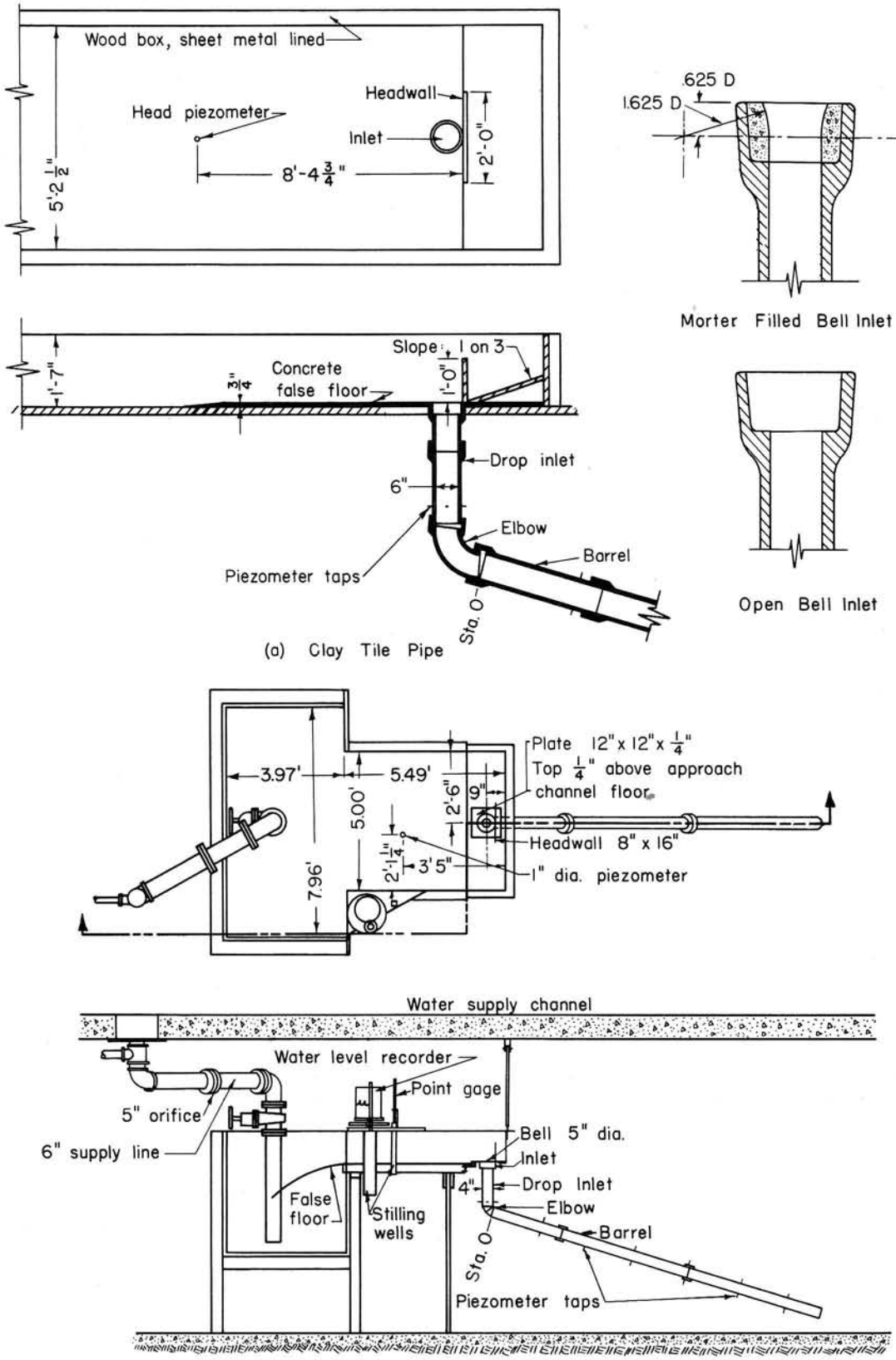


Fig. II-1 - Test Setups and Drop Inlet Spillways.

The 6-in. pipe was very rough for vitrified tile. Instead of having a smooth glazed surface, there were burnt grains scattered over the surface, as well as occasional small surface swellings. A photograph of this surface is shown in Fig. II-2. In spite of this rough surface, the average value of Manning's n was found to be about 0.0080 with a maximum of about 0.0092. The Darcy-Weisbach friction factor was assumed to be constant at 0.015 when making the friction head loss calculations. The transparent pipe was considered to be hydraulically smooth for the friction head loss calculations, this assumption being based on tests by others and later tests on closed conduit spillways.

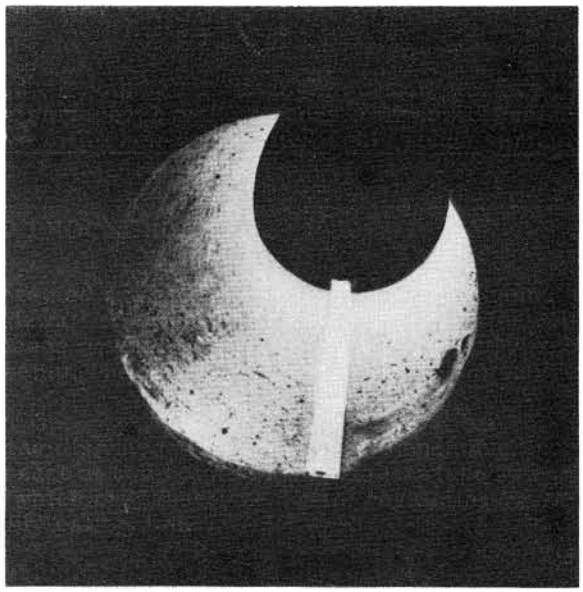

Fig. II-2 - Surface of 6-in. Vitrified Clay Tile Pipe.

A number of piezometers were used to determine the pressures within the spillway. The piezometer locations are shown schematically in Fig. II-1. The piezometers were formed by drilling the tile pipe from the outside. This ordinarily chipped the wall of the pipe. The chip was overfilled with paraffin and the paraffin scraped even with the pipe surface. Piezometers for the transparent pipe were easily formed by drilling through the pipe from the outside. The locations of all piezometers are given in Table II-2. Unless otherwise designated, all piezometers were located on the conduit invert. Pressures were measured in open manometer columns.

Variables included in the test program were length of conduit, which also caused the total drop Z through the spillway to vary, and the height of the drop inlet $Z_1$. The magnitudes of these variables are given in Table II-1.

TABLE II-2

PIEZOMETER LOCATIONS AND LOCAL PRESSURE DEVIATION

FROM HYDRAULIC GRADE LINE SERIES I, II, III, IV, VIII, IX, L-1, L-2 AND L-3

| Piezometer Location | Series I | | Series II | | Series III | | Series IV | | Series VIII | | Series IX | | Series L-1 | | Series L-2 | | Series L-3 | |
|---|---|---|---|---|---|---|---|---|---|---|---|---|---|---|---|---|---|---|
| | Station | $h_n/h_{vp}$ | Station | $h_n/h_{vp}$ | Station | $h_n/h_{vp}$ | Station | $h_n/h_{vp}$ | Station | $h_n/h_{vp}$ | Station | $h_n/h_{vp}$ | Station | $h_n/h_{vp}$ | Station | $h_n/h_{vp}$ | Station | $h_n/h_{vp}$ |
| Left* | -4.08D | +0.23 | -4.08D | +0.25 | -4.08D | +0.19 | -4.08D | +0.28 | -3.95D | -- | -4.07D | +0.57 | -1.60D | +0.20 | -1.59D | +0.20 | -1.59D | +0.20 |
| Upstream* | -4.09D | +0.21 | -4.09D | +0.22 | -4.09D | +0.16 | -4.06D | +0.27 | -3.97D | -- | -4.05D | +0.51 | -1.62D | +0.32 | -1.59D | +0.32 | -1.60D | +0.31 |
| Right* | -4.06D | +0.19 | -4.06D | +0.21 | -4.06D | +0.18 | -4.04D | -- | -3.95D | -- | -4.07D | +0.59 | -1.62D | +0.21 | -1.62D | +0.21 | -1.60D | +0.20 |
| Downstream* | -4.04D | +0.36 | -4.04D | +0.38 | -4.04D | +0.33 | -4.04D | +0.35 | -3.97D | -- | -4.05D | +0.61 | -1.60D | +0.01 | -1.60D | +0.01 | -1.60D | +0.00 |
| Crown | | | | | | | | | 1.03D | -- | 1.03D | -0.12 | 0.75D | -0.29 | 0.75D | -0.32 | 0.75D | -0.35 |
| Invert | | | | | | | | | 1.13D | -- | 1.13D | +0.08 | 0.75D | -0.11 | 0.75D | -0.11 | 0.75D | -0.11 |
| Crown | 3.57D | +0.07 | 3.57D | +0.03 | 3.57D | +0.04 | 3.57D | +0.07 | 4.62D | -- | 4.62D | -0.04 | | | | | | |
| Invert | 3.45D | +0.13 | 3.45D | +0.16 | 3.45D | +0.10 | 3.45D | +0.19 | 4.54D | -- | 4.54D | +0.00 | 5.75D | +0.02 | 5.75D | +0.02 | 5.75D | +0.02 |
| Invert | 11.34D | +0.06 | 11.34D | +0.08 | 11.34D | +0.04 | 11.34D | +0.07 | 11.36D | -- | 11.36D | -0.02 | 10.76D | -0.01 | 10.76D | -0.00 | 10.76D | 0.00 |
| Invert | 19.27D | +0.02 | 19.27D | +0.04 | 19.27D | +0.04 | 19.27D | +0.07 | 19.32D | -- | 19.32D | -0.06 | 15.76D | -0.00 | 15.76D | -0.00 | 15.88D | -0.00 |
| Invert | | | | | 27.20D | -0.02 | 27.20D | +0.00 | 27.22D | -- | 27.22D | -0.06 | 20.77D | -0.03 | 20.77D | -0.03 | 20.76D | -0.03 |
| Invert | | | | | 35.14D | +0.00 | 35.14D | +0.00 | 35.12D | -- | 35.12D | -0.08 | 25.76D | -0.02 | 25.76D | -0.02 | 25.76D | -0.02 |
| Invert | | | | | 43.06D | | 43.06D | +0.12 | 43.02D | -- | 43.02D | -0.05 | 30.76D | -0.01 | 30.76D | -0.02 | 30.76D | -0.02 |
| Invert | | | | | | | 50.99D | +0.04 | 51.00D | -- | 51.00D | +0.01 | | | | | | |
| Invert | | | | | | | 58.89D | +0.01 | 58.90D | -- | 58.90D | +0.07 | | | | | | |

*Side of drop inlet.

## APPARATUS AND PROCEDURE

The channels in which the spillways were tested are shown in Fig. II-1. The channels were wide enough so there were probably no sidewall effects, but greater channel sidewall heights would have permitted the use of higher heads over the drop inlet crest. The approach to the drop inlet was essentially level for each setup. The differences between the two setups can be seen in Fig. II-1.

For the tile pipe setup shown in Fig. II-1 the discharge was measured, depending upon the rate of flow, by means of the differential pressure at two points in a 12-in. tee (used as an elbow) or by a 3-1/2-in. orifice in a 4-in. line which by-passed the 12-in. regulating valve. Both of the measuring devices had been previously calibrated.

For the transparent pipe setup shown in Fig. II-1, the discharge was measured by a 5-in. orifice in the 6-in. supply line. This orifice was calibrated before it was placed in use.

The test procedure consisted of setting a flow, waiting until the water level in the headpool became constant, then determining the rate of flow, the head on the drop inlet crest, and the pressures within the spillway. For the transparent pipe tests pressures were sometimes recorded photographically when they fluctuated. This was done by placing dye in the manometer columns and taking double exposure photographs of the manometer board at the maximum and minimum pressures. Notes on the flow conditions were also recorded. This procedure was repeated until the complete range of heads and discharges had been covered.

Periodic fluctuations in the headpool water level due to alternating control sections in the spillway were frequently observed, so a water-level recorder was installed to measure these fluctuations during the transparent pipe tests. The rate of change of headpool level, determined from the water-level recorder chart, was multiplied by the headpool area to give the flow rate going into storage or being subtracted from storage. The steady inflow rate through the supply line into the headpool was corrected by the quantity going into or being subtracted from storage to determine the actual rate of flow through the spillway. A water-level recorder was also used for the tile pipe tests after Series IV had been completed. However, its purpose was to insure that the water level was approximately steady prior to taking readings, and the records were not used to correct for storage.

## DESCRIPTION OF FLOW

The tile pipe tests were the first laboratory tests made with a steep pipe slope. Therefore the performance of the spillway was not clearly understood and the descriptions of the flow may be deficient in some respects. However, indications are that the control changed from the weir at the drop inlet crest to the pipe without going through orifice or short tube controls. This is true except for Series VIII, where the control apparently changed from weir to orifice. The water-level recorder records and the notes taken during the experiments indicate that pipe flow may have occurred for short periods during one test. However, no data were obtained for the full pipe condition. Apparently the riser height for Series VIII is too short to insure that orifice flow will not occur. The other riser heights tested are apparently

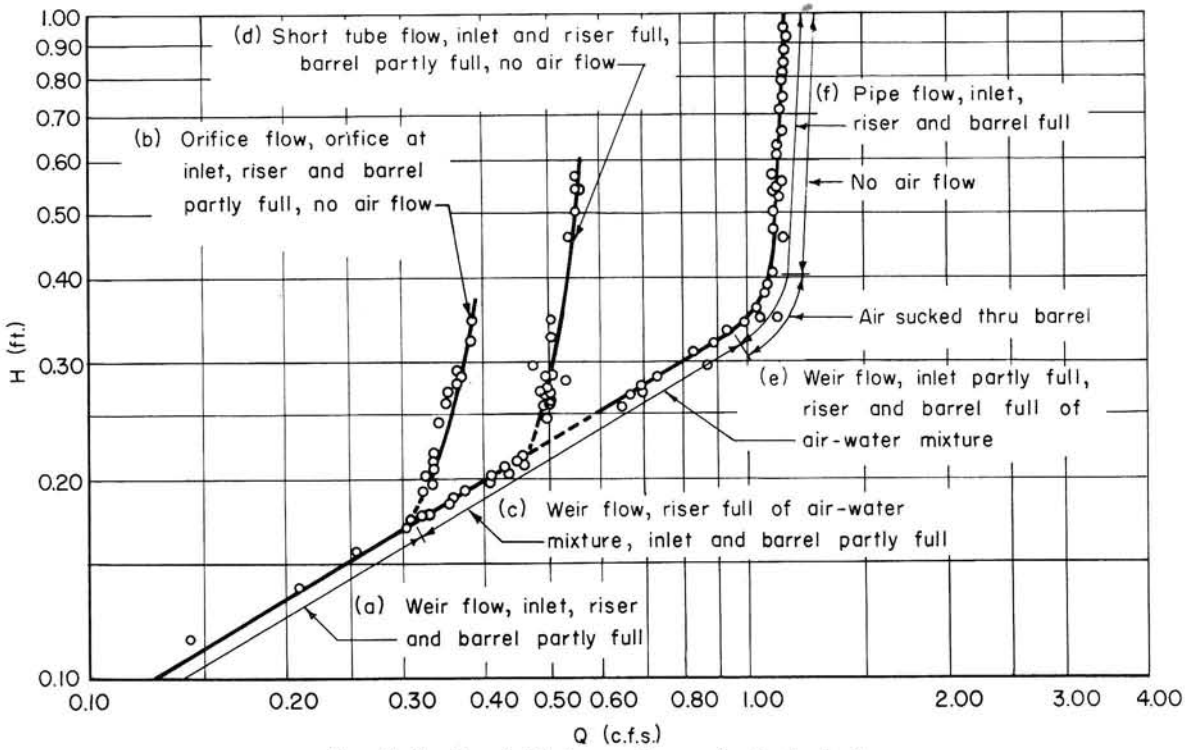


Fig. II-3 - Head-Discharge Curves for Series L-3.

great enough to insure that only the desirable weir and pipe controls exist. It should be remembered, however, that these early tests were not as complete as later tests, and it is entirely possible that the presence of orifice and short tube controls could have been missed. Later tests indicate the desirability of drop inlets having an area greater than that of the barrel. It appears that the type of drop inlet represented by the clay pipe tests should be used with caution, especially in view of the results of the transparent pipe tests described below.

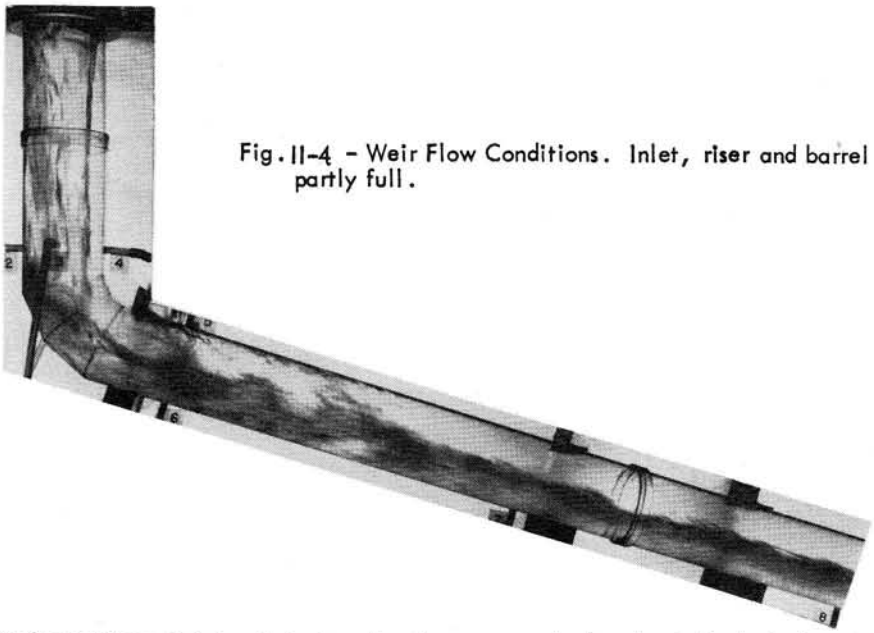

Fig. II-4 - Weir Flow Conditions. Inlet, riser and barrel partly full.

Control sections obtained during the transparent pipe tests included weir, orifice, short tube and pipe. For Series L-1 orifice control was not observed for some unknown reason. The following description of flow conditions is taken from the annual report of the Soil Conservation Service project located at the St. Anthony Falls Hydraulic Laboratory for the calendar year 1943 and applies specifically to Series L-3, but it is typical of Series L-2 and is typical

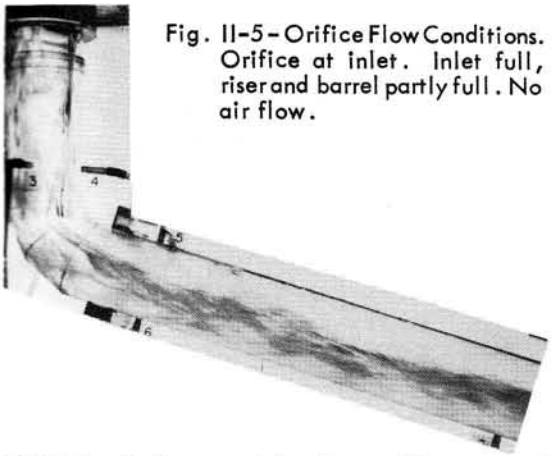

Fig. II-5 - Orifice Flow Conditions. Orifice at inlet. Inlet full, riser and barrel partly full. No air flow.

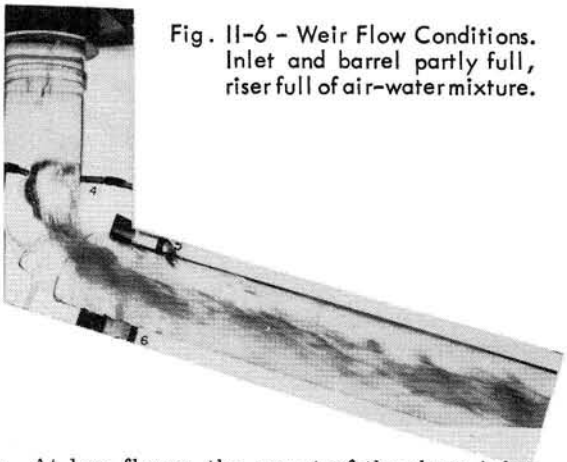

Fig. II-6 - Weir Flow Conditions. Inlet and barrel partly full, riser full of air-water mixture.

of Series L-1 except for the orifice control portion. At low flows, the crest of the drop inlet acts as a weir in controlling the flow, and the drop inlet and barrel are partly full. See head-discharge curve Section (a), Fig. II-3 and Fig. II-4. At a slightly greater flow the inlet is flooded out and acts as an orifice in controlling the flow, and the drop inlet and barrel are partly full. See Section (b), Fig. II-3 and Fig. II-5. At a still higher flow the drop inlet will fill and air will be sucked through it, the barrel will be partly full, and the sucking of the water away from the drop inlet crest due to the additional head caused by the drop inlet flowing full of a water-air mixture permits the drop inlet crest to again act as a weir in controlling the flow.

See Section (c), Fig. II-3 and Fig. II-6. As the flow increases still further the drop inlet crest will again be drowned out, air flow through the drop inlet will stop, the barrel will still be partly full, and the drop inlet, acting as a short tube, will control the flow. See Section (d), Fig. II-3 and Fig. II-7. The next thing that happens as the flow increases is the formation of a hydraulic jump at the entrance to the barrel. The hydraulic jump travels through the conduit sucking an air-water mixture through the drop inlet as it does so. See Fig. II-8. As the traveling hydraulic jump passes out of the barrel at its lower end the flow conditions may revert to either orifice or short tube flow, or the pipe may continue to flow full of an air-water mixture. In this latter case, the additional head caused by the spillway flowing full of mixture will suck water away from the drop inlet and permit the drop inlet crest to again control the flow. See Section (e), Fig. II-3 and Fig. II-9. As the flow still further increases the air flow will gradually decrease until the spillway flows completely full of water. See Fig. II-10. For this case, pipe flow controls the discharge. See Section (f), Fig. II-3. It is also possible for the flow to alternate between weir, orifice, short tube and pipe while the rate of flow to the headpool is steady and constant, the control section at any given time being indeterminate.

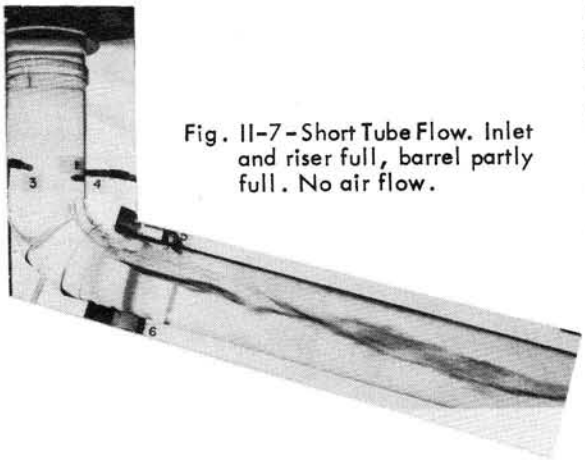

Fig. II-7 - Short Tube Flow. Inlet and riser full, barrel partly full. No air flow.

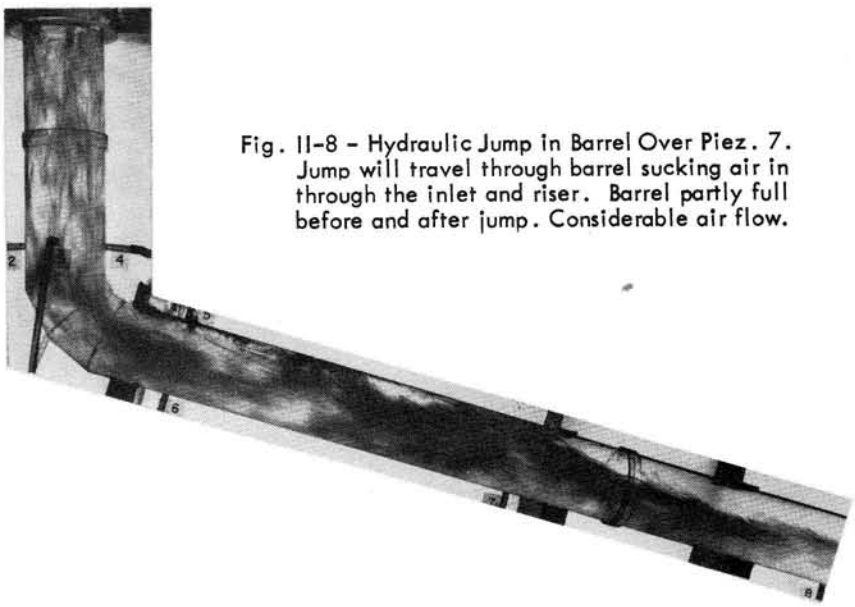

Fig. II-8 - Hydraulic Jump in Barrel Over Piez. 7. Jump will travel through barrel sucking air in through the inlet and riser. Barrel partly full before and after jump. Considerable air flow.

## DISCHARGE COEFFICIENTS

The determination of the flow through any closed conduit spillway requires a knowledge of the discharge coefficients. The determinations of these coefficients for the drop inlet crest acting as a weir, the drop inlet crest acting as an orifice, the drop inlet acting as a short tube, and the entrance loss coefficient for full pipe flow are given in the following paragraphs.

### Weir Coefficient

The value of the discharge coefficient C in Eqs. I-1 and I-2 is given by the solid curves of Figs. II-11b, II-12b and II-13b, for the three different drop inlet crest types covered by this report. It will be noticed that the data points scatter somewhat--lines parallel to the recommended curve for C are drawn 5 per cent above and below the C curves to indicate the precision represented. Just why the coefficients of Series VIII and IX in Fig. II-12b are so much higher than those for the other series is not known.

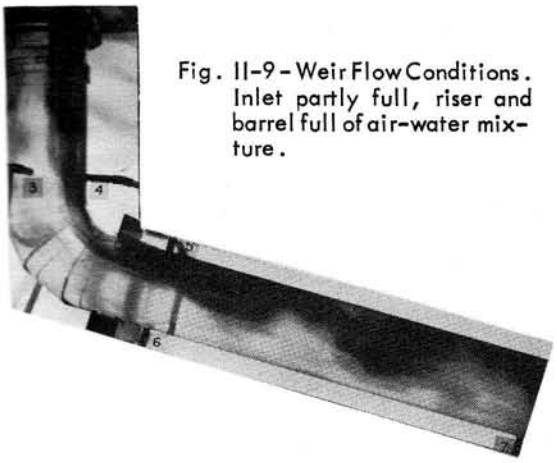

Fig. II-9 - Weir Flow Conditions. Inlet partly full, riser and barrel full of air-water mixture.

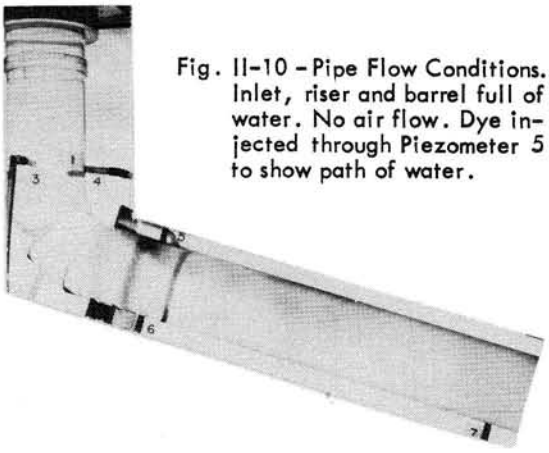

Fig. II-10 - Pipe Flow Conditions. Inlet, riser and barrel full of water. No air flow. Dye injected through Piezometer 5 to show path of water.

It would have been very difficult to draw a representative curve through these data points if other means had not been used to define the curve. The recommended C curve was defined by plotting $(Q/D^{5/2})^{2/3}$ against H/D. This method has previously been adopted when analyzing data on the box inlet drop spillways [I-10]. It can be seen in Figs. II-11a, II-12a and II-13a that the data are well represented by two straight lines. The lower line is probably representative of true weir flow over the crest. The upper line still represents weir control, but is

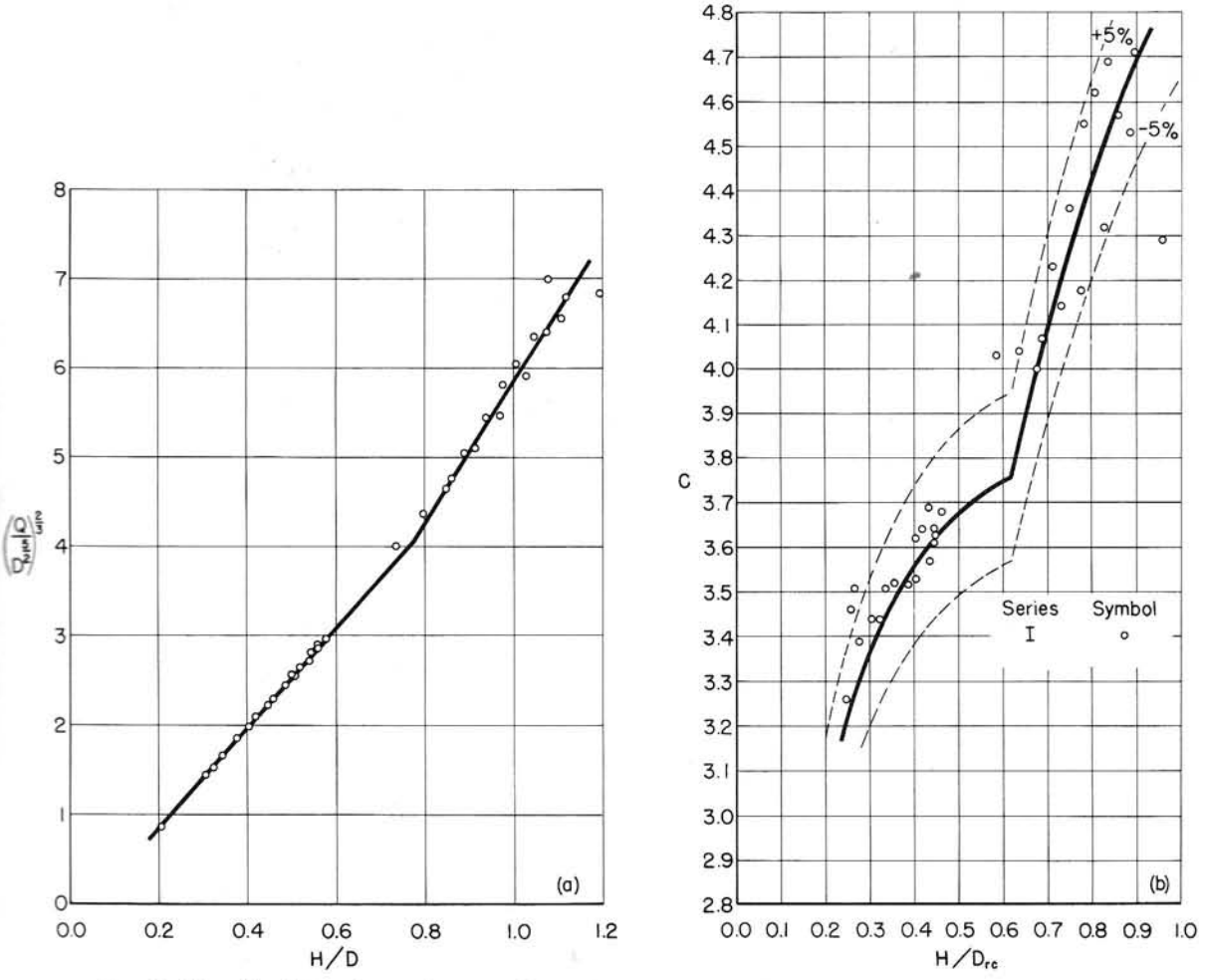


Fig. II-11 - Head-Discharge Curve and Head-Coefficient Curve for Weir Flow, Series I.

probably affected by such things as interference of the converging nappes or suction of air through the drop inlet. The equations of these curves are, for Fig. II-11a,

$$\frac{Q}{D_{rc}^{5/2}} = 4.14 \frac{L}{D_{rc}} \left[ \frac{H}{D_{rc}} - 0.038 \right]^{3/2} \qquad \text{(II-1a)}$$

when $H/D_{rc} < 0.619$ and

$$\frac{Q}{D_{rc}^{5/2}} = 6.98 \frac{L}{D_{rc}} \left[ \frac{H}{D_{rc}} - 0.209 \right]^{3/2} \qquad \text{(II-1b)}$$

when $H/D_{rc} > 0.619$

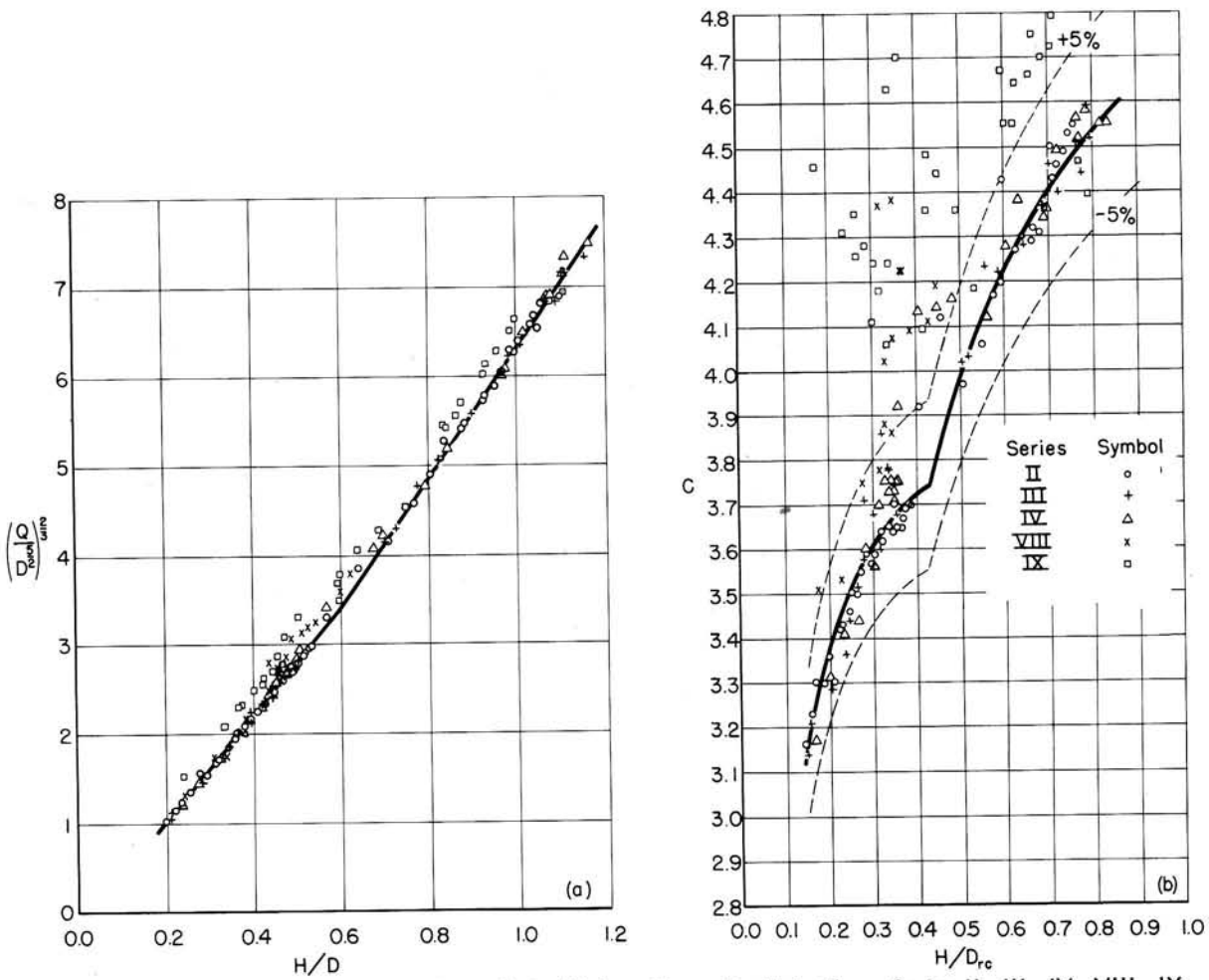


Fig. II-12 - Head-Discharge Curve and Head-Coefficient Curve for Weir Flow, Series II, III, IV, VIII, IX.

for Fig. II-12a,

$$\frac{Q}{D_{rc}^{5/2}} = 4.07 \frac{L}{D_{rc}} \left[ \frac{H}{D_{rc}} - 0.023 \right]^{3/2} \qquad \text{(II-2a)}$$

when $H/D_{rc} < 0.423$ and

$$\frac{Q}{D_{rc}^{5/2}} = 5.50 \frac{L}{D_{rc}} \left[ \frac{H}{D_{rc}} - 0.096 \right]^{3/2} \qquad \text{(II-2b)}$$

when $H/D_{rc} > 0.423$

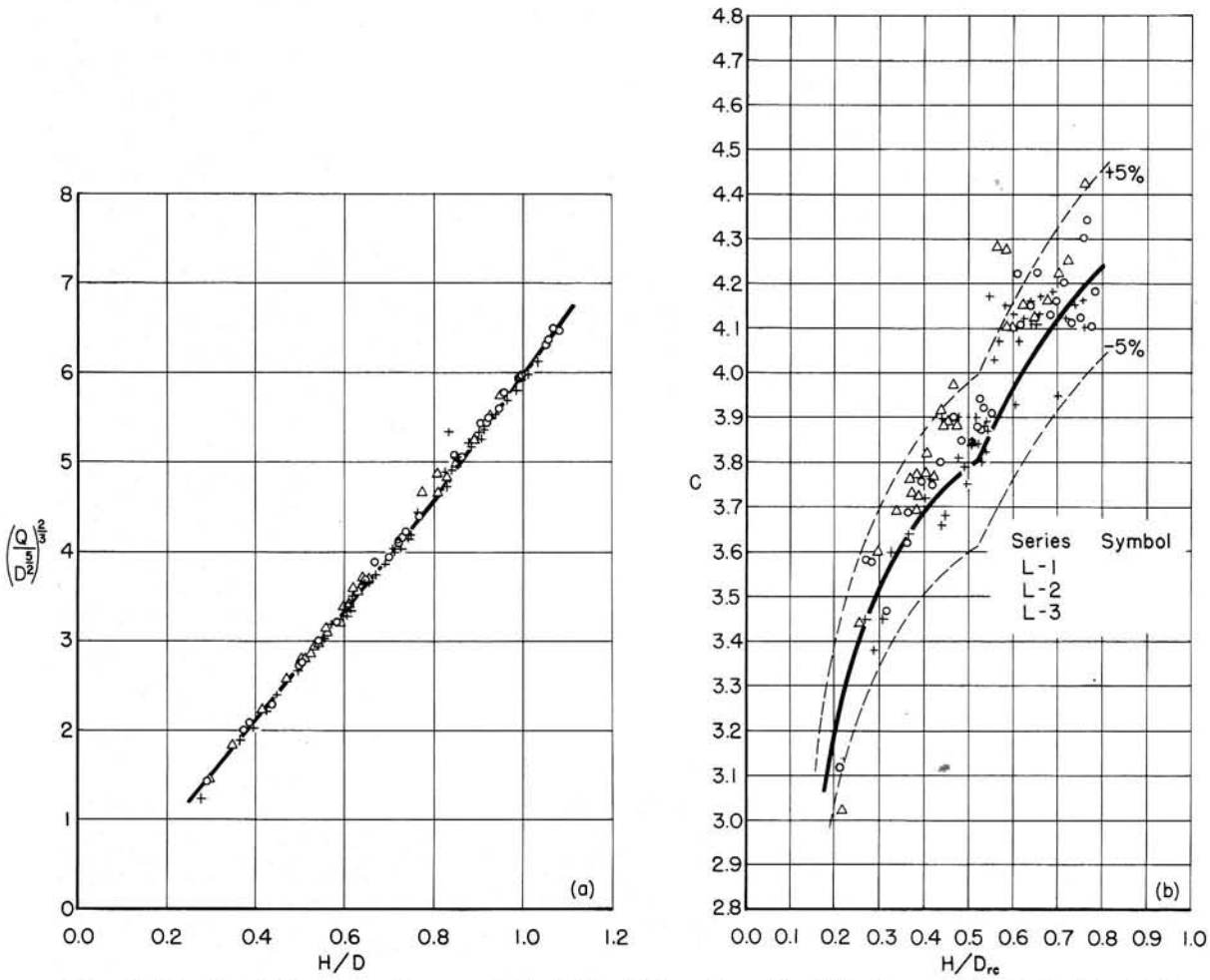


Fig. II-13 - Head-Discharge Curve and Head-Coefficient Curve for Weir Flow, Series L-1, L-2, L-3.

and for Fig. II-13a,

$$\frac{Q}{D_{rc}^{5/2}} = 4.20 \frac{L}{D_{rc}} \left[ \frac{H}{D_{rc}} - 0.033 \right]^{3/2} \qquad \text{(II-3a)}$$

when $H/D_{rc} < 0.521$ and

$$\frac{Q}{D_{rc}^{5/2}} = 5.12 \frac{L}{D_{rc}} \left[ \frac{H}{D_{rc}} - 0.094 \right]^{3/2} \qquad \text{(II-3b)}$$

when $H/D_{rc} > 0.521$.

The curves of Figs. II-11a, II-12a and II-13a were transferred to Figs. II-11b, II-12b and II-13b respectively, after correcting for the change from conduit diameter D to drop

inlet crest diameter $D_{rc}$ which is taken as the inside diameter of the bell for the bell entrance. This was done so as to facilitate the extrapolation to other ratios of $D_{rc}/D$, since it is $D_{rc}$ that determines the crest length rather than D. It should be remembered that the crest of Fig. II-12 is representative of bell ended tile and is somewhat rounded, whereas the crest of Fig. II-11 is a square-edged bellmouth inlet and the crest of Fig. II-13 is a square-edged pipe bell entrance.

Especially to be noted is the variation of discharge coefficient with relative head. The method of analysis presented here suggests that this variation is a result of the fact that the head-discharge curve does not pass through the origin of coordinates as one would expect. The reason for this remains for future explanation.

## Orifice Coefficient

Strangely, evidence of orifice control at the drop inlet crest was not obtained for all drop inlets included in the similar series reported here. The reason for this inconsistency is not known. It seems likely that the designer should plan as if orifice control would exist, because, if the assumption were in error, he would be on the safe side in planning for a lower capacity that he would actually have.

Orifice control was in evidence for Series VIII, and was known to exist for Series L-2 and L-3. It should be remembered that these were the earliest tests conducted on closed conduit spillways and that the presence of orifice flow could have been easily overlooked for other series. Values of the orifice discharge coefficients $C_o$ in Eq. I-6 are given in Table II-1 for those series where orifice flow was observed. The head was measured from the water surface to the bottom of the bell entrance, since the orifice control was observed to be at that point.

Orifice flow extended to a head of $1.28\ H_o/D$ for Series L-2, to a head of $1.41\ H_o/D$ for Series L-3, and to a head of $2.55\ H_o/D$ for Series VIII. The maximum head which is obtained for orifice flow is apparently fortuitous, and heads greater than those observed are by no means out of the range of possibility.

## Short Tube Coefficient

Short tube flow--when the drop inlet is full of water and the barrel is partly full--was observed only for Series L-1, L-2 and L-3. It could have been present for some of the tile pipe tests, but if so it could not be observed visually and the head-discharge data shows no evidence of the existence of short tube flow. Values of the short tube discharge coefficient $C_s$ in Eq. I-7 are given in Table II-1 for those instances where it was observed.

Short tube flow was observed at maximum heads of $6.18\ H_s/D$ for Series L-1, $5.10\ H_s/D$ for Series L-2, and $4.27\ H_s/D$ for Series L-3. As for orifice flow, the maximum head for short tube flow is apparently fortuitous.

## Entrance Loss Coefficient

Entrance loss coefficients $K_e$ for use in Eq. I-5 are given in Table II-1, except for Series VIII. The spillway never ran completely full for Series VIII and it was therefore impossible to evaluate $K_e$. The tabulated values of $K_e$ for the tile pipe series are the averages for a very small number of tests, and they are of low precision. Also the pipe friction factor for the tile pipe was of low precision, and this enters directly into the determination of $K_e$. Values of $K_e$ for the transparent pipe are based on more tests, are of much higher precision, and can be used with some confidence. The loss caused by the elbow is also included in $K_e$ and would undoubtedly increase if flatter slopes (greater angular change at the elbow) were used. The tests reported here were made using only one slope and no indication of the effect of pipe slope on $K_e$ is forthcoming from them.

## PRESSURE COEFFICIENTS

Average values of the local pressure deviations $h_n/h_{vp}$ computed for full flow in a horizontal frictionless conduit are given in Table II-2. These pressures should be zero along the barrel beyond the influence of the drop inlet and elbow. The differences between the observed averages and zero are small. This could be due to small imperfections in the piezometers, to errors in determining the conduit friction factor, or because the hydraulic grade line was assumed to pass through the center of the conduit exit which is not necessarily a correct assumption. This assumption also means that the tabulated values of $h_n/h_{vp}$ are not necessarily exactly correct. In any case, the differences are small and can safely be neglected.

The tabulated values of $h_n/h_{vp}$ for the drop inlet are always positive. However, the friction grade line is so low that the pressures computed from Eq. I-14 will be negative and the hydraulic grade line will be below the conduit. This is because the barrel is on a slope that is much steeper than the friction slope.

Maximum pressures for part full flow $h_p/D$ were observed at the first invert piezometer in the barrel. The maximum pressures observed during each series are given in Table II-3 together with the location of the piezometer. In most instances this piezometer was so far downstream that it probably did not record the actual maximum impact pressures caused by water falling down the drop inlet. It is apparent from Table II-3 that the maximum recorded pressures are approximately equal to the pipe diameter and are so low as to cause the designer no concern.

TABLE II-3

MAXIMUM OBSERVED PRESSURE FOR PART FULL FLOW

| Series | I | II | III | IV | VIII | IX | L-1 | L-2 | L-3 |
|---|---|---|---|---|---|---|---|---|---|
| Piez. | 3.45D | 3.45D | 3.45D | 3.45D | 1.13D | 1.13D | 0.75D | 0.75D | 0.75D |
| $h_p/D$ | 0.88 | 0.78 | 1.05 | 1.05 | 1.11 | 1.47 | 0.99 | 0.84 | 0.78 |

## CONCLUSIONS AND RECOMMENDATIONS

The preceding discussion has shown that the flow through closed conduit spillways having a drop inlet of the same diameter as that of the barrel is determined by weir, orifice, short tube, and pipe control sections. The only safe way to determine the maximum assured capacity is to assume weir and orifice controls. This will give the minimum capacity at any given head. It should be realized that the possibility of short tube and pipe flow is real and that the spillway capacity at times may be considerably greater than the orifice flow for which the spillway should be designed.

All things considered, the proportions of the closed conduit spillway described in this part of the report are not recommended for use under field conditions.

If, in spite of the preceding, this spillway design is adopted, the proportions for the drop inlet may be taken from Fig. II-1 and Table II-1; the weir discharge coefficients may be taken from Figs. II-11, II-12 and II-13; the orifice, short tube and entrance coefficients may be taken from Table II-1; and the local pressure constants may be taken from Table II-2.

## Part III

## Enlarged Circular Drop Inlet with Pipe Elbow at Base and Vitrified Clay Tile Reducer Barrel Entrance

### DESCRIPTION OF SPILLWAY

The tests reported here were conducted on a spillway made of vitrified clay tile pipe. The drop inlet was of 8-in. (actually 0.666 ft) diameter pipe with the bell acting as the crest. An 8-in. 90-degree elbow was used at the bottom of the riser. This was followed by an 8-in. by 6-in. reducer to complete the inlet. The barrel was the same 6-in. (actually 0.496 ft) diameter pipe used for the tests reported in Part II. The drop inlet is shown in Fig. III-1. The nominal conduit slope was 30 per cent, actual slopes being given in Table III-1. The outlet discharged freely; that is, the outlet was not submerged.

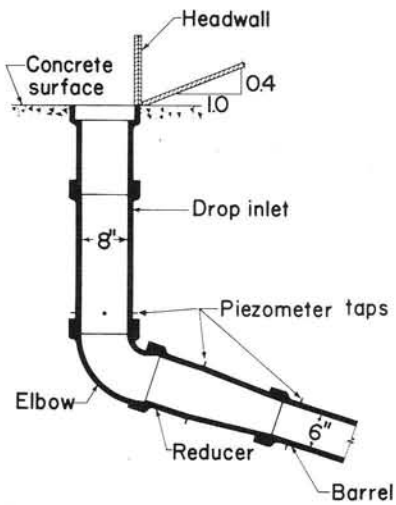


Fig. III-1 - Drop Inlet for Series V, VI and VII.

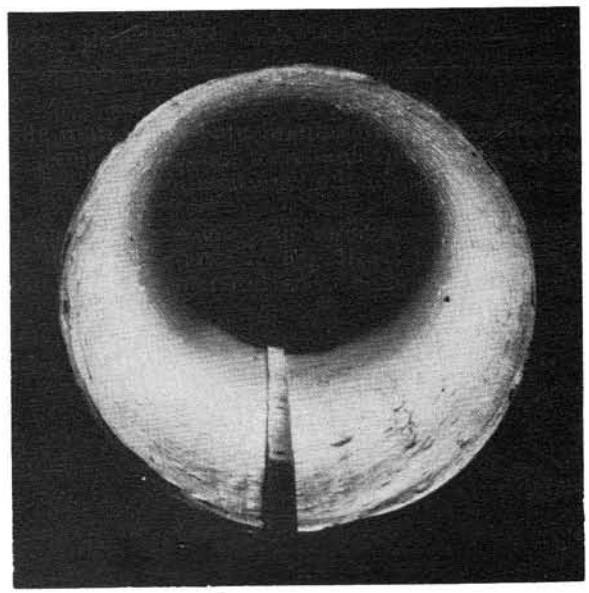

Fig. III-2 - Surface of 8-in. Vitrified Clay Tile Pipe.

TABLE III-1

PROPORTIONS OF SPILLWAYS AND DISCHARGE COEFFICIENTS

| Series | D (ft) | $D_r/D$ | $D_{rc}/D$ | $\ell/D$ | S | Z/D | $Z_1/D$ | Inlet Crest | Conduit Entrance | Anti-Vortex Device | $C_o$ | $N_o$ | $C_s$ | $N_s$ | $K_e$ | $N_e$ |
|---|---|---|---|---|---|---|---|---|---|---|---|---|---|---|---|---|
| V | 0.496 | 1.34 rd. | 1.77 rd. | 55.40 | 0.310 | 26.51 | 9.84 | Bell | Elbow and reducer | Tangent wall | -- | -- | -- | -- | 0.25 | 9 |
| VI | 0.496 | 1.34 rd. | 1.77 rd. | 55.40 | 0.311 | 24.42 | 7.64 | Bell | Elbow and reducer | Tangent wall | -- | -- | -- | -- | 0.06 | 5 |
| VII | 0.496 | 1.34 rd. | 1.77 rd. | 55.40 | 0.314 | 21.39 | 4.52 | Bell | Elbow and reducer | Tangent wall | -- | -- | -- | -- | 0.14 | 6 |

The 8-in. tile was much smoother than the 6-in. tile. This is apparent upon comparing Fig. III-2 with Fig. II-2. As in Part II of this report, the Darcy-Weisbach friction factor was assumed to be constant at 0.015 when making the friction head loss calculations.

Pressures were determined by means of piezometers and open manometer columns located along the spillway. Those in and near the inlet are shown in Fig. III-1. Locations of all piezometers are given in Table III-2. The piezometers were installed as described in Part II.

The only controlled variable in this group of tests was the height of the drop inlet. This also caused the total drop through the spillway to vary. The drop inlet heights included in the test program are given in Table III-1.

## APPARATUS AND PROCEDURE

The general test setup was identical with that described in Part II and shown in Fig. II-1a.

In spite of the greater length of weir crest, the channel approaching the drop inlet was still wide enough for the sidewall effects to be so small that they could be safely ignored.

The test procedure was the same as that described in Part II for the tile pipe tests.

TABLE III-2

PIEZOMETER LOCATIONS AND LOCAL PRESSURE DEVIATION FROM HYDRAULIC GRADE LINE, SERIES V, VI AND VII

| Piezometer Location | Series V Station | Series V $h_n/h_{vp}$ | Series VI Station | Series VI $h_n/h_{vp}$ | Series VII Station | Series VII $h_n/h_{vp}$ |
|---|---|---|---|---|---|---|
| Left* | -6.73D | +0.85 | -6.73D | +0.74 | -6.81D | +0.69 |
| Upstream* | -6.73D | +0.86 | -6.73D | +0.72 | -6.73D | +0.76 |
| Right* | -6.75D | +0.84 | -6.75D | +0.70 | -6.83D | +0.74 |
| Downstream* | -6.75D | +0.80 | -6.75D | +0.66 | -6.83D | +0.64 |
| Crown | -2.54D | +0.74 | -2.54D | +0.61 | -2.54D | +0.66 |
| Invert | -2.50D | +0.75 | -2.50D | +0.63 | -2.50D | +0.71 |
| Crown | 0.52D | +0.11 | 0.52D | +0.01 | 0.52D | +0.06 |
| Invert | 0.52D | +0.13 | 0.52D | +0.02 | 0.52D | +0.06 |
| Invert | 7.32D | +0.08 | 7.34D | -0.03 | 7.34D | +0.01 |
| Invert | 15.27D | +0.06 | 15.32D | -0.05 | 15.32D | -0.02 |
| Invert | 23.26D | +0.00 | 23.23D | -0.05 | 23.23D | -0.03 |
| Invert | 31.12D | -0.01 | 31.13D | -0.05 | 31.13D | -0.05 |
| Invert | 39.04D | +0.02 | 39.05D | -0.03 | 39.05D | -0.01 |
| Invert | 47.02D | -0.10 | 47.14D | -0.03 | 47.14D | +0.05 |
| Invert | 54.88D | +0.01 | 54.96D | -0.01 | 54.96D | -0.02 |

*Side of drop inlet.

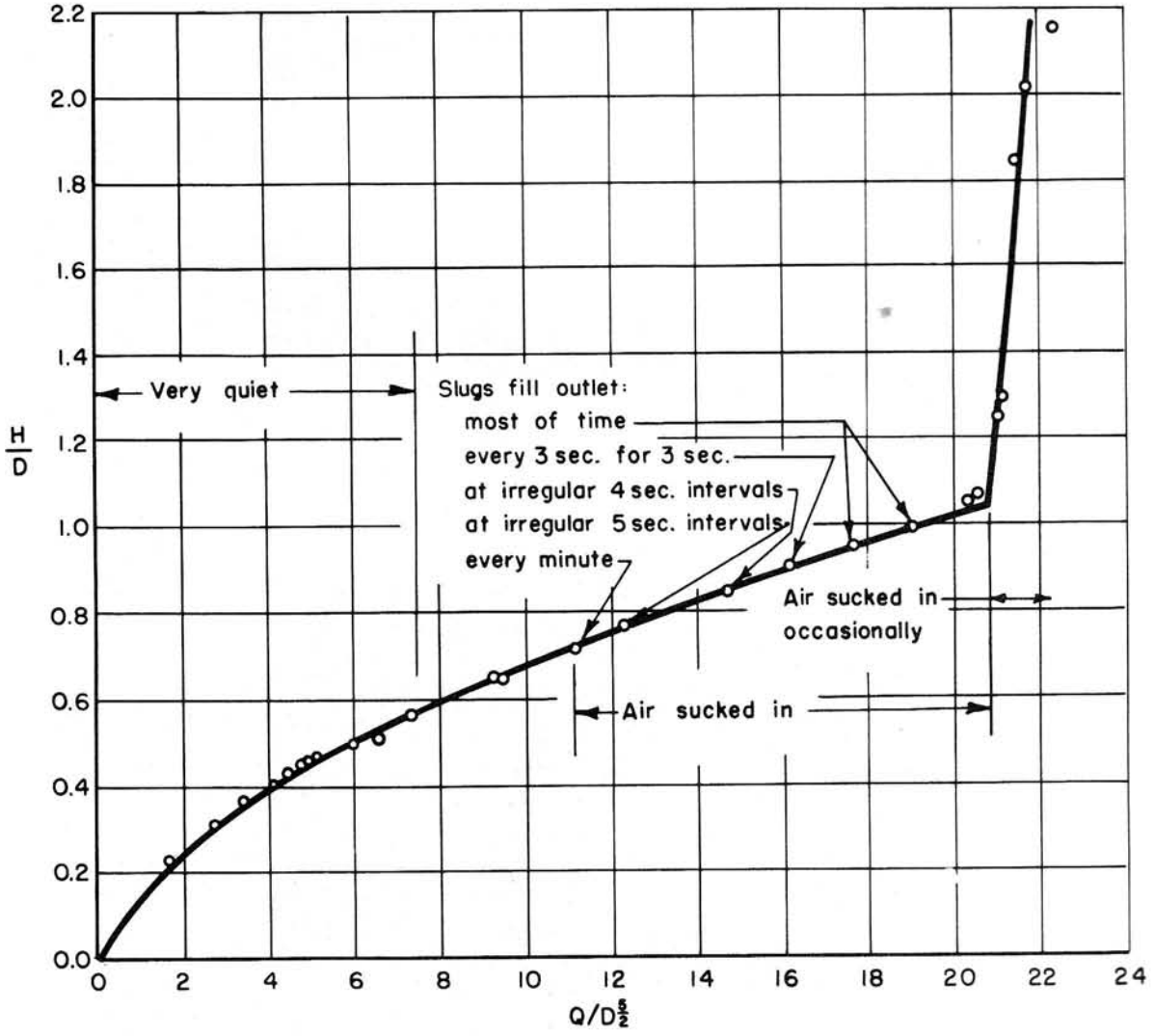


Fig. III-3 - Head-Discharge Curve, Series VII.

The only controlled variable in this group of tests was the height of the drop inlet. This also caused the total drop through the spillway to vary. The drop inlet heights included in the test program are given in Table III-1.

## APPARATUS AND PROCEDURE

The general test setup was identical with that described in Part II and shown in Fig. II-1a.

In spite of the greater length of weir crest, the channel approaching the drop inlet was still wide enough for the sidewall effects to be so small that they could be safely ignored.

The test procedure was the same as that described in Part II for the tile pipe tests.

TABLE III-2

PIEZOMETER LOCATIONS AND LOCAL PRESSURE DEVIATION FROM HYDRAULIC GRADE LINE, SERIES V, VI AND VII

| Piezometer Location | Series V Station | Series V $h_n/h_{vp}$ | Series VI Station | Series VI $h_n/h_{vp}$ | Series VII Station | Series VII $h_n/h_{vp}$ |
|---|---|---|---|---|---|---|
| Left* | -6.73D | +0.85 | -6.73D | +0.74 | -6.81D | +0.69 |
| Upstream* | -6.73D | +0.86 | -6.73D | +0.72 | -6.73D | +0.76 |
| Right* | -6.75D | +0.84 | -6.75D | +0.70 | -6.83D | +0.74 |
| Downstream* | -6.75D | +0.80 | -6.75D | +0.66 | -6.83D | +0.64 |
| Crown | -2.54D | +0.74 | -2.54D | +0.61 | -2.54D | +0.66 |
| Invert | -2.50D | +0.75 | -2.50D | +0.63 | -2.50D | +0.71 |
| Crown | 0.52D | +0.11 | 0.52D | +0.01 | 0.52D | +0.06 |
| Invert | 0.52D | +0.13 | 0.52D | +0.02 | 0.52D | +0.06 |
| Invert | 7.32D | +0.08 | 7.34D | -0.03 | 7.34D | +0.01 |
| Invert | 15.27D | +0.06 | 15.32D | -0.05 | 15.32D | -0.02 |
| Invert | 23.26D | +0.00 | 23.23D | -0.05 | 23.23D | -0.03 |
| Invert | 31.12D | -0.01 | 31.13D | -0.05 | 31.13D | -0.05 |
| Invert | 39.04D | +0.02 | 39.05D | -0.03 | 39.05D | -0.01 |
| Invert | 47.02D | -0.10 | 47.14D | -0.03 | 47.14D | +0.05 |
| Invert | 54.88D | +0.01 | 54.96D | -0.01 | 54.96D | -0.02 |

*Side of drop inlet.

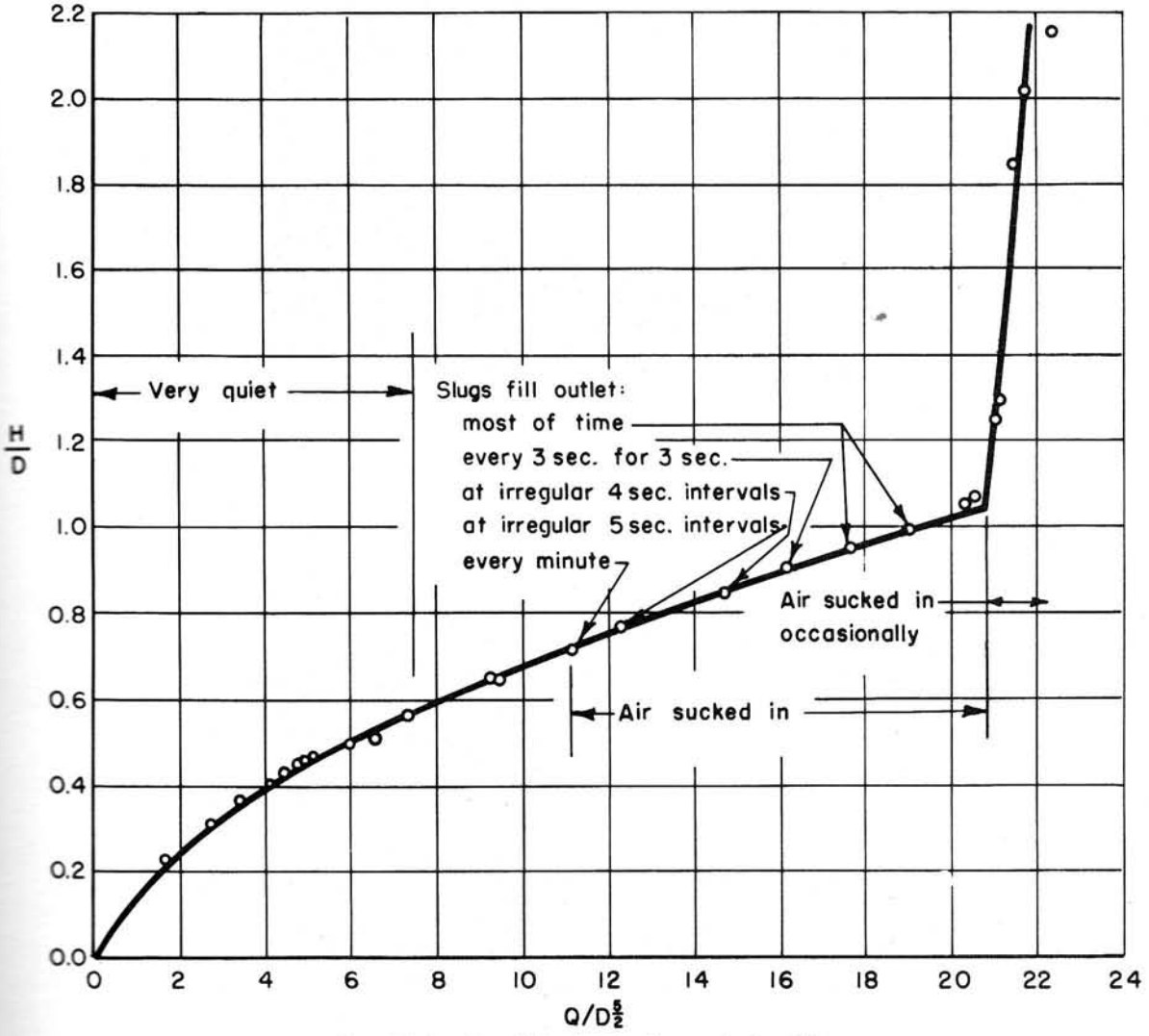


Fig. III-3 - Head-Discharge Curve, Series VII.

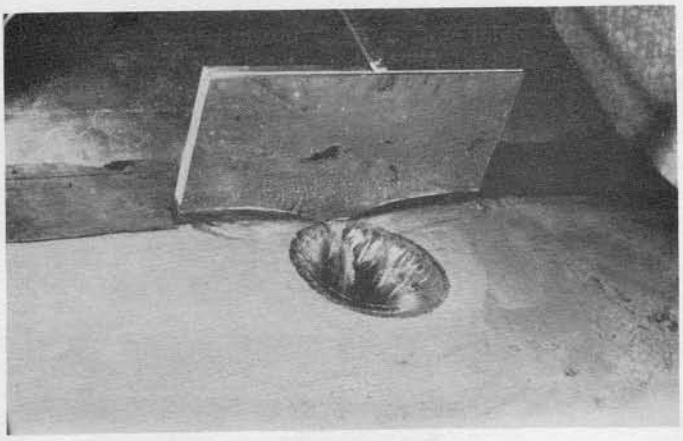

Fig. III-4 - Weir Flow at Crest of Drop Inlet, Barrel Partly Full, H/D = 0.36.

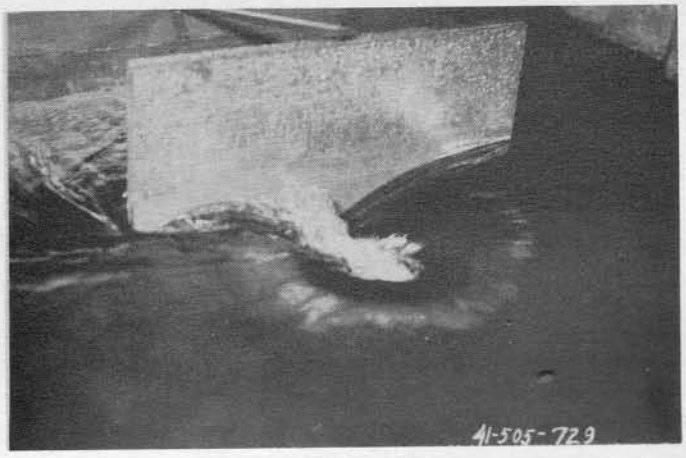


Fig. III-5 - Weir Flow at Crest of Drop Inlet, Slugs in Barrel, Circulation Around Headwall, H/D = 0.94.

Fig. III-6 - Conduit Completely Full, Circulation Around Headwall, H/D = 1.40.

## DESCRIPTION OF FLOW

The head-discharge relationship for the type of closed conduit spillway shown in Fig. III-1 exhibits only the desirable weir and pipe controls. A typical rating curve is shown in Fig. III-3. The same rating curve is obtained for both rising and falling stages. The flow condition for many tests is also noted in Fig. III-3. These notes were taken during the tests. The notes on air flow indicate that air was carried through the spillway during the time traveling hydraulic jumps or slugs filled the conduit and traveled through it. The slugs increased in frequency with increases in the flow until the conduit flowed continuously full of an air-water mixture. Subsequent increases in the water flow reduced the air flow until the spillway flowed completely full of water alone, except for occasional gulps of air through a vortex.

A typical view of weir flow at a low head is shown in Fig. III-4. The weir also controls the head-discharge relationship for the flow shown in Fig. III-5, as can be seen by referring to Fig. III-3. There the conduit is flowing completely full most of the time, but air is being sucked in at the inlet. The conduit is flowing completely full of water for the inlet condition shown in Fig. III-6 and the control is the pipe. However, an occasional gulp of air is carried down through the disturbance at the left end of the headwall and through the spillway.

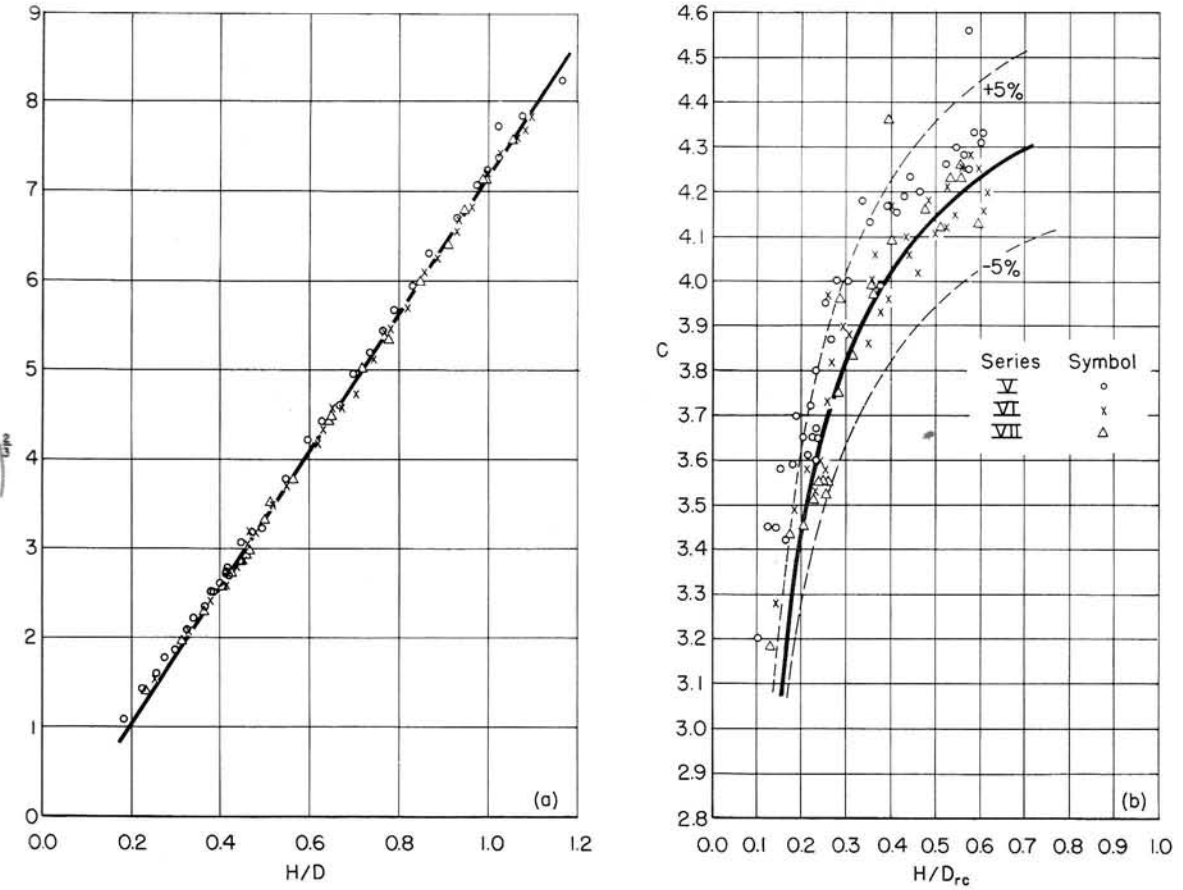


Fig. III-7 - Head-Discharge Curve and Head-Coefficient Curve for Weir Flow, Series V, VI, VII.

The circulation around in back of the headwall shown in Figs. III-5 and III-6 was found in later tests to cause a considerable reduction in the capacity of the spillway. Mention is made of it here since it is an undesirable condition and means should be taken to eliminate circulation around the headwall.

After the conclusion of Series V, it was discovered that a string of oakum used to calk the joint in the drop inlet was hanging across the drop inlet. It is not known just when this occurred, so some of the prior observations may be in error. The joint was tight when installed, but apparently opened by about 5/8 in. some time during the experiment.

## DISCHARGE COEFFICIENTS

Since only weir and pipe controls existed for this spillway, only the weir coefficient and the entrance loss coefficient were determined.

### Weir Coefficient

The value of the weir-flow coefficient in Eq. I-1 is given by the solid line in Fig. III-7b. Dash lines have been drawn 5 per cent above and below the solid line to indicate the spread of the data.

The coefficient curve was computed from the curve shown in Fig. III-7a which, with the coordinates used, is a straight line. A better fit at the low heads could have been obtained by using two straight lines as in Fig. II-12a. Since only a few points at the low and ordinarily most unimportant heads are affected, the single curve is used. This curve has the equation

$$\frac{Q}{D_{rc}^{5/2}} = 4.66 \frac{L}{D_{rc}} \left[ \frac{H}{D_{rc}} - 0.037 \right]^{3/2} \qquad \text{(III-1)}$$

The coefficient curve of Fig. III-7b is computed from the equation

$$C = 4.66 \left[ 1 - \frac{0.037}{H/D_{rc}} \right]^{3/2} \qquad \text{(III-2)}$$

Many of the comments made in Part II concerning the weir coefficient also apply here.

### Entrance Loss Coefficient

Entrance loss coefficients $K_e$ for use in Eq. I-5 are given in Table III-1. There is a considerable variation in the tabulated values of $K_e$ and this is not conducive to confidence in them. It is possible that the omission of small storage corrections may have caused this variation. Vortices caused by circulation around the headwall are an additional source of error in all these early experiments.

## PRESSURE COEFFICIENTS

The average pressure coefficients $h_n/h_{vp}$ for a horizontal frictionless pipe are given in Table III-2. These may be inserted in Eq. I-14 to determine the actual pressure. The tabulated pressure coefficients along the barrel are close to the theoretical zero except for the piezometers located close to the contraction; the small deviation from zero downstream from the influence of the inlet may be neglected for all practical purposes. Possible reasons for this deviation are given in Part II. In the inlet the pressure coefficients are above zero, as one would expect. The pressure coefficients in the inlet are referenced to the velocity head in the barrel and not to the lower velocity head which exists in the drop inlet.

Pressures should always be computed to determine whether or not they are close to or below the vapor pressure. If they are in the vicinity of the vapor pressure or below, steps should be taken to secure higher pressures within the spillway.

TABLE III-3

MAXIMUM OBSERVED PRESSURE FOR PART FULL FLOW

Values of $h_p/D$

| Series | V | VI | VII |
|---|---|---|---|
| Piezometer: | | | |
| -2.50D | 2.68 | 1.63 | 1.03 |
| +0.52D | 0.60 | 0.66 | 0.66 |

Maximum pressures for the condition of part full flow in the barrel were observed at invert Piezometer -2.50D. This piezometer is located just downstream from the elbow and just precedes the reducer. Maximum pressures observed at this piezometer and at Piezometer 0.52D, the first piezometer downstream of the reducer, are given in Table III-3.

## CONCLUSIONS AND RECOMMENDATIONS

From a hydraulic point of view, the spillway shown in Fig. III-1 is entirely satisfactory and is recommended for use under field conditions. The spillway proportions may be taken from Fig. III-1 and Table III-1; weir discharge coefficients may be taken from Fig. III-7; the entrance coefficient may be taken from Table III-1; and the local pressure constants may be taken from Table III-2.

It is recommended that some means be employed to eliminate circulation around the headwall. This circulation reduces the capacity of the spillway.

## Part IV

## Square Drop Inlet with Square-Edged Crest and Bell Barrel Entrance

### DESCRIPTION OF SPILLWAY

The drop inlets for these spillways were 24, 18, 12 and 8 in. square in plan and 48 in. deep. Their dimensions are given in Fig. IV-1 and Table IV-1. The crests of the drop inlets were square edged. The headwall on the downstream side of the drop inlets extended completely across the test channel; there was no opportunity for circulation in back of it.

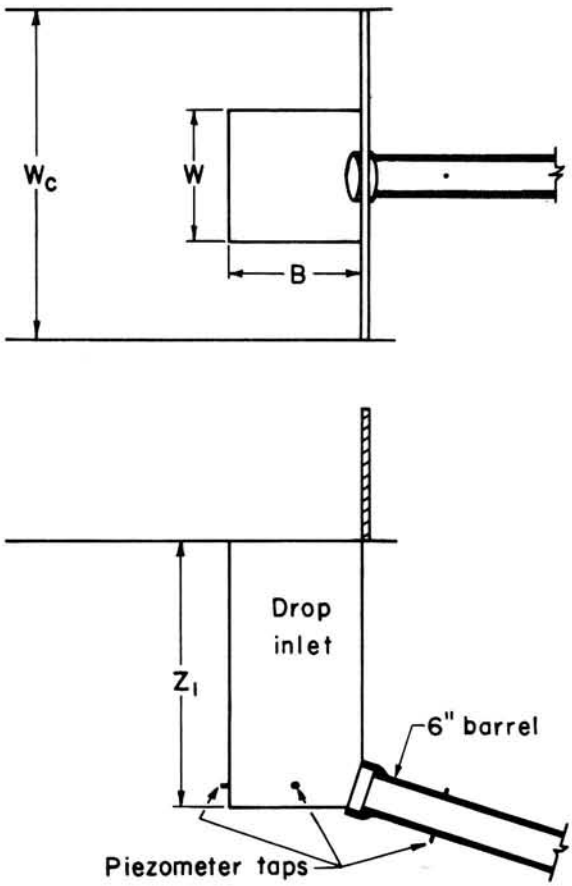


TABLE

| Series | B and W |
|---|---|
| X-A to XIV-A | 2.002 ft. |
| XV | 1.500 ft. |
| XVI | 1.000 ft. |
| XVII | 0.672 ft. |

Fig. IV-1 - Drop Inlet for Series X-A to XVII Inclusive.

TABLE IV-1

PROPORTIONS OF SPILLWAYS AND DISCHARGE COEFFICIENTS

| Series | D (ft) | $D_r/D$ | $D_{ro}/D$ | $\ell/D$ | S | Z/D | $Z_1/D$ | Inlet Crest | Conduit Entrance | Anti-Vortex Device | $C_o$ | $N_o$ | $C_s$ | $N_s$ | $K_e$ | $N_e$ |
|---|---|---|---|---|---|---|---|---|---|---|---|---|---|---|---|---|
| XA | 0.496 | 4.04 sq. | 4.04 sq. | 59.37 | 0.098 | 13.32 | 8.03 | Square edge | Bell | Tangent wall | -- | -- | -- | -- | 0.13 | 9 |
| XI | 0.496 | 4.04 sq. | 4.04 sq. | 59.37 | 0.203 | 19.53 | 7.99 | Square edge | Bell | Tangent wall | -- | -- | -- | -- | 0.12 | 11 |
| XII | 0.496 | 4.04 sq. | 4.04 sq. | 59.37 | 0.301 | 25.42 | 8.01 | Square edge | Bell | Tangent wall | -- | -- | -- | -- | 0.17 | 10 |
| XIII | 0.496 | 4.04 sq. | 4.04 sq. | 39.56 | 0.301 | 19.45 | 8.02 | Square edge | Bell | Tangent wall | -- | -- | -- | -- | 0.17 | 8 |
| XIV | 0.496 | 4.04 sq. | 4.04 sq. | 19.82 | 0.301 | 13.53 | 8.04 | Square edge | Bell | Tangent wall | -- | -- | -- | -- | 0.16 | 11 |
| XIVA | 0.496 | 4.04 sq. | 4.04 sq. | 19.82 | 0.302 | 13.58 | 8.08 | Square edge | Bell* | Tangent wall | -- | -- | -- | -- | 0.20 | 16 |
| XV | 0.496 | 3.02 sq. | 3.02 sq. | 59.53 | 0.302 | 25.97 | 8.21 | Square edge | Bell | Tangent wall | -- | -- | -- | -- | 0.22 | 16 |
| XVI | 0.496 | 2.02 sq. | 2.02 sq. | 59.53 | 0.300 | 25.62 | 8.23 | Square edge | Bell | Tangent wall | -- | -- | -- | -- | 0.23 | 12 |
| XVII | 0.496 | 1.35 sq. | 1.35 sq. | 59.53 | 0.300 | 25.51 | 8.15 | Square edge | Bell | Tangent wall | -- | -- | -- | -- | 0.41 | 9 |

*Downstream face of drop inlet filled in flush with end of bell. Bell projects into drop inlet for other series.

The barrel left the drop inlet at the base of the drop inlet. The barrel was the same 6-in. (actually 0.496 ft) diameter bell and spigot vitrified clay tile pipe used in the tests described in Parts II and III of this paper. The bell was used as the barrel entrance. The inside bottom of the bell was flush with the floor of the drop inlet and the top of the bell was in the plane of the downstream face of the drop inlet. The sides of the bell therefore projected into the drop inlet. The conduit entrance shown in Fig. IV-2 was used except for Series XIVA where the downstream side of the riser was filled in to make it flush with the face of the bell, as is shown in Fig. IV-3.

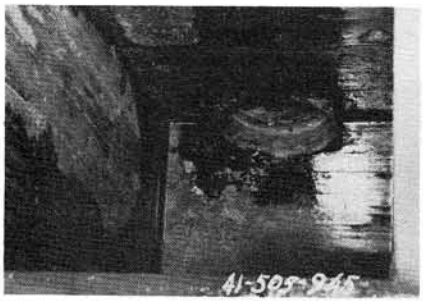

Fig. IV-2 - Drop Inlet and Barrel Entrance Except for Series XIV-A.

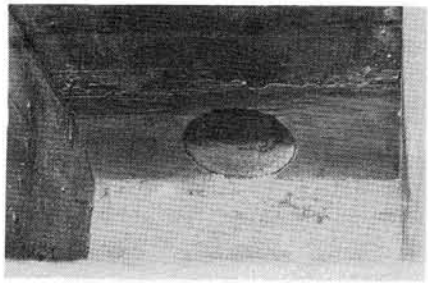

Fig. IV-3 - Drop Inlet and Barrel Entrance for Series XIV-A.

Reference is made to Part II of this paper for a discussion of the surface of the tile pipe and its friction factor. It is pertinent to note here that just before the tests of Series XIV were begun it was noticed that each pipe had settled in the bell of the following pipe, so that its invert was about 1/16 in. low. Just what effect this misalignment had on the results or just when it occurred is not known. Apparently the pipe was relaid before beginning Series XV.

Piezometers were installed near the base of the drop inlet in the upstream wall and in the two sidewalls. In addition, piezometers were located at intervals along the invert of the barrel. Their locations are indicated in Table IV-2. The piezometers were installed as described in Part II, and open manometer columns, read visually, were used to determine the magnitude of the pressure. Before beginning Series XIV it was noted that the paraffin in Piezometer 19.3D was missing. It was replaced. Also at Piezometer 11.3D the paraffin had lifted slightly, but apparently it was not replaced because of its inaccessibility. The piezometric data seemed to be little affected by these things.

TABLE IV-2

PIEZOMETER LOCATIONS AND LOCAL PRESSURE DEVIATION FROM HYDRAULIC GRADE LINE, SERIES X-A TO XVII

| Piezometer Location | Series XA | | Series XI | | Series XII | | Series XIII | | Series XIV | | Series XIVA | | Series XV | | Series XVI | | Series XVII | |
|---|---|---|---|---|---|---|---|---|---|---|---|---|---|---|---|---|---|---|
| | Station | $h_n/h_{vp}$ | Station | $h_n/h_{vp}$ | Station | $h_n/h_{vp}$ | Station | $h_n/h_{vp}$ | Station | $h_n/h_{vp}$ | Station | $h_n/h_{vp}$ | Station | $h_n/h_{vp}$ | Station | $h_n/h_{vp}$ | Station | $h_n/h_{vp}$ |
| Left* | -2.33D | +1.12 | -2.25D | +1.11 | -2.17D | +1.17 | -2.15D | +1.16 | -2.17D | +1.15 | -2.17D | +1.19 | -1.68D | +1.20 | -1.17D | +1.17 | -- | -- |
| Upstream* | -2.33D | +1.12 | -2.25D | +1.11 | -2.17D | +1.17 | -2.15D | +1.16 | -2.17D | +1.15 | -2.17D | +1.19 | -1.68D | +1.20 | -1.17D | +1.17 | -0.84D | +1.19 |
| Right* | -2.33D | +1.12 | -2.25D | +1.11 | -2.17D | +1.17 | -2.15D | +1.16 | -2.17D | +1.15 | -2.17D | +1.19 | -1.68D | +1.20 | -1.17D | +1.17 | -- | -- |
| Invert | 4.48D | +0.08 | 4.48D | +0.05 | 4.48D | +0.09 | 4.42D | +0.10 | 4.47D | +0.10 | 4.47D | +0.12 | 3.45D | +0.13 | 3.45D | +0.13 | 3.45D | +0.17 |
| Invert | 11.31D | +0.01 | 11.31D | -0.00 | 11.31D | +0.02 | 11.23D | +0.06 | 11.31D | +0.10 | 11.31D | +0.15 | 8.54D | +0.13 | 8.54D | +0.13 | 8.54D | +0.18 |
| Invert | 19.26D | -0.01 | 19.26D | -0.02 | 19.26D | +0.01 | 19.21D | +0.02 | 19.31D | +0.01 | 19.31D | +0.10 | 15.01D | +0.09 | 15.01D | +0.10 | 15.01D | +0.14 |
| Invert | 27.18D | -0.02 | 27.18D | -0.03 | 27.18D | 0.00 | 27.12D | +0.01 | | | | | 23.32D | +0.03 | 23.32D | +0.06 | 23.32D | +0.09 |
| Invert | 35.05D | -0.06 | 35.05D | -0.06 | 35.05D | -0.04 | 35.00D | -0.03 | | | | | 27.28D | +0.05 | 27.28D | +0.07 | 27.28D | +0.10 |
| Invert | 42.94D | -0.02 | 42.94D | -0.03 | 42.94D | -0.02 | | | | | | | 35.21D | +0.04 | 35.21D | +0.07 | 35.21D | +0.10 |
| Invert | 50.91D | +0.04 | 50.91D | +0.04 | 50.91D | +0.05 | | | | | | | 43.12D | -0.00 | 43.12D | +0.05 | 43.12D | +0.08 |
| Invert | 58.87D | +0.08 | 58.87D | +0.09 | 58.87D | +0.07 | | | | | | | 51.03D | +0.03 | 51.03D | +0.05 | 51.03D | +0.08 |
| Invert | | | | | | | | | | | | | 59.00D | +0.02 | 59.00D | +0.02 | 59.00D | +0.02 |

*Side of drop inlet.

Variables included in the test program were the drop inlet dimensions mentioned previously, the slope of the barrel and the length of the barrel. Nominal slopes of 10, 20 and 30 per cent were used. Nominal barrel lengths were 20, 40 and 60 pipe diameters. Actual values are given in Table IV-1.

## APPARATUS AND PROCEDURE

The same equipment, channels and test methods were used for these tests as were used for the tile pipe tests described in Parts II and III. The test setup is shown in Fig. II-1a.

The test channel was so narrow that the sidewall effects are undoubtedly significant for the two or three largest drop inlets. This has been shown in connection with a study of box inlet drop spillways [I-11]. The effect of the relatively narrow approach channel will be discussed further in the subsection below entitled "Weir Coefficient."

## DESCRIPTION OF FLOW

The nappe clings to the sides of the riser at the very lowest heads. For this condition a data point cannot be expected to fall on the normal weir curve. As the flow increases the nappe springs clear of the crest as can be seen in Fig. IV-4. There the nappe is still clinging near the upstream end. This is because the water depth on the crest is shallow at that point as a result of the high approach velocity and relatively narrow approach channel. At the very lowest flows the inlet to the barrel is only partly full, and the barrel entrance acts as a weir and exercises a secondary control that, of course, has no effect on the headpool elevation. However, even at as low a flow as in Fig. IV-4 the barrel entrance is submerged and air is sucked into the barrel. With further increases in the flow, slugs form in the barrel and travel either all or part of the way through it. There is a considerable and very audible suction of air under these conditions. Also, the nappes alternately fall and rise as the air flow starts and stops as a result of the slugs forming, traveling through the barrel, and leaving the barrel. Pressures under the nappe were observed to fluctuate from zero to -0.01 ft of water for Series XV, while for Series XVI the pressure was observed to fluctuate from +0.11 to -0.04 ft of water. These measurements were very crude and do not necessarily represent maximum or minimum pressures under the nappe. The effect of these variations in pressure under the nappe was apparently not sufficient to be noticed on the head-discharge curve.

The frequency of formation of the traveling hydraulic jumps or slugs increases with the flow until the barrel flows continuously full of an air-water mixture. The air flow then gradually decreases with further increases in water flow, the barrel flowing full all the time and the depth in the drop inlet gradually increasing. In Fig. IV-5 little if any air is being carried through the spillway in spite of the white water in the drop inlet. The barrel is flowing full and the head between the water surface in the drop inlet and the centerline of the barrel exit is consumed in pipe flow losses. However, the control at the drop inlet crest is obviously of the weir type and the headpool level is therefore governed by the weir flow formula.

According to the head-discharge curve, the flow shown in Fig. IV-6 can be computed by either the weir or the pipe equations since it is at the intersection of the weir and pipe curves. Increasing the flow by only 0.08 cfs results in the condition shown in Fig. IV-7 which is obviously pipe flow. Increasing the flow by another 0.22 cfs completely submerges the drop inlet crest as shown in Fig. IV-8. The movement of the water surface can be seen from the confetti streaks.

The presence of vortices was noted for Series XIV and XIVA. No mention of vortices was made in the notes for other series. Careful examination of the water surface shown in Fig. IV-8 shows small depressions suggestive of incipient vortices. Vortex effects were apparently negligible for the series discussed in Part IV of this paper.

Only the desirable weir and pipe controls influenced the head-discharge relationship for this spillway.

## DISCHARGE COEFFICIENTS

The weir and pipe discharge coefficients will be discussed in the following subsections. Mention will also be made of the orifice at the base of the drop inlet even though it had no effect on the headpool elevation.

Fig. IV-4 - Weir Flow at Crest of Drop Inlet. Nappe clinging only at upstream corner. Barrel entrance is submerged. Air is carried through barrel. H/D = 0.34.

Fig. IV-5 - Weir Flow at Crest of Drop Inlet. Barrel full. No air flow. H/D = 0.57.

Fig. IV-6 - Either the Weir or the Pipe Equation May be Used to Compute the Flow for these Conditions. H/D = 0.61.

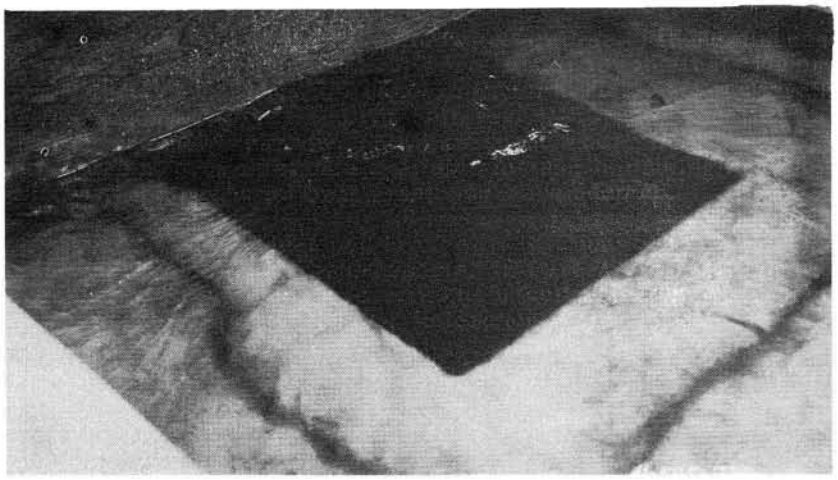

Fig. IV-7 - Pipe Equation Determines Discharge. Flow is only 0.08 cfs greater than that for Fig. IV-6. H/D = 0.70.

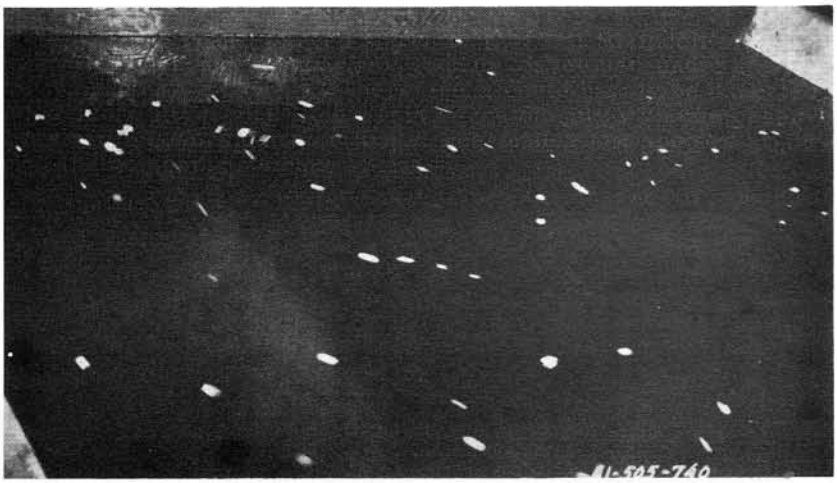

Fig. IV-8 - Inlet is Completely Submerged. Confetti shows little movement of water surface. H/D = 2.14.

Weir Coefficient

The drop inlets discussed here are similar to those discussed in Part V of this report. However, the approach channels were "wide" for the tests reported in Part V and "narrow" for the tests reported in this part except for Series XVII. According to the report on "Hydraulic Design of the Box Inlet Drop Spillway" [I-11], a channel width correction must be applied when the channel is narrow. This introduced a complication into the analysis, especially since there were no drop inlet data available for use in making the approach channel width corrections. Therefore the following methods were adopted.

The equations developed for the two sections of the head-discharge curve (see Fig. II-12 for a typical plot of the data) reported in Part V were assumed to be correct. The discharge given by these equations was computed, corrected for the effect of approach channel width shown in Table III or Fig. IV of Reference I-11, and compared with the observed discharge. The discharge was also computed according to Reference I-11 assuming the control to be at the box (drop) inlet crest. This discharge was also compared with the observed discharge.

For the lower portion of the head-discharge curve it was found that the discharges computed according to Reference I-11 agreed better with the observed discharges than did the discharges computed from the equation developed from the data reported in Part V. For the upper portion of the head-discharge curve, the equation given in Part V gave closer agreement with the observed discharges than did the discharges computed from Reference I-11.

The two rating curves shown in Fig. 9 of Blaisdell's thesis [I-8] intersect at $Q/D^{5/2} = 5.25$. At about that discharge a vacuum developed under the nappe which increased the effective head on the crest. Therefore it could hardly be expected that the discharge as computed from Reference I-11 would agree closely with the observed discharges at the higher flows while good agreement could reasonably be expected at the lower discharges. This is what the comparisons have shown.

Best results will be obtained if the discharges are computed as in Reference I-11 when $Q/D^{5/2}$ is less than 4, and from the equation

$$\frac{Q}{D^{5/2}} = 4.1 \frac{L}{D}\left[\frac{H}{D} - 0.060\right]^{3/2} \qquad \text{(V-2b)}$$

when $Q/D^{5/2}$ is greater than 4.

## Orifice Coefficient

The orifice is located at the bottom of the drop inlet and is the entrance to the barrel. Actually no orifice coefficient was obtained, but some discussion of the barrel entrance acting as an orifice is in order.

During the 1930's and into the 1940's a drop inlet closed conduit spillway was assumed never to flow full if the barrel slope was steeper than the friction slope. For this condition the control sections were taken as the drop inlet crest acting as a weir or the barrel entrance acting as an orifice--whichever gave the least flow being the control.

The tests reported here show that the barrel becomes sealed off intermittently soon after the water level submerges the barrel entrance. The resulting slugs suck air through the barrel entrance. It appears that the barrel entrance acting as an orifice exercises control over the discharge only momentarily between the time one slug leaves the barrel and the succeeding slug forms. The turbulence caused by the weir nappes plunging into the drop inlet undoubtedly contributes to the sealing off of the barrel and the elimination of the orifice as a control section for this drop inlet closed conduit spillway.

## Entrance Loss Coefficient

Entrance loss coefficients $K_e$ for use in Eq. I-5 are given in Table IV-1. The tabulated values represent the average of from 8 to 16 determinations. They are, therefore, probably more reliable than the values of $K_e$ listed in Tables II-1 and III-1 where the average was obtained from only 2 to 9 observations on the vitrified clay tile pipe. Also more attention was given to insuring reasonably constant headpool elevations during these later series. Even so, the headpool fluctuated somewhat during the observations in spite of all efforts to insure constant pool levels. The headpool fluctuation during a typical 10-minute observation period was commonly 0.01 ft.

# PRESSURE COEFFICIENTS

The average pressure coefficients $h_n/h_{vp}$ reduced to a horizontal frictionless pipe are given in Table IV-2. In general, the pressure coefficients along the barrel are reasonably close to the theoretical zero, except close to the drop inlet, and for all practical purposes may be assumed to be zero. (There is a discussion in Part II of possible reasons why $h_n/h_{vp}$ is not zero.) Pressure coefficients in the drop inlet are above zero as one would expect. However, actual pressures almost anywhere within the spillway may be below atmospheric pressure and they should be checked.

Maximum pressures for part-full flow were observed to occur some distance downstream from the barrel entrance. They were quite likely the result of imperfections in the piezometer. No values of $h_p/D$ are given here since it is felt that a better indication of the pressures can be obtained through computation of the depth of flow.

# CONCLUSIONS AND RECOMMENDATIONS

All the drop inlets shown in Fig. IV-1 are entirely satisfactory and geometrically similar structures are recommended for use under field conditions. The spillway proportions may be taken from Fig. IV-1 and Table IV-1; the capacity of the crest acting as a weir may be computed using Reference I-11 up to $Q/D^{5/2} = 4$, while for greater flows Eq. V-2b should be used; the entrance coefficient may be taken from Table IV-1; and the local pressure constants for use in Eq. I-14 may be taken from Table IV-2.

## Part V

## Square Drop Inlet With Square-Edged Crest and Square-Edged Barrel Entrance

### DESCRIPTION OF SPILLWAY

The drop inlets for all of these tests were constructed of Lucite or Plexiglas and were square in plan. Their dimensions are defined in Fig. V-1 and are tabulated in Table V-1. Most of the drop inlets were 1.25D square in plan and 5D deep although these dimensions were varied in Series L-20 through Series L-24. The crest was square edged. An anti-vortex wall located on the downstream crest of the drop inlet was used for all tests except those of Series L-7, where the wall was omitted. A dike from the anti-vortex wall to the downstream end of the test channel was used to prevent circulation in back of the wall except for Series L-7 and L-8.

The barrel left the drop inlet at its base. The barrel invert was tangent to the bottom of the drop inlet and the barrel crown was tangent to the downstream face of the drop inlet. The downstream face of the drop inlet at its base was filled in to make it flush with the barrel entrance as in Fig. IV-3. The barrel was circular Lucite pipe for all tests. The inside diameters were 1-1/8 in., 2-1/4 in. and 4-1/2 in. The 2-1/4-in. pipe was used for most of the tests. Conduit lengths were either 20D, 40D or 100D, the latter length being adopted for the later tests. The conduit outlet discharged freely; it was not submerged.

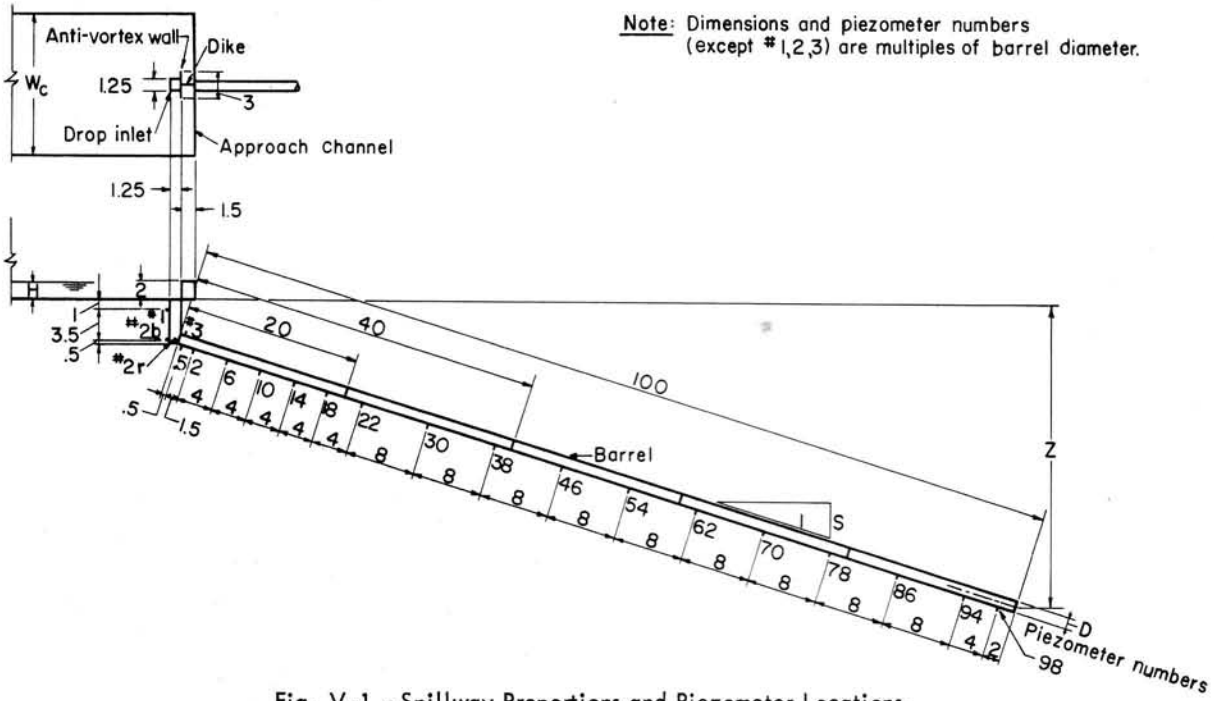


Fig. V-1 - Spillway Proportions and Piezometer Locations, Series L-4B to L-19 Inclusive.

The polished Lucite pipe used for these tests was assumed to be hydraulically smooth. The "smooth" curve for f presented by Rouse [I-44, p. 405, Fig.11] was used in computing friction losses through the spillway. The average friction factor for the 20 series L-14 through L-33 was 1.7 per cent less than the friction factor for smooth pipe, the range of deviation being from +9 per cent to -9 per cent as can be seen by referring to Tables V-1 and VI-1.

Piezometers were installed in the drop inlet and conduit to determine the pressures at the points indicated in Fig. V-1 and Table V-2. Pressures were indicated in open manometer columns and recorded photographically.

Variables included in the test program were the drop inlet area and drop inlet depth to determine how these dimensions affected the performance of the spillway; the conduit size to

## TABLE V-1

## PROPORTIONS OF SPILLWAYS AND DISCHARGE COEFFICIENTS

| Series | D (ft) | $D_r/D$ | $D_{rc}/D$ | $\ell/D$ | S | Z/D | $Z_1/D$ | Inlet Crest | Conduit Entrance | Anti-Vortex Wall | Deviation of f From "Smooth", % | $C_o$ | $N_o$ | $C_s$ | $N_s$ | $K_e$ | $N_e$ |
|---|---|---|---|---|---|---|---|---|---|---|---|---|---|---|---|---|---|
| L-4B | 0.376 | 1.25 sq. | 1.25 sq. | 20 | 0.298 | 10.43 | 5.00 | Square edge | Square edge | Tangent and dike | -- | -- | -- | -- | -- | 0.84 | 16 |
| L-5A | 0.0924 | 1.25 sq. | 1.25 sq. | 20 | 0.293 | 10.66 | 5.00 | Square edge | Square edge | Tangent and dike | -- | -- | -- | -- | -- | 0.74 | 10 |
| L-6 | 0.0924 | 1.25 sq. | 1.25 sq. | 40 | 0.301 | 16.87 | 5.00 | Square edge | Square edge | Tangent and dike | -- | -- | -- | -- | -- | 0.62 | 6 |
| L-7 | 0.1875 | 1.25 sq. | 1.25 sq. | 20 | 0.299 | 10.58 | 5.00 | Square edge | Square edge | None | -- | -- | -- | -- | -- | -- | -- |
| L-8 | 0.1875 | 1.25 sq. | 1.25 sq. | 20 | 0.299 | 10.58 | 5.00 | Square edge | Square edge | Tangent | -- | -- | -- | -- | -- | 1.24 | 6 |
| L-9 | 0.1875 | 1.25 sq. | 1.25 sq. | 20 | 0.296 | 10.35 | 5.00 | Square edge | Square edge | Tangent and dike | -- | -- | -- | -- | -- | 0.77 | 17 |
| L-10 | 0.1875 | 1.25 sq. | 1.25 sq. | 20 | 0.025 | 4.99 | 5.00 | Square edge | Square edge | Tangent and dike | -- | -- | -- | -- | -- | 0.94 | 11 |
| L-11 | 0.1875 | 1.25 sq. | 1.25 sq. | 20 | 0.050 | 5.49 | 5.00 | Square edge | Square edge | Tangent and dike | -- | -- | -- | -- | -- | 0.93 | 12 |
| L-12 | 0.1875 | 1.25 sq. | 1.25 sq. | 20 | 0.100 | 6.49 | 5.00 | Square edge | Square edge | Tangent and dike | -- | -- | -- | -- | -- | 0.88 | 8 |
| L-13 | 0.1875 | 1.25 sq. | 1.25 sq. | 20 | 0.204 | 8.49 | 5.00 | Square edge | Square edge | Tangent and dike | -- | -- | -- | -- | -- | 0.79 | 7 |
| L-14 | 0.1875 | 1.25 sq. | 1.25 sq. | 100 | 0.025 | 7.12 | 5.00 | Square edge | Square edge | Tangent and dike | +4.0 | -- | -- | -- | -- | 1.09 | 22 |
| L-15 | 0.1875 | 1.25 sq. | 1.25 sq. | 100 | 0.049 | 9.44 | 5.00 | Square edge | Square edge | Tangent and dike | +0.4 | -- | -- | -- | -- | 0.96 | 19 |
| L-16 | 0.1875 | 1.25 sq. | 1.25 sq. | 100 | 0.102 | 14.65 | 5.00 | Square edge | Square edge | Tangent and dike | +0.0 | -- | -- | -- | -- | 0.80 | 6 |
| L-17 | 0.1875 | 1.25 sq. | 1.25 sq. | 100 | 0.200 | 24.70 | 5.00 | Square edge | Square edge | Tangent and dike | -5.1 | -- | -- | -- | -- | 0.80 | 13 |
| L-18 | 0.1875 | 1.25 sq. | 1.25 sq. | 100 | 0.199 | 24.39 | 5.00 | Square edge | Square edge | Tangent and dike | +0.7 | -- | -- | -- | -- | 0.87 | 19 |
| L-19 | 0.1875 | 1.25 sq. | 1.25 sq. | 100 | 0.303 | 34.77 | 5.00 | Square edge | Square edge | Tangent and dike | -1.1 | -- | -- | -- | -- | 0.84 | 19 |
| L-20 | 0.1875 | 1.25 sq. | 1.25 sq. | 100 | 0.299 | 31.44 | 2.00 | Square edge | Square edge | Tangent and dike | +9.3 | 4.44 | 34 | -- | -- | 0.92 | 19 |
| L-21 | 0.1875 | 1.25 sq. | 1.25 sq. | 100 | 0.298 | 33.30 | 4.00 | Square edge | Square edge | Tangent and dike | +4.8 | 3.97 | 4 | -- | -- | 0.87 | 10 |
| L-22 | 0.1875 | 2.00 sq. | 2.00 sq. | 100 | 0.302 | 33.25 | 3.50 | Square edge | Square edge | Tangent and dike | +1.8 | 4.70 | 22 | -- | -- | 0.61 | 8 |
| L-23 | 0.1875 | 1.50 sq. | 1.50 sq. | 100 | 0.302 | 33.23 | 3.50 | Square edge | Square edge | Tangent and dike | +2.0 | 4.83 | 5 | -- | -- | 0.74 | 11 |
| L-24 | 0.1875 | 1.00 sq. | 1.00 sq. | 100 | 0.302 | 33.22 | 3.50 | Square edge | Square edge | Tangent and dike | -0.4 | 4.09 | 7 | -- | -- | 1.31 | 10 |

determine the scale effect, if any; and the barrel slope to determine its effect on the performance and entrance loss coefficient. Conduit length was not a fundamental variable after the method of analyzing the data had been established; the length was determined by space considerations and by the length necessary to establish uniform flow downstream from the drop inlet and provide sufficient length for the determination of the friction factor.

## TABLE V-2

## PIEZOMETER LOCATIONS AND LOCAL PRESSURE DEVIATION FROM HYDRAULIC GRADE LINE, SERIES L-4B to L-24

| Piezometer Location | Series | L-4B | L-5A | L-6 | L-8 | L-9 | L-10 | L-11 | L-12 | L-13 | L-14 | L-15 | L-16 | L-17 | L-18 | L-19 | L-20 | L-21 | L-22 | L-23 | L-24 |
|---|---|---|---|---|---|---|---|---|---|---|---|---|---|---|---|---|---|---|---|---|---|
| | Station | | | | | | | | | | $h_a/h_{vp}$ | | | | | | | | | | |
| Upstream* Right* | No. 1[a] | +1.22 | +1.23 | +1.15 | +1.52 | +1.23 | +1.36 | +1.36 | +1.32 | +1.24 | +1.58 | +1.37 | +1.21 | +1.20 | +1.30 | +1.27 | -- | +1.29 | +1.51 | +1.43 | +1.04 |
| Upstream* | No. 2r[b] | +1.44 | +1.41 | +1.30 | +1.73 | +1.47 | +1.57 | +1.60 | +1.55 | +1.45 | +1.71 | +1.61 | -- | +1.44 | +1.47 | +1.44 | +1.39 | +1.50 | +1.54 | +1.55 | +1.42 |
| | No. 2b[b] | +1.44 | +1.43 | +1.32 | +1.82 | +1.49 | +1.58 | +1.60 | +1.55 | +1.46 | +1.70 | +1.64 | +1.44 | +1.46 | +1.52 | +1.50 | +1.42 | +1.48 | +1.53 | +1.52 | +1.39 |
| Crown | No. 3[c] | -1.29 | -0.95 | -0.98 | -1.30 | -1.29 | -1.46 | -1.38 | -1.38 | -1.17 | -1.34 | -1.15 | -1.21 | -1.21 | -1.01 | -1.06 | -1.30 | -0.95 | -0.78 | -0.88 | -1.44 |
| Invert | D/2 | -0.30 | -0.04 | -0.16 | -0.17 | -0.31 | -0.27 | -0.22 | -0.26 | -0.23 | -0.28 | -0.22 | -0.13 | -0.17 | -0.18 | -0.21 | -0.27 | -0.05 | -0.26 | -0.10 | +0.09 |
| Invert | 2D | -0.20 | +0.04 | -0.05 | -0.06 | -0.16 | -0.17 | -0.14 | -0.15 | -0.12 | -0.14 | -0.16 | -0.07 | -0.28 | -0.05 | -0.06 | -0.12 | -0.01 | -0.02 | 0.00 | -0.05 |
| Invert | 6D | -0.00 | +0.07 | +0.02 | +0.01 | -0.03 | -0.01 | +0.00 | +0.01 | +0.02 | +0.07 | +0.05 | +0.04 | +0.07 | -0.02 | +0.00 | +0.01 | +0.02 | -0.01 | +0.01 | +0.02 |
| Invert | 10D | +0.00 | +0.05 | -0.02 | +0.03 | -0.02 | -0.01 | -0.00 | +0.01 | -0.01 | +0.07 | +0.05 | +0.04 | +0.02 | +0.05 | +0.05 | +0.04 | +0.05 | -0.04 | +0.04 | +0.05 |
| Invert | 14D | 0.00 | +0.00 | -0.03 | -0.01 | -0.03 | -0.02 | -0.02 | -0.01 | -0.00 | +0.06 | +0.05 | +0.04 | +0.02 | +0.04 | +0.04 | | | | | |
| Invert | 18D | -0.01 | +0.01 | -0.03 | -0.03 | -0.03 | -0.01 | -0.02 | -0.00 | -0.02 | +0.04 | +0.03 | +0.02 | +0.00 | +0.00 | +0.02 | | | | | |
| Invert | 22D | | | -0.04 | | | | | | | +0.09 | +0.07 | +0.06 | +0.05 | +0.11 | +0.08 | | | | | |
| Invert | 30D | | | -0.04 | | | | | | | +0.04 | +0.03 | +0.02 | -0.00 | +0.03 | +0.03 | +0.03 | +0.02 | +0.02 | +0.03 | +0.02 |
| Invert | 38D | | | -0.03 | | | | | | | +0.02 | +0.01 | +0.01 | -0.00 | +0.01 | +0.01 | | | | | |
| Invert | 46D | | | | | | | | | | +0.04 | +0.00 | +0.00 | -0.02 | +0.03 | +0.02 | | | | | |
| Invert | 54D | | | | | | | | | | +0.01 | -0.01 | -0.01 | -0.02 | +0.00 | -0.00 | -0.01 | 0.00 | 0.00 | 0.00 | -0.01 |
| Invert | 62D | | | | | | | | | | +0.05 | +0.01 | +0.01 | +0.01 | +0.03 | +0.02 | | | | | |
| Invert | 70D | | | | | | | | | | -0.03 | -0.01 | -0.02 | -0.03 | -0.01 | -0.03 | -0.04 | -0.01 | -0.01 | -0.01 | -0.02 |
| Invert | 78D | | | | | | | | | | -0.00 | -0.02 | -0.02 | -0.02 | -0.01 | -0.01 | | | | | |
| Invert | 86D | | | | | | | | | | -0.05 | -0.03 | -0.04 | -0.03 | -0.02 | -0.03 | | | | | |
| Invert | 94D | | | | | | | | | | -0.00 | -0.03 | -0.03 | -0.02 | -0.02 | -0.03 | | | | | |
| Invert | 98D | | | | | | | | | | -0.03 | -0.02 | -0.02 | -0.02 | -0.02 | -0.02 | -0.07 | -0.03 | -0.02 | -0.02 | -0.02 |
| Invert | 99D | | | | | | | | | | -0.09 | -0.06 | -0.02 | -0.03 | | | | | | | |
| Invert | 99-3/4D | | | | | | | | | | -0.10 | -0.07 | | | | | | | | | |
| Invert | 99.9D | | | | | | | | | | | | -0.08 | -0.05 | | | | | | | |

*Side of drop inlet. [a]At -4D. [b]At -D/2. [c]At D/2.

TABLE V-3

CHARACTERISTICS OF TEST SETUPS

| Characteristic | Setup for Series | | | |
|---|---|---|---|---|
| | L-4B | L-5A to L-13 inc. | L-14 to L-17 inc. | L-18 and L-19 |
| Water supply | Supply channel | Supply channel | Supply channel | Recirculated |
| Head available | 11.0' | 11.8' | 8.5' | 11.9' |
| Flow measurements | | | | |
| Instrument | 5" orifice in 6" line | 1.0' HS flume | 1.0' HS flume | 1.0" orifice in 2" line and 2.1" orifice in 4" line |
| Head measurement | Water manometer | Point gage | Point gage | Water manometer and mercury manometer |
| Approach channel | | | | |
| Width, length, depth | 5.0' x 5.5' x 1.1' | 2.0' x 6.3' x 1' | 2.0' x 6.3' x 1.0' | 3.0' x 15.0' x 2.0' |
| Photograph | Fig. V-2a | Fig. V-3a | Fig. V-3a | Fig. V-4a |
| Model installation | | | | |
| Photograph | Fig. V-2b | Fig. V-3b | | Fig. V-4b |

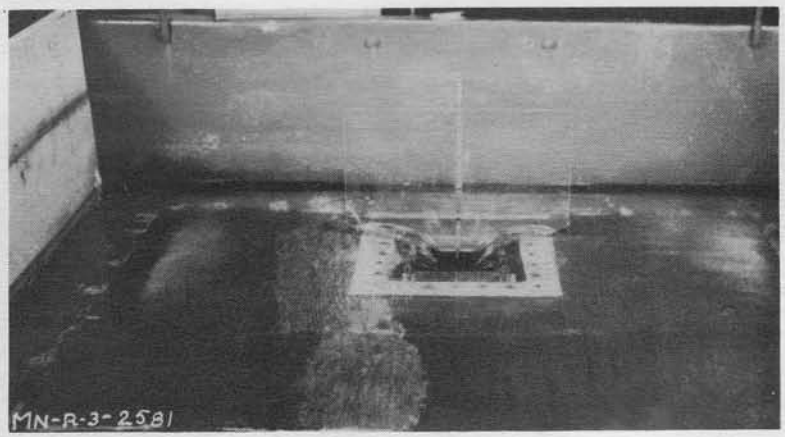


(a) Approach to drop inlet

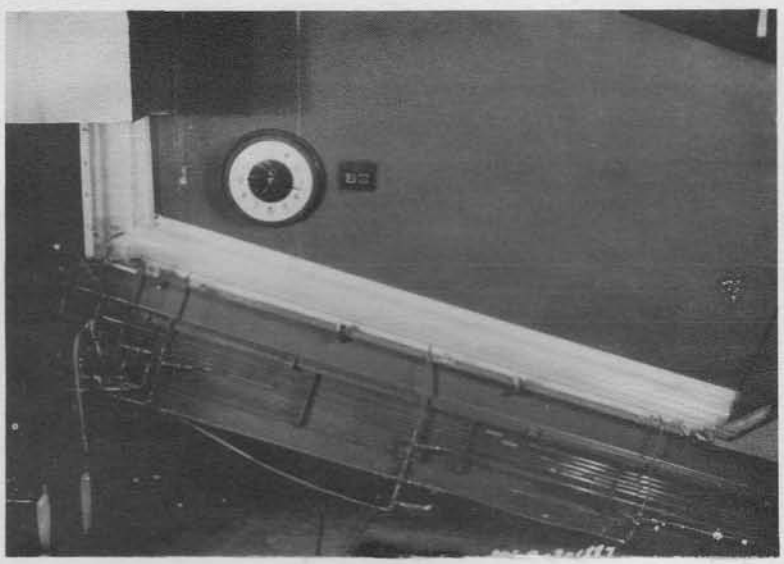

(b) Model, showing connection to manometers and pressur recorders

Fig. V-2 - Test Setup for Series L-4B.

## APPARATUS AND PROCEDURE

Four different test setups were used to make these tests. The important features of the setups and the series tested on each are given in Table V-3.

The water supply for the first three setups was obtained from the Mississippi River through the main Laboratory supply channel. The fourth setup was assembled to eliminate operational difficulties which were traced to this source of supply. The principal difficulty experienced was that the transparent plastic used in the models has a fairly high coefficient of thermal expansion. When the model was installed at room temperature and operated during the winter months using water at temperatures close to freezing, the pipes shrank, opening joints and permitting leakage of air into and water out of the model. These difficulties were overcome in the fourth setup by recirculating water at room temperature and by using a constant level tank to insure steady flow.

The devices for measuring flow rates were calibrated to insure their accuracy.

A special effort was made in all of the installations to insure that the velocity distribution in the approach channel was symmetrical. Only partial success was obtained as is evidenced by the discussion in the section entitled "Circulation Around Headwall."

All of the models were installed in much the same manner. This is apparent from Figs. V-2, V-3 and V-4. Each pipe was attached to a base or girder which could be adjusted as to longitudinal position, elevation, and slope. The waste receiver was arranged so that flow from the pipe would be unimpeded (free).

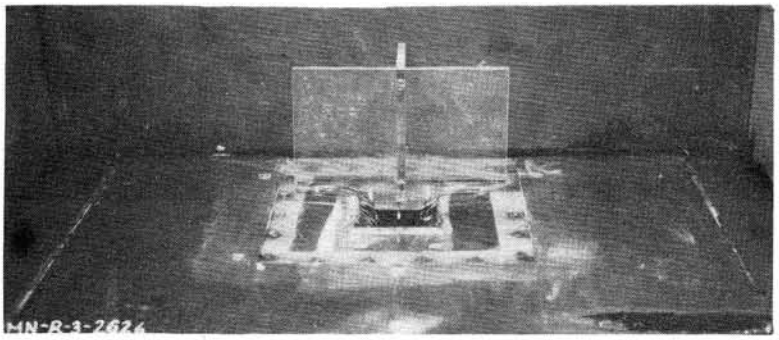


(a) Approach to drop inlet

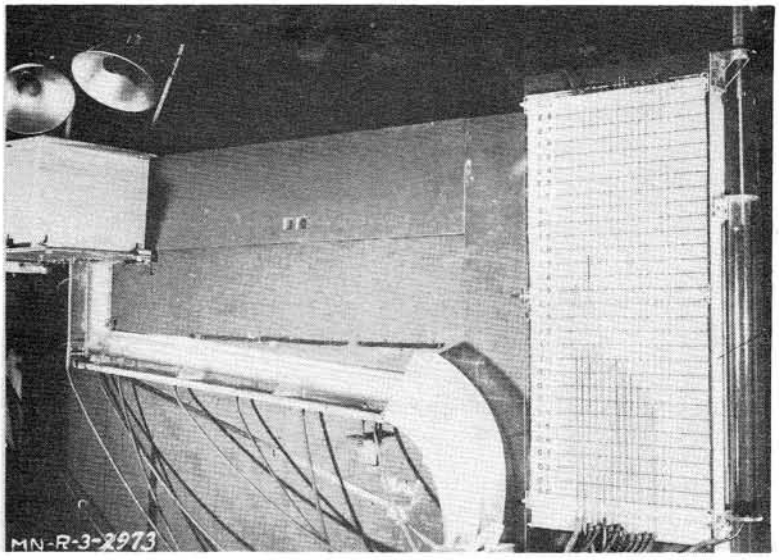


(b) Model and manometer board for Series L-13

Fig. V-3 - Test Setup for Series L-5A to L-13 Inclusive.

Heads on the drop inlet crest were measured by a point gage located over a stilling well which was connected to the headpool. For two setups a recorder was used to determine when the level in the headpool became constant; a Stevens type M water level recorder was used on the first setup and an Esterline-Angus bellows-type pressure recorder on the fourth setup.

The Stevens type M water level recorder was substituted for the Esterline-Angus recorder for tests subsequent to Series L-19 so that its greater accuracy could be utilized to make storage corrections in the headpool.

Pressures from the piezometers located along the conduits were carried to manometer boards where the manometers were grouped for convenience to permit photographic recording of the instantaneous pressures upon a single negative. The manometers were glass tubes about 3 mm in inside diameter. The tubes were so small that the readings were undoubtedly

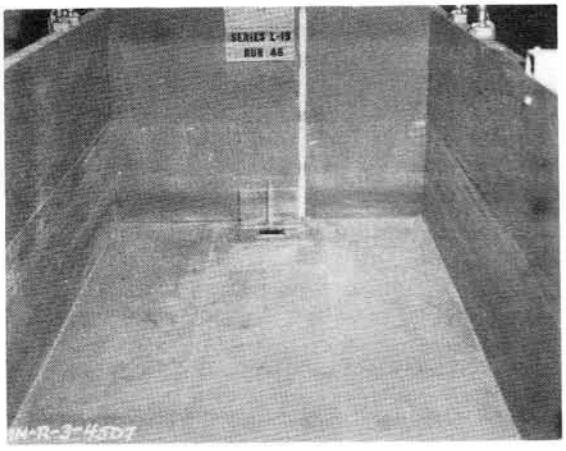

(a) Approach to drop inlet

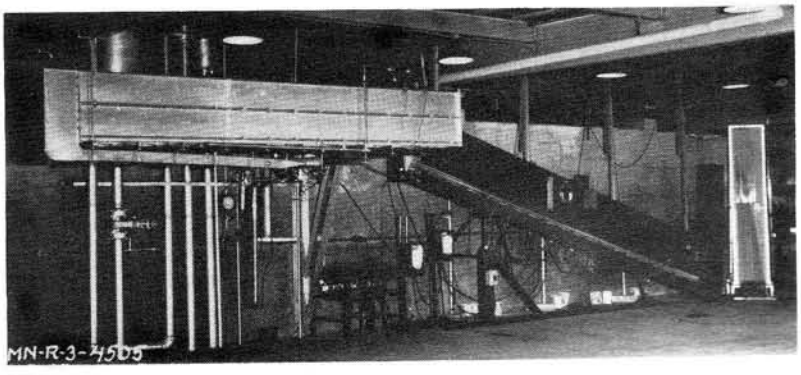

(b) General view of test setup showing approach channel, model and manometer board for Series L-19.

Fig. V-4 - Test Setup for Series L-18 and L-19.

influenced by capillary effects. However, the more rapid response to fluctuating pressures through the use of small manometer tubes is believed to more than compensate for any effects of capillarity. Since the pressures fluctuated rapidly under some flow conditions, inertia must also affect some of the readings.

All readings were obtained photographically in order to simultaneously record the pressure in each of the tubes. This method was necessary to obtain the readings when pressures fluctuated and was used for the other runs to insure a permanent record. Pressures were read from the negatives or prints to 0.01 ft with the aid of a magnifying glass. This procedure was most satisfactory. Esterline-Angus pressure recorders were also used with some setups to provide a record of the fluctuating pressures at some of the piezometer locations.

Photographs of the inlet and pipe were obtained for most runs to provide a record of flow conditions at these locations.

## DESCRIPTION OF FLOW

The first description of flow applies only to Series L-4B to L-19 inclusive, Series L-7 excepted. For these series the drop inlet was 5D deep and only the desirable weir and pipe controls governed the head-discharge relationship.

The nappes could be made to cling to the sides of the drop inlet at values of H/D up to 0.85, although runs were made throughout this range of head with the nappes free. When H/D was greater than about 0.85, the nappes clung to the sides of the drop inlet in spite of all efforts to free them. Views of the clinging nappes are shown in Fig. V-5 and views of the free nappes in Fig. V-6. It will be noted in Fig. V-6b that the free nappes intersect in the drop inlet. This condition is conducive to entrainment of air, and some air was carried through the pipe under these conditions. Under the condition of Fig. V-5b, the air movement was not sufficient to cause its presence to be noted.

No noticeable fluctuation in head over the crest was observed when H/D was less than 0.55. However, considerable fluctuation in head was observed when the nappes were free and H/D was between approximately 0.55 and 0.85. When the nappes clung to the side of the drop inlet, no head fluctuation took place. A view of the clinging nappes is shown in Fig. V-7. Close observation of Fig. V-7b shows that there is an air pocket in the drop inlet. The air pocket expands as the flow accelerates down the drop inlet. The upper end of the barrel is also full of a water-air mixture. Views of the free nappes are shown in Figs. V-8 and V-9. In Fig. V-8b slugs are forming and breaking in the upper end of the barrel. These slugs create suction that draws air noisily in through the drop inlet and the partial vacuum in effect increases the head over the weir and draws down the headpool. These slugs form only intermittently and between times the suction and capacity of the inlet are reduced. This causes the headpool to rise. Fig. V-9a shows that under these conditions the space above the nappes is full of water, while it can be seen in Fig. V-9b that no slugs are forming in the barrel and no suction is being applied to the drop inlet. The air bubbles shown in the drop inlet in Fig. V-9b represent the air shown in Fig. V-8b which is now being mixed with the water and carried out into the barrel.

The head was steady and it was not possible to free the nappes when H/D was greater than 0.85. Considerable amounts of air were sucked noisily into the structure, the air flow decreasing as the water flow increased. The barrel and drop inlet were continuously full of a water-air mixture. Fig. X-10 shows the flow conditions. It should be emphasized that even though the barrel is full of a mixture of water and air, nappes are in evidence, and the discharge varies as the 3/2 power of the head over the drop inlet crest.

As the water flow increases, the air flow eventually stops and the conduit becomes completely full of water. The flow through the structure is then computed as if it were a pipe.

For Series L-20 to L-24 inclusive the drop inlet was less than 5D deep with the result that the orifice at the base of the drop inlet controlled the head-discharge relationship in addition to weir and pipe controls. Orifice flow is illustrated in Fig. V-11. There it can be seen that the drop inlet is completely full, there is no flow of air, and the conduit is partly full.

## DISCHARGE COEFFICIENTS

### Weir Coefficient

The weir head-discharge curve for the drop inlets discussed here is in two parts (see Fig. II-12 for a typical plot of the data). The reasons for the two curves are explained in Part IV of this report. Equations for the two parts of the weir rating curve were determined by the aid of the least squares method using data obtained during Series L-4B to L-21 inclusive. These equations are

$$\frac{Q}{D^{5/2}} = 0.42\sqrt{2g}\,\frac{L}{D}\left[\frac{H}{D} - 0.004\right]^{3/2} \qquad (V\text{-}1)$$

up to $Q/D^{5/2} = 4$. At higher discharges the equation becomes

$$\frac{Q}{D^{5/2}} = 0.51\sqrt{2g}\,\frac{L}{D}\left[\frac{H}{D} - 0.060\right]^{3/2} \qquad (V\text{-}2a)$$

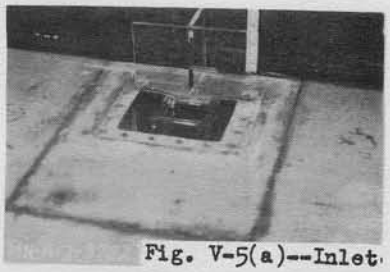

Fig. V-5(a)--Inlet

Fig. V-6(a)--Inlet

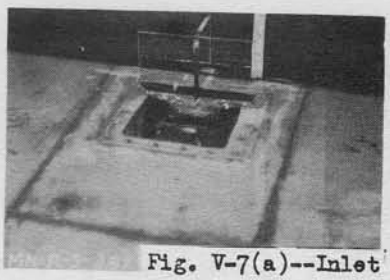

Fig. V-7(a)--Inlet

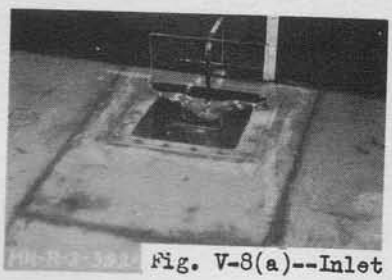

Fig. V-8(a)--Inlet

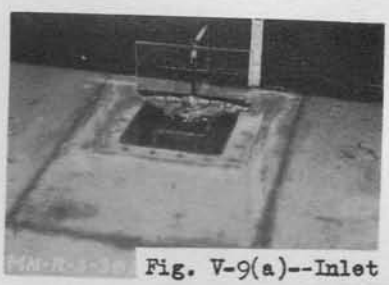

Fig. V-9(a)--Inlet

Fig. V-10(a)--Inlet

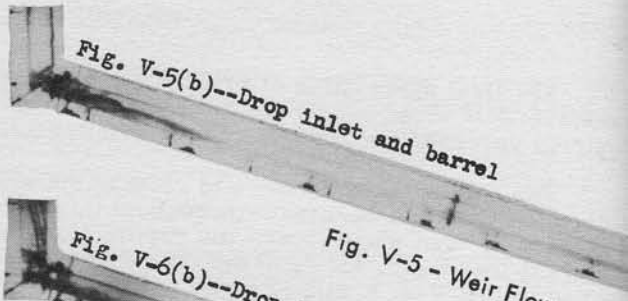

Fig. V-5(b)--Drop inlet and barrel

Fig. V-5 - Weir Flow at Cre

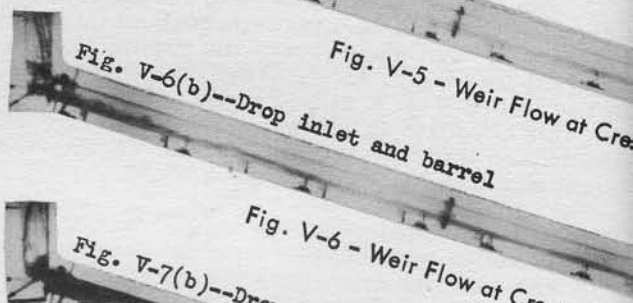

Fig. V-6(b)--Drop inlet and barrel

Fig. V-6 - Weir Flow at Crest of Dro

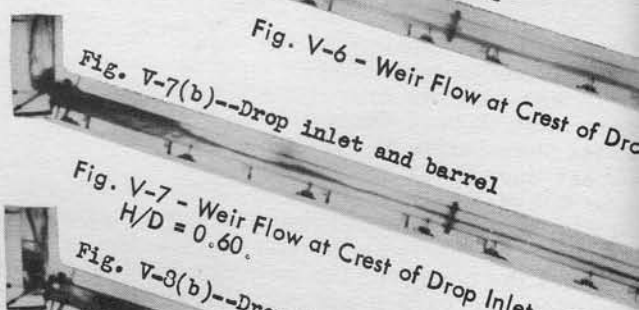

Fig. V-7(b)--Drop inlet and barrel

Fig. V-7 - Weir Flow at Crest of Drop Inlet. Clingin
H/D = 0.60.

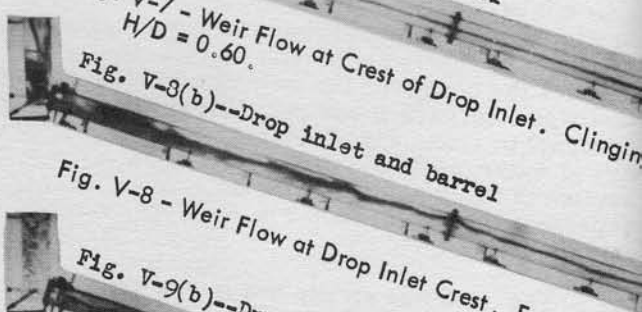

Fig. V-8(b)--Drop inlet and barrel

Fig. V-8 - Weir Flow at Drop Inlet Crest. Free Nappes

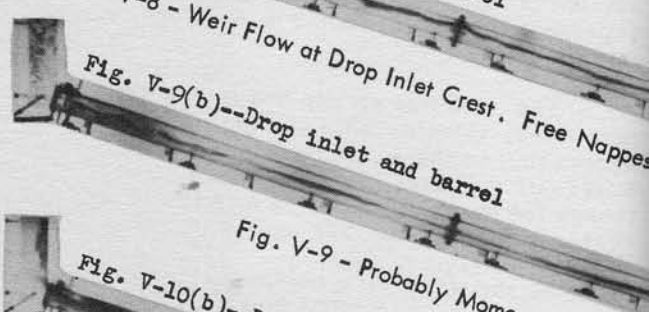

Fig. V-9(b)--Drop inlet and barrel

Fig. V-9 - Probably Momentary Orifice

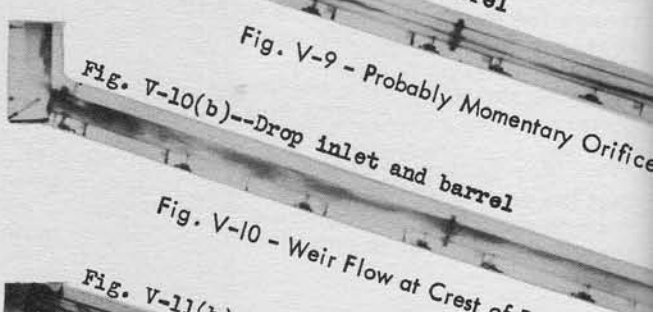

Fig. V-10(b)--Drop inlet and barrel

Fig. V-10 - Weir Flow at Crest of Drop Inlet.

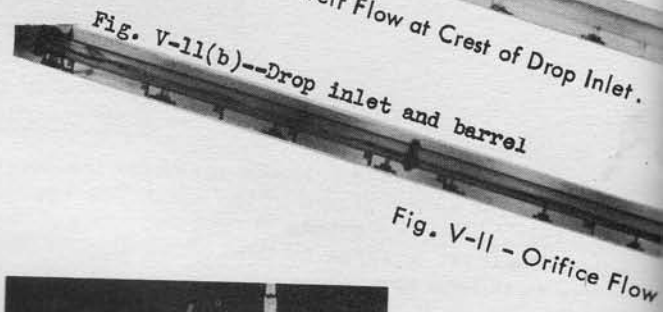

Fig. V-11(b)--Drop inlet and barrel

Fig. V-11 - Orifice Flow

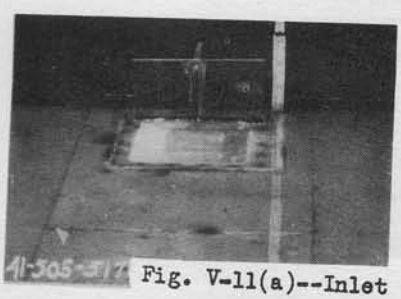

Fig. V-11(a)--Inlet

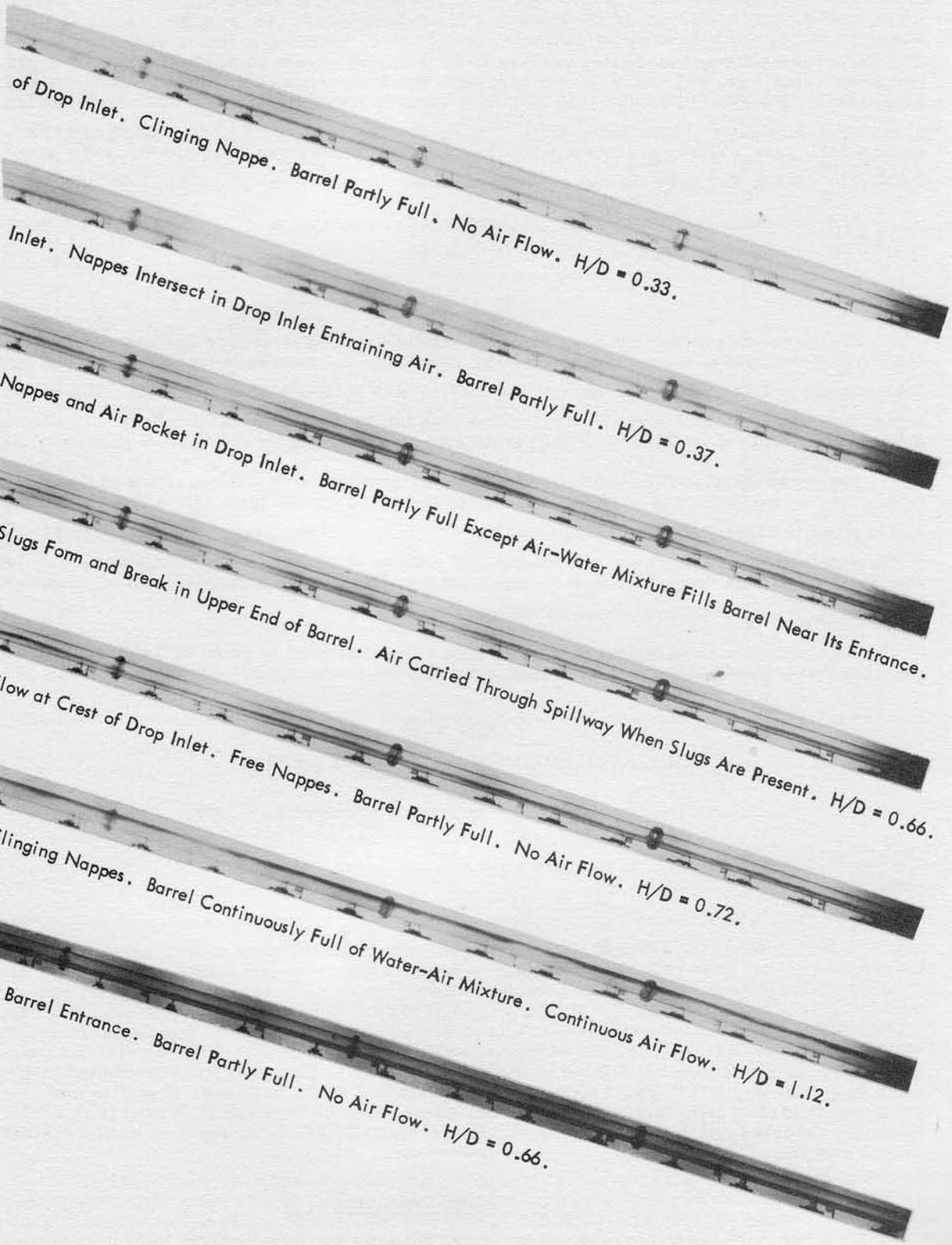

of Drop Inlet. Clinging Nappe. Barrel Partly Full. No Air Flow. H/D = 0.33.

Inlet. Nappes Intersect in Drop Inlet Entraining Air. Barrel Partly Full. H/D = 0.37.

Nappes and Air Pocket in Drop Inlet. Barrel Partly Full Except Air-Water Mixture Fills Barrel Near Its Entrance.

Slugs Form and Break in Upper End of Barrel. Air Carried Through Spillway When Slugs Are Present. H/D = 0.66.

Flow at Crest of Drop Inlet. Free Nappes. Barrel Partly Full. No Air Flow. H/D = 0.72.

Clinging Nappes. Barrel Continuously Full of Water-Air Mixture. Continuous Air Flow. H/D = 1.12.

at Barrel Entrance. Barrel Partly Full. No Air Flow. H/D = 0.66.

or

$$\frac{Q}{D^{5/2}} = 4.1 \frac{L}{D}\left[\frac{H}{D} - 0.060\right]^{3/2} \qquad \text{(V-2b)}$$

The observed discharges for Series L-4B to L-24 inclusive were compared with the discharges computed using Eqs. V-1 and V-2, and also with the discharges computed using the method explained in "Hydraulic Design of the Box Inlet Drop Spillway" [I-11]. For the lower portion of the head-discharge curve where $Q/D^{5/2} < 4$, the discharge computed according to Reference I-11 gave closer agreement with the observed discharges than did Eq. V-1. When $Q/D^{5/2} > 4$, Eq. V-2 gave the closest agreement.

Best results will be obtained if the discharges are computed after Reference I-11 when $Q/D^{5/2} < 4$, and from Eq. V-2 when $Q/D^{5/2} > 4$.

## Orifice Coefficient

The barrel entrance at the base of the drop inlet acted as an orifice to control the head-discharge relationship when the height of the drop inlet $Z_1$ was less than 5D, that is for Series L-20 to L-24 inclusive. No orifice control was obtained when $Z_1 = 5D$, that is for Series L-4B to L-19 inclusive. Therefore, the drop inlet should be at least 5D deep to eliminate the possibility of the square-edged barrel entrance affecting the elevation of the headpool.

The presence of orifice control permits the determination of the magnitude of the coefficient $C_o$ in Eq. I-7. The coefficient has been computed for Series L-20 to L-24 inclusive and is given in Table V-1. The listed values of $C_o$ represent the average of from 5 to 34 individual determinations. There are insufficient data to draw any general conclusions as to how $C_o$ varies with drop inlet size or depth, but the data do give a general idea of the magnitude of $C_o$ for the square-edged conduit entrance.

The maximum head observed when orifice control existed is given in Table V-4. It is possible that higher heads could have been obtained; the listed figures are those actually ob-

TABLE V-4

INDICATED MINIMUM DROP INLET DEPTH

| Series | h/D* | Actual $Z_1/D$ | Indicated Minimum $Z_1/D$ |
|---|---|---|---|
| L-20 | 3.12 | 2.00 | 5.12 |
| L-21 | 0.98 | 4.00 | 4.98 |
| L-22 | 2.15 | 3.50 | 5.65 |
| L-23 | 1.85 | 3.50 | 5.35 |
| L-24 | 2.20 | 3.50 | 5.70 |

*Maximum value above crest at which orifice control was observed.

served. These heads have been added to the actual drop inlet depth to give an indicated minimum drop inlet depth that would eliminate the possibility of the existence of orifice control. Presumably these depths could be reduced by some depth of flow over the drop inlet crest. However, the data do indicate that the drop inlet depth should be 5D or more to insure against orifice control.

## Entrance Loss Coefficient

Entrance loss coefficients $K_e$ for use in Eq. I-5 are given in Table V-1. The values listed represent the average of from 6 to 22 determinations.

Fig. V-12 shows the effect of barrel slope on the entrance loss coefficient. It is well known that the loss coefficient at a bend increases with the angle of the bend. The angle through which the flow turns at the base of the drop inlet increases as the barrel slope decreases. Therefore, the highest loss coefficients are to be expected at the lowest slopes--and this is what is shown in Fig. V-12. Although there is some scatter to the data, the maximum error in the discharge should not exceed 15 per cent if the curve shown is used for design purposes.

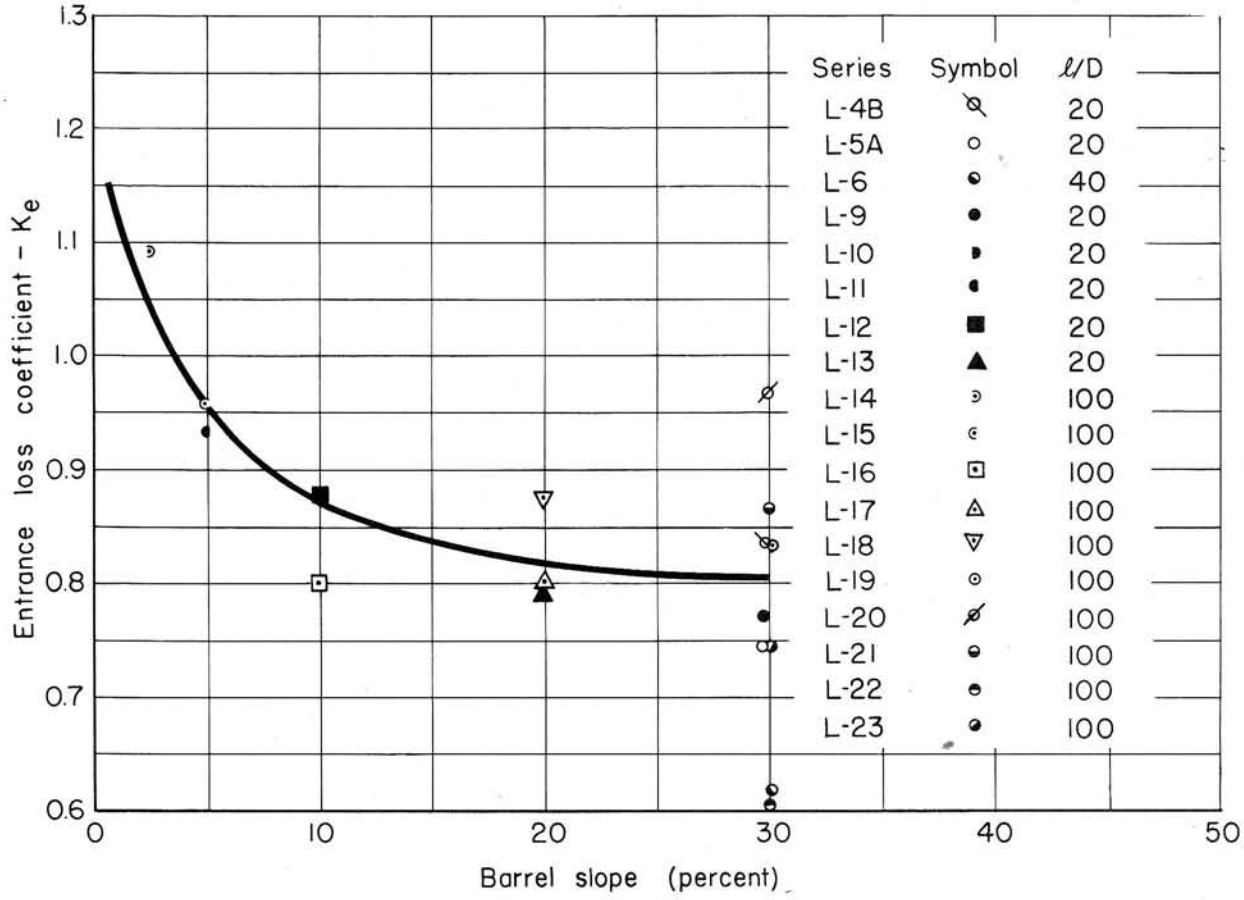


Fig. V-12 - Effect of Barrel Slope on Entrance Loss Coefficient.

## PRESSURE COEFFICIENTS

The average pressure coefficients $h_n/h_{vp}$ reduced to a horizontal frictionless pipe are given in Table V-2. It will be noticed that the pressure coefficients along the barrel are close to the theoretical zero except in the vicinity of the drop inlet. The very low pressures just inside the barrel entrance should be noted. Cavitation at this location is a definite possibility. If pressures below the vapor pressure are likely the design should be changed to secure higher pressures and eliminate the possibility of damage from cavitation. Pressure coefficients in the drop inlet are above zero, but actual pressures below atmospheric can be readily obtained and they should be determined.

## CIRCULATION AROUND ANTI-VORTEX WALL

Early in the test program, considerable difficulty was experienced in obtaining similar head-discharge curves for supposedly similar spillways that differed only in size. This was finally traced to the effect of different amounts of circulation around the headwall. Excellent agreement was obtained after all circulation around the headwall was prevented by means of a dike between the headwall and the downstream end of the test channel.

The effects of circulation are illustrated by Series L-7, L-8 and L-9, the results of these tests being plotted in Fig. V-13. As can be seen in Fig. V-14, there was no anti-vortex wall at all for Series L-7. An anti-vortex wall but no dike was used for Series L-8. This is shown in Fig. V-15. An anti-vortex wall plus a dike, as shown in Fig. V-16, was used for Series L-9. It can be seen in Fig. V-13 that the flow is increased by the use of an anti-vortex

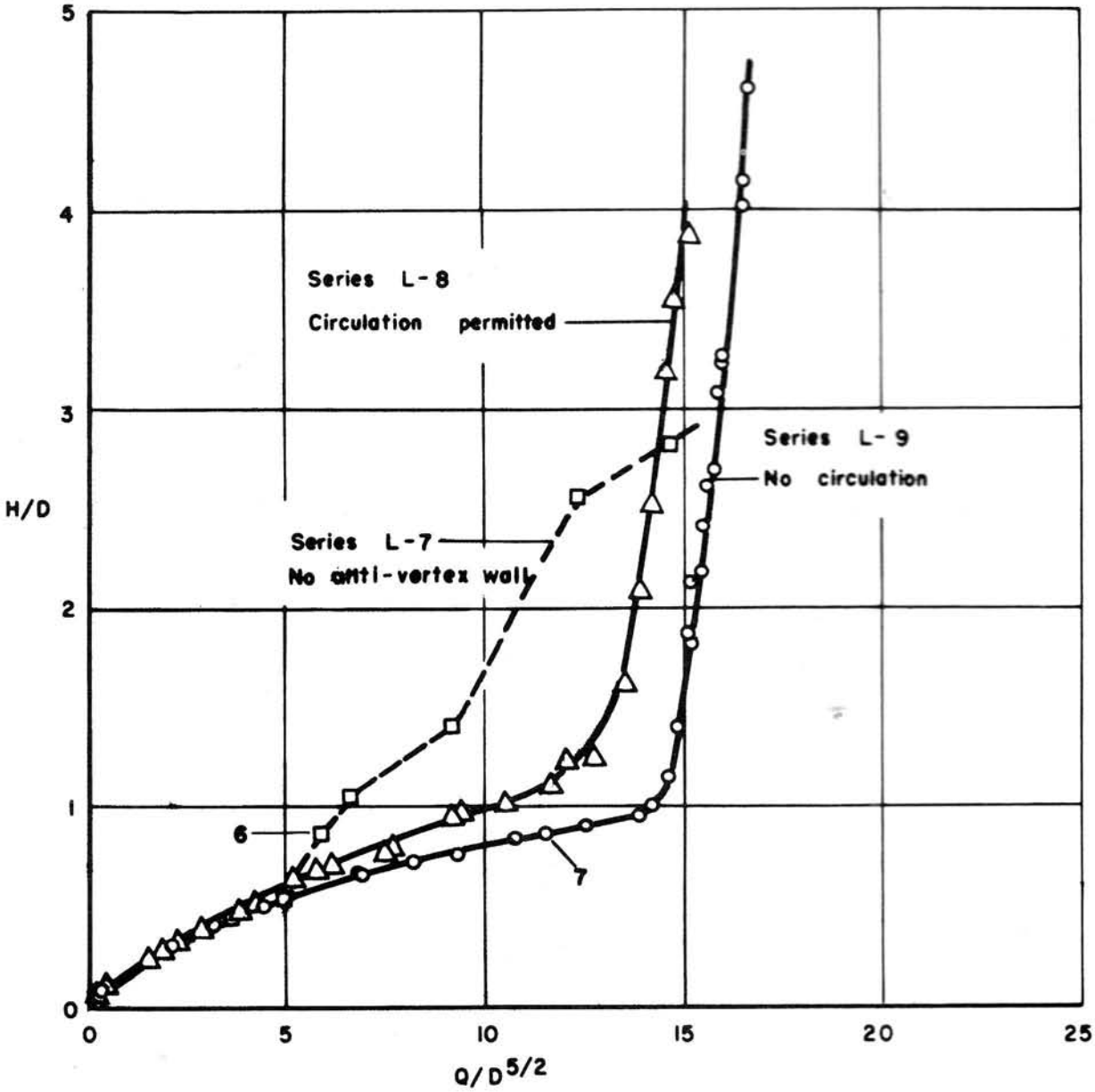


Fig. V-13 - Head-Discharge Curves for Series L-7, L-8, L-9.

wall even though this cuts off access to one-fourth of the drop inlet crest. The reduction of the circulation in the case of Series L-8 and its complete elimination in the case of Series L-9 is the reason. Compare Figs. V-14, V-15 and V-16.

Some circulation was observed after the anti-vortex wall was submerged, but if the wall is sufficiently high the capacity of the spillway is not affected. The anti-vortex wall dimensions used during these tests are given in Fig. V-1.

This group of tests shows that anti-vortex walls are needed and should be used on all drop inlets.

Fig. V-14 - No Headwall Was Used for Series L-7. Confetti shows circulation. $H/D = 0.85$. $Q/D^{5/2} = 5.8$.


Fig. V-15 - A Headwall But No Dike Was Used for Series L-8. Depression at left end of headwall is caused by circulation in back of headwall. $H/D = 1.00$. $Q/D^{5/2} = 10.5$.

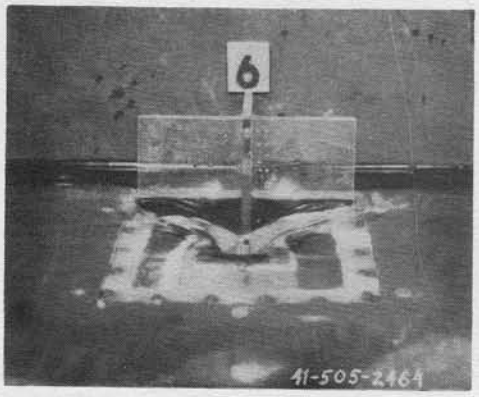


Fig. V-16 - Use of Dike Plus a Headwall for Series L-9 Eliminates Circulation. $H/D = 0.82$. $Q/D^{5/2} = 10.6$.

## CONCLUSIONS AND RECOMMENDATIONS

Drop inlets having the form shown in Fig. V-1 are satisfactory and geometrically similar structures are recommended for field installation provided:

1. The drop inlet depth is 5D or more.
2. An anti-vortex wall and dike are used to prevent circulation.

Tests on various sized spillways in the laboratory have verified the laws of similitude and the methods of analysis given in Part I of this report series.

The capacity of the drop inlet crest acting as a weir may be determined for values of $Q/D^{5/2} < 4$ through the use of Reference I-11. Eq. V-2 should be used when $Q/D^{5/2} > 4$.

The entrance loss coefficients may be interpolated from Table V-1 and Fig. V-12.

The local pressure constants for use in Eq. I-14 may be taken from Table V-2.

## Part VI

## Circular Drop Inlet With Square-Edged and Rounded Crests and Concrete-Pipe-Groove Barrel Entrance

### DESCRIPTION OF SPILLWAY

The proportions of the drop inlet and the spillway are given in Fig. VI-1 and Table VI-1. These circular drop inlets had two different diameters but only one depth. The drop inlet crests were either square-edged or rounded to the quadrant of a circle.

A number of different types of headwall or vortex inhibitor were tried and, in this respect, these tests are the most comprehensive conducted thus far. The splitter type vortex inhibitor shown in Fig. VI-1b was 2D/9 thick and extended back into the dam fill. It was 0.75D high for Series L-25, L-27 and L-31; and 2D high for Series L-33. The tangent anti-vortex wall shown in Fig. VI-1c was 0.33D thick, 0.75D high, and 3.5D long. The cover anti-vortex

TABLE VI-1

PROPORTIONS OF SPILLWAYS AND DISCHARGE COEFFICIENTS

| Series | D (ft) | $D_r/D$ | $D_{ro}/D$ | $\ell/D$ | S | $Z/D$ | $Z_1/D$ | Inlet Crest | Conduit Entrance | Anti-Vortex Wall | Deviation of f From "Smooth", % | $C_o$ | $N_o$ | $C_s$ | $N_s$ | $K_e$ | $N_e$ |
|---|---|---|---|---|---|---|---|---|---|---|---|---|---|---|---|---|---|
| L-25 | 0.1875 | 1.78 rd. | 1.78 rd. | 100 | 0.200 | 21.47 | 1.96 | Square edge | Concrete pipe groove | Splitter | -3.2 | -- | -- | -- | -- | 0.66 | 9 |
| L-26 | 0.1875 | 1.78 rd. | 2.28 rd. | 100 | 0.200 | 21.48 | 1.96 | 0.25D rad. | Concrete pipe groove | None | -2.4 | -- | -- | -- | -- | 0.42 | 10 |
| L-27 | 0.1875 | 1.78 rd. | 2.28 rd. | 100 | 0.200 | 21.48 | 1.96 | 0.25D rad. | Concrete pipe groove | Splitter | -5.7 | -- | -- | -- | -- | 0.42 | 12 |
| L-28 | 0.1875 | 1.78 rd. | 2.28 rd. | 100 | 0.200 | 21.48 | 1.96 | 0.25D rad. | Concrete pipe groove | Tangent | -5.6 | -- | -- | -- | -- | 0.50 | 12 |
| L-29 | 0.1875 | 1.78 rd. | 2.28 rd. | 100 | 0.200 | 21.48 | 1.96 | 0.25D rad. | Concrete pipe groove | Cover | -6.4 | -- | -- | -- | -- | 0.46 | 11 |
| L-29A | 0.1875 | 1.78 rd. | 2.28 rd. | 100 | 0.200 | 21.48 | 1.96 | 0.25D rad. | Concrete pipe groove | Cover | -- | -- | -- | -- | -- | 0.53 | 7 |
| L-30 | 0.1875 | 1.25 rd. | 1.25 rd. | 100 | 0.200 | 21.52 | 1.96 | Square edge | Concrete pipe groove | Special | -8.8 | -- | -- | -- | -- | 1.06 | 11 |
| L-31 | 0.1875 | 1.25 rd. | 1.75 rd. | 100 | 0.200 | 21.52 | 1.96 | 0.25D rad. | Concrete pipe groove | Splitter | -5.8 | -- | -- | -- | -- | 0.62 | 12 |
| L-32 | 0.1875 | 1.25 rd. | 1.75 rd. | 100 | 0.200 | 21.52 | 1.96 | 0.25D rad. | Concrete pipe groove | Splitter | -6.0 | -- | -- | -- | -- | 0.72 | 13 |
| L-33 | 0.1875 | 1.25 rd. | 1.75 rd. | 100 | 0.200 | 21.52 | 1.96 | 0.25D rad. | Concrete pipe groove | Splitter | -5.8 | -- | -- | -- | -- | 0.61 | 13 |

plate shown in Fig. VI-1d was 2D/9 thick, 4.25D in diameter, and its bottom surface was 0.75D above the drop inlet crest. A few tests were made with the bottom surface 0.625D above the drop inlet crest. The three piers were 2D/9 thick by 1.24D long. The splitter in the drop inlet shown in Fig. VI-1e was 2D/9 thick by 0.75D high. The inlet shown in Fig. VI-1f was 1.25D high by 0.375D thick. The opening at crest level extended around 180 degrees of the upstream side of the drop inlet circumference and was 0.75D high.

The entrance to the conduit at the base of the drop inlet was formed as by butting the groove end of the concrete pipe against the circular riser form, wrapping sheet metal around the outside of the pipe, and extending it to fill the space between the end of the pipe and the riser. The sheet metal served as the inside form. The groove end of the concrete pipe was proportioned so that the 0.1875 ft diameter test pipe represented 24-in. concrete pipe, a scale of 1:10.7. This gave an enlarged entrance to the conduit that helped reduce the contraction of the flow at that point. The conduit was 100D long and its slope was 20 per cent for all tests.

The polished Lucite pipe was assumed to be hydraulically smooth. Rouse's "smooth" curve [I-44, p. 405, Fig. 11] was used in computing friction losses. The measurements of the friction factor given in Table VI-1 indicate that the pipe was smoother than smooth. This is presumably impossible and can possibly be laid to the fact that the piezometric pressure measurements were consistently in error in one direction. Accurate piezometric pressure measurements require the utmost care.

Piezometers were installed in the drop inlet and conduit to determine the pressures at the points indicated in Figs. V-1, VI-1a and Table VI-2.

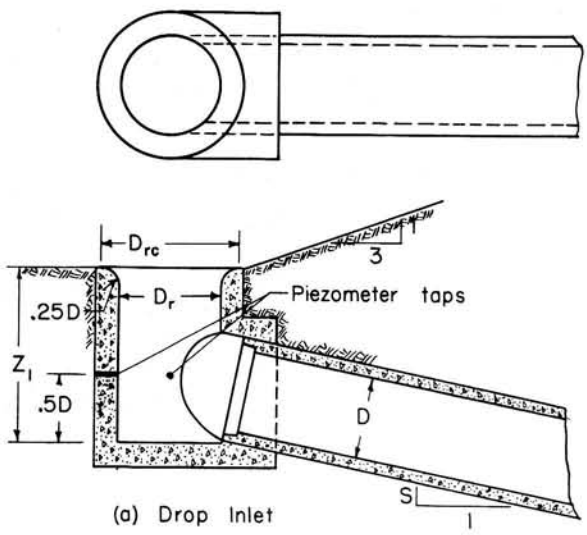


(a) Drop Inlet

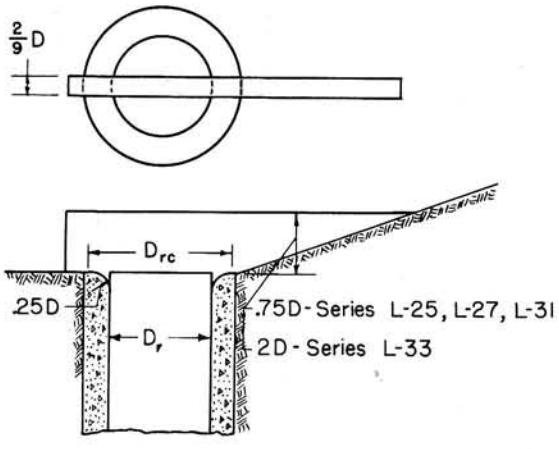


(b) Splitter Anti-vortex Wall

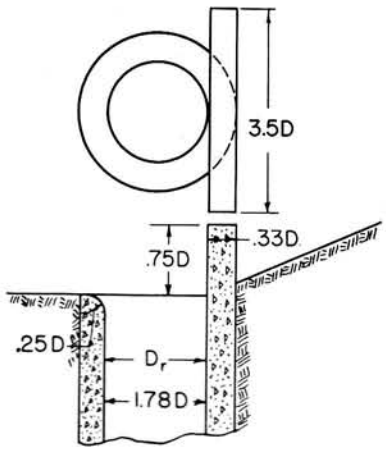


(c) Tangent Anti-vortex Wall

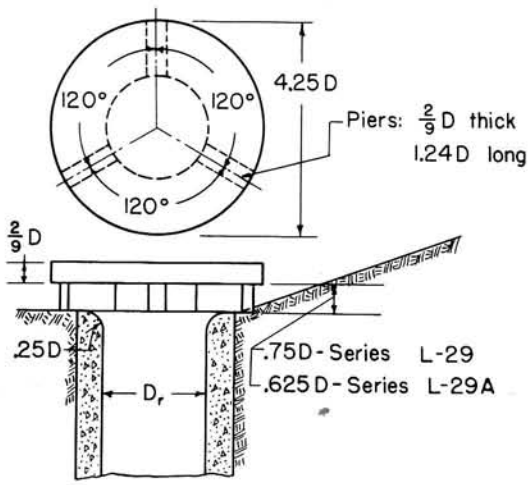


(d) Cover Anti-vortex Plate

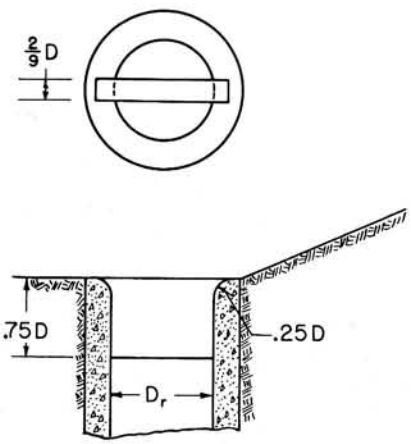


(e) Splitter in Drop Inlet

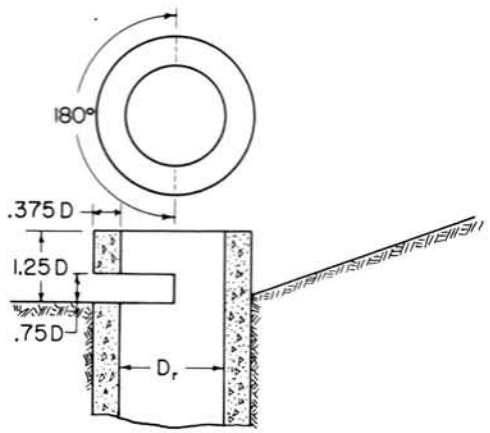


(f) Special

Fig. VI-1 - Drop Inlet Dimensions, Anti-Vortex Walls, and Piezometer Locations.

## APPARATUS AND PROCEDURE

The apparatus and the test procedure used for the tests described here are identical to that described in Part V for the series subsequent to Series L-19.

## DESCRIPTION OF FLOW

As the flow through the spillway increases from zero, the first condition noted is weir flow over the drop inlet crest with the conduit flowing only partly full and little air flow. An increase in the rate of flow next produces the condition of weir flow over the drop inlet crest with the conduit first containing slugs or traveling hydraulic jumps which suck air in through the drop inlet as they travel down the conduit. Further increases in the flow increase the frequency of the slugs until the conduit is flowing continuously full of an air-water mixture. The final flow condition is reached when the water flow is sufficient to replace the air flow, after which the spillway flows continuously full and the discharge then is computed as for a pipe.

### TABLE VI-2

### PIEZOMETER LOCATIONS AND LOCAL PRESSURE DEVIATION FROM HYDRAULIC GRADE LINE, SERIES L-25 TO L-33

| Piezometer Location | Series | L-25 | L-26 | L-27 | L-28 | L-29 | L-30 | L-31 | L-32 | L-33 |
|---|---|---|---|---|---|---|---|---|---|---|
| | Station | $h_n/h_{vp}$ | | | | | | | | |
| Right* | No. 2r[a] | +1.38 | +1.36 | +1.35 | +1.39 | +1.41 | +1.33 | +1.28 | +1.41 | +1.26 |
| Upstream* | No. 2b[a] | +1.37 | +1.34 | +1.37 | +1.32 | +1.41 | +1.34 | +1.28 | +1.39 | +1.22 |
| Crown | No. 3[b] | +0.12 | +0.07 | -0.02 | +0.11 | +0.13 | -0.12 | -0.09 | +0.02 | -0.11 |
| Invert | D/2 | +0.20 | +0.08 | +0.07 | +0.10 | +0.09 | +0.08 | -0.01 | +0.05 | -0.01 |
| Invert | 2D | +0.16 | +0.10 | +0.10 | +0.13 | +0.12 | +0.10 | +0.03 | +0.04 | +0.03 |
| Invert | 6D | +0.03 | +0.01 | +0.01 | +0.01 | +0.03 | -0.02 | -0.05 | -0.06 | -0.06 |
| Invert | 10D | +0.05 | +0.02 | +0.03 | +0.04 | +0.05 | +0.03 | +0.01 | 0.00 | 0.00 |
| Invert | 30D | +0.01 | -0.01 | -0.01 | 0.00 | +0.01 | +0.00 | -0.02 | -0.02 | -0.04 |
| Invert | 54D | -0.03 | -0.02 | -0.05 | -0.04 | -0.05 | -0.05 | -0.06 | -0.06 | -0.06 |
| Invert | 70D | -0.03 | -0.04 | -0.06 | -0.06 | -0.06 | -0.08 | -0.06 | -0.07 | -0.07 |
| Invert | 98D | -0.03 | -0.03 | -0.04 | -0.04 | -0.04 | -0.04 | -0.04 | -0.04 | -0.04 |

*Side of drop inlet. [a]At -D/2. [b]At D/2.

It should be especially noted that, through the use of circular drop inlets and conduit entrances of the type described, a drop inlet only 2D deep gives completely satisfactory flow conditions. In each case, there were no headpool fluctuations, no multiple discharge at any head, and the transition from weir control to pipe control was abrupt and satisfactory.

The performance of the anti-vortex devices received considerable attention and will be described in detail.

No anti-vortex device at all was used for Series L-26. A study of the experimental rating curve (see Fig. VII-1) and the notes taken during the experiments show that the spillway performance was satisfactory as long as weir flow existed over the drop inlet crest. However, vortices formed when the control changed to pipe flow and the discharge through the spillway decreased as much as 44 per cent. The vortices decreased the flow until the head over the crest reached 7D. Their effect at higher heads, if any, was not noticeable. The appearance of the vortices and their effect on the flow are shown in Fig. VI-2. The results of this test show that some type of vortex inhibitor is essential.

The splitter type anti-vortex device shown in Fig. VI-1b was used for Series L-25, L-27, L-31 and L-33. The splitter was 0.75D high except for Series L-33 where the splitter was 2D high. The lower splitter prevented vortex formation until the splitter became submerged. Vortices formed after submergence of the splitter and caused reductions in the spillway capacity. When the splitter height was raised, as for Series L-33, vortex formation was eliminated or reduced to such an extent that any effect on the flow could not be detected. This proved true even after the higher splitter was completely submerged. A comparison of the vortex formation at identical heads is presented in Fig. VI-3. In Fig. VI-3a air is sucked in through the vortex, while in Fig. VI-3b the vortex tendency appears as a small dimple in the water surface through which, according to the notes, slight amounts of air were sucked in at rare intervals.

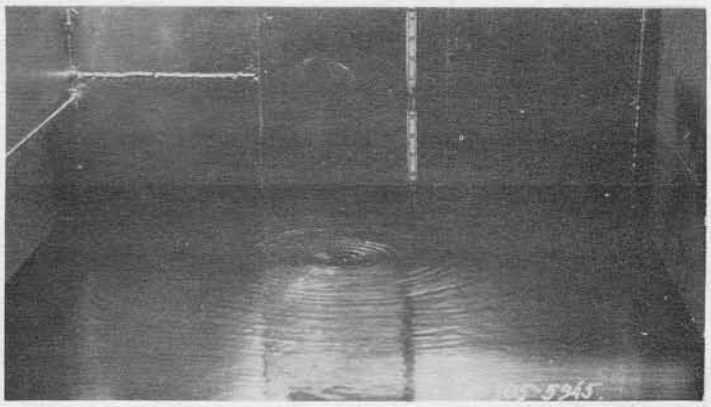

(a) H/D = 2.2
Reduction in discharge due to vortex is 42 per cent

(b) H/D = 3.2
Reduction in discharge due to vortex is 13 per cent

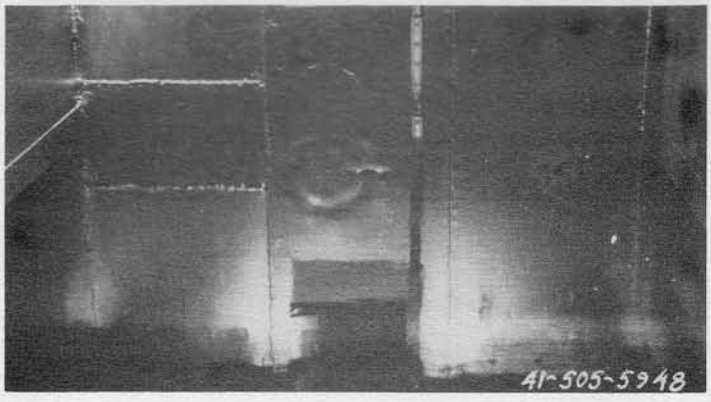


(c) H/D = 4.4
Reduction in discharge due to vortex is 5 per cent


(d) H/D = 7.5
Reduction in discharge due to vortex is 0 per cent

**Fig. VI-2** - Effect of Vortex on Capacity When No Anti-Vortex Device is Used.

The anti-vortex wall tangent to the downstream side of the drop inlet shown in Fig. VI-1c was used for Series L-38. Water was permitted to circulate between the wall and the end of the test channel and this aided vortex formation. Also the wall height of 0.75D was too low. Indications are that the prevention of circulation around the wall, using the dike described in Part V, and a wall 2D high would be satisfactory. However, the tangent anti-vortex wall does prevent free access to more of the drop inlet crest than does the splitter and higher heads, for the same discharge, are to be expected.

The circular cover supported on piers shown in Fig. VI-1d was used during Series L-29. It proved to be the most satisfactory of any of the types reported in Part VI. Its height over the drop inlet crest was varied only slightly and its diameter was not varied at all, so the op-

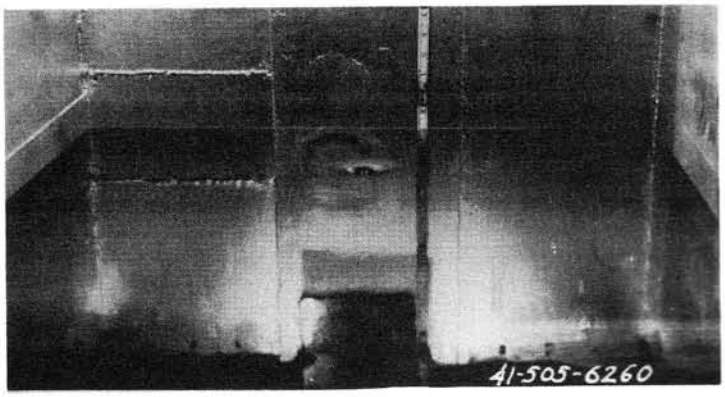


(a) Splitter 0.75D high

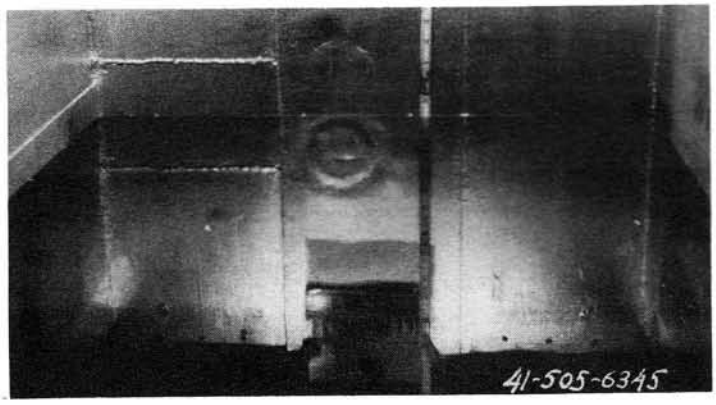


(b) Splitter 2D high

Fig. VI-3 - Effect of Height of Splitter on Vortex Formation. H/D = 4.3.

timum dimensions are unknown. However, the cover was only slightly better than the high splitter used for Series L-33.

The splitter in the drop inlet shown in Fig. VI-1e was used during Series L-32. It is unsatisfactory as a vortex inhibitor and its use is not recommended.

The arrangement shown in Fig. VI-1f was used in Series L-30. It performed poorly and its use is also not recommended.

To summarize the results of these tests on vortex inhibitors, it may be said, on the basis of performance, that the cover, the splitter (Fig. VI-1b), and the tangent anti-vortex devices are recommended in that order. However, the difference between the performance of these types of vortex inhibitors is so small that the governing consideration should be cost of construction. While the tests reported here have permitted a description of the performance of various types of vortex inhibitors, they were not extensive enough to definitely determine their optimum size.

## DISCHARGE COEFFICIENTS

### Weir Coefficient

The discharge coefficient C for use in Eqs. I-1 and I-2 is given by the solid curve of Fig. VI-4. The data points are those obtained during the laboratory tests. The dash lines drawn 5 per cent above and below the solid curve indicate the precision. Individual curves could be drawn for each of the different inlets, but the additional precision obtained in estimating the coefficient of discharge is not warranted from a practical standpoint. The crest length L for use in Eqs. I-1 and I-2 is the net length; i.e., the gross length minus the width of the anti-vortex walls. The equation for the solid curve of Fig. VI-4 is

$$C = 3.60\left[1 - \frac{0.013}{H/D_{rc}}\right]^{3/2} \qquad \text{(VI-1)}$$

which, when inserted in Eq. I-2, gives

$$\frac{Q}{D_{rc}^{5/2}} = 3.60\,\frac{L}{D_{rc}}\left[\frac{H}{D_{rc}} - 0.013\right]^{3/2} \qquad \text{(VI-2)}$$

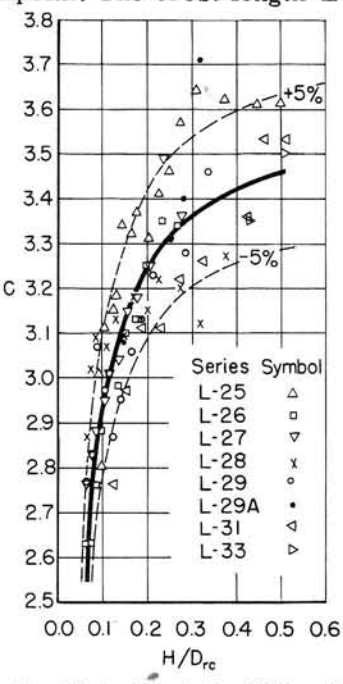


Fig. VI-4 - Head-Coefficient Curve for Circular Drop Inlets.

### Entrance Loss Coefficient

Entrance loss coefficients $K_e$ for use in Eq. I-5 are given in Table VI-1. The values listed are the average of from 7 to 13 determinations. They were determined with the barrel on a 20 per cent slope and are reliable for this one slope only.

## PRESSURE COEFFICIENTS

The average pressure coefficients $h_n/h_{vp}$ reduced to a horizontal frictionless pipe are given in Table VI-2. The concrete groove entrance to the barrel apparently gives considerably higher pressure just inside the barrel entrance than does the square-edged entrance. This reduces the chance of the occurrence of cavitation damage. Nevertheless, the pressure should be computed to indicate whether or not cavitation damage is a possibility.

## CONCLUSIONS AND RECOMMENDATIONS

Circular drop inlets having a diameter as small as 1.25D and a depth of 2D are satisfactory if the barrel entrance is formed as described here.

Some form of anti-vortex device is an absolute necessity. The cover shown in Fig. VI-1d, the splitter shown in Fig. VI-1b, and the tangent wall shown in Fig. VI-1c are recommended in the order given, although the differences in the performances are small. The height of the splitter and tangent anti-vortex walls should be sufficient to extend above the maximum water surface or have a maximum height of 2D, whichever gives the lesser height. The arrangements shown in Figs. VI-1e and VI-1f should not be used.

The capacity of the drop inlet crest, acting as a weir, can be determined from Eq. I-1 and the solid curve of Fig. VI-4 or from Eq. VI-2.

The entrance loss coefficients for full conduit flow are given in Table VI-1. They should be modified if the barrel slope is other than 20 per cent.

The local pressure constants for use in Eq. I-14 may be taken from Table VI-2.

## Part VII

## Effect of Vortex at Inlet on Spillway Discharge

### INTRODUCTION

The justification for devoting a part of this report exclusively to the effect of the vortex on the discharge lies in the extreme reduction in the discharge which a vortex can cause, and in the fact that many designers and field engineers are not aware that the elimination of an anti-vortex device is a very serious omission. Insisting on the proper installation of a suitable anti-vortex device is just as important as insisting that the proper size conduit be used. This will be shown below.

Some information on the effect of vortices has been obtained from experiments conducted on closed conduit spillways at the St. Anthony Falls Hydraulic Laboratory, but the most thorough studies have been conducted by others. Much of the information given below has, therefore, been abstracted from a few published reports that have been selected because they bring out the great reduction in capacity caused by vortices.

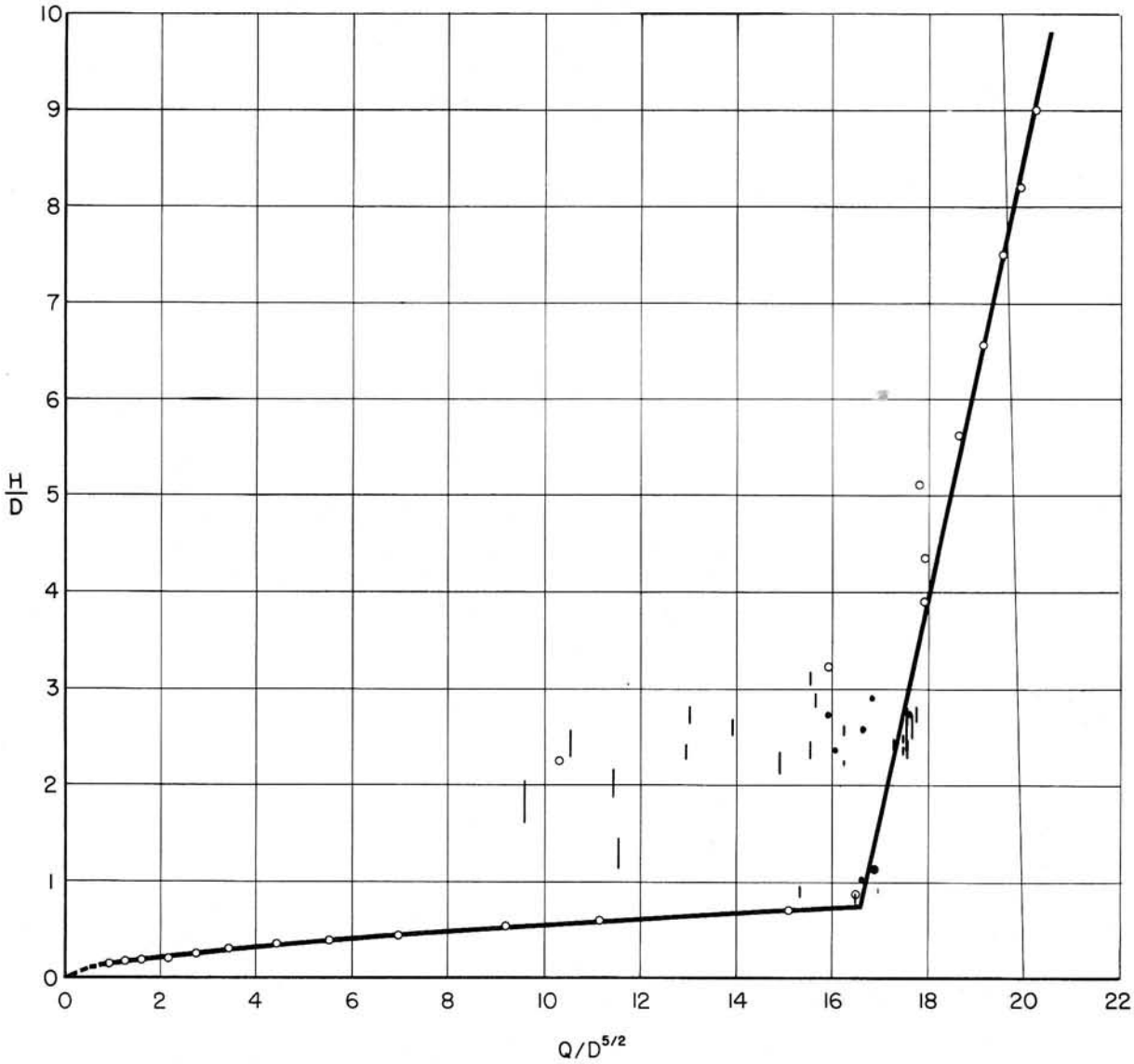


Fig. VII-1 - Effect of Vortices on Head-Discharge Curve for Series L-26.

## CLOSED CONDUIT SPILLWAY SERIES L-7, L-8 AND L-9

The effect of circulation and vortex formation on one closed conduit spillway has been presented in Part V under the heading, "Circulation Around Anti-Vortex Wall." The results are given in Fig. V-13. Runs labeled "6" for Series L-7 and "7" for Series L-9 were made at the same head over the drop inlet crest, yet the flow through the spillway was doubled when circulation around the anti-vortex wall was prevented, even though the crest length was shortened by one-fourth by the installation of the wall. The reduced flow caused by the circulation, although impressive, is not as much as other investigators have found for other types of spillway.

At a head of 1.2H/D in Fig. V-13, the conduit is flowing as a pipe. The discharge at this head for Series L-8, where circulation in back of the wall is permitted, is 13 per cent less than for Series L-9, where circulation is prevented. The dike, therefore, serves to increase the spillway capacity. The discharge at this same head for Series L-7, where no wall is used, is 39 per cent less than that for Series L-9. Moreover, the rating curve is difficult to define because different vortex intensities greatly affect the flow through the spillway.

Vortices, which may vary in intensity, make it impossible to predict the flow through the spillway in addition to causing a reduction in the flow through the spillway. The former deficiency is probably more serious than the latter. The only reliable solution is to eliminate vortices or to reduce their effect to negligible proportions.

## CLOSED CONDUIT SPILLWAY SERIES L-26

The head-discharge curve for Series L-26 is presented in Fig. VII-1. It will be noticed, as stated in Part VI, that the weir flow portion of this curve is well defined. However, vortices were generated as soon as pipe flow began. With the formation of these vortices, air was carried through the spillway and the rate of outflow became very erratic. The extreme scatter of the data between values of H/D of 1 and 3 is a result of the varying influence of the vortex. All of the data in Fig. VII-1 which is represented by vertical lines and dots were obtained with one rate of flow into the headpool, that is $Q/D^{5/2} = 16.8$. Outflow rates--flow through the spillway--were obtained by correcting for storage in the headpool. The outflow rate was constant only for an average of between one and two minutes and, during this constant outflow, the water level in the headpool was usually changing. The range in headpool level during a constant outflow rate is indicated by the length of the vertical lines in Fig. VII-1.

The reduction in discharge at H/D = 2 from an indicated $Q/D^{5/2}$ for pipe flow of 17.2 to an observed 9.6--a reduction of 44 per cent--is quite serious in itself, but there is no indication that the minimum possible discharge was actually observed. A vortex of greater strength could well have caused a further reduction in discharge. Moreover, the actual flow through the spillway at any one time is unknown, for data were obtained everywhere between $Q/D^{5/2} = 9.6$ and 17.7 for a single rate of flow to the headpool. In other words, it is impossible to define the head-discharge curve in this range.

When the depth over the drop inlet crest exceeded about 7D, air did not enter the spillway through the vortices and a well-defined rating curve was then obtained. Apparently, high submergence of the drop inlet decreases the vortex effect. Nevertheless, it appears prudent to provide means for controlling vortex formation at closed conduit spillways because of its extremely adverse effect on the discharge at moderate heads.

## EFFECT OF VORTEX ON ORIFICE DISCHARGE

Experiments concerning the effect of the vortex on the discharge of a horizontal circular orifice in the floor of a tank are reported by C. J. Posey and Hsieh-ching Hsu [I-40]. All experiments were run with a constant head. The vortex was formed by admitting water radially or tangentially in proportions which were varied to vary the strength. The tangential water was admitted through two or four nozzles which were set at different radii $r_j$ from the orifice. The size of the vortex was found to depend on the average tangential component of the velocity. This ratio is designated as $\tan \theta$.

The results obtained by Posy and Hsu [I-40] are presented in Fig. VII-2, which is copied from their paper. The right-hand scale, which shows the per cent reduction in discharge due

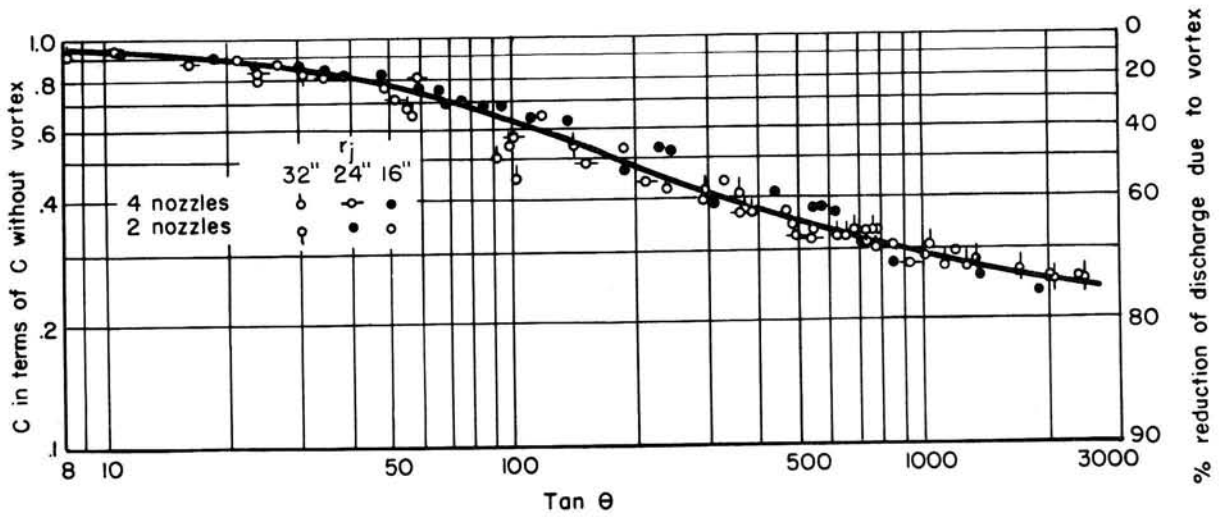


Fig. VII-2 - Effect of Vortex on Orifice Discharge.

to the vortex, indicates that reductions up to 75 per cent are possible. In other words, the flow through an orifice with a vortex can be as little as one-fourth the flow which would pass through the orifice if there were no vortex.

The data presented in Fig. VII-2 emphasize the comments made previously that a vortex causes a great reduction in the capacity of a spillway and that means should be taken to insure that vortices will not form.

## EFFECT OF VORTEX ON DISCHARGE OF VERTICAL PIPES

Flow into a vertical pipe is closely akin to flow in the drop inlet of a closed conduit spillway. Therefore the experiments on vertical pipes and the effect of vortices on their discharge which have been reported by A. M. Binnie and G. A. Hookings [I-5] and Lennart Rahm [I-41] are of interest.

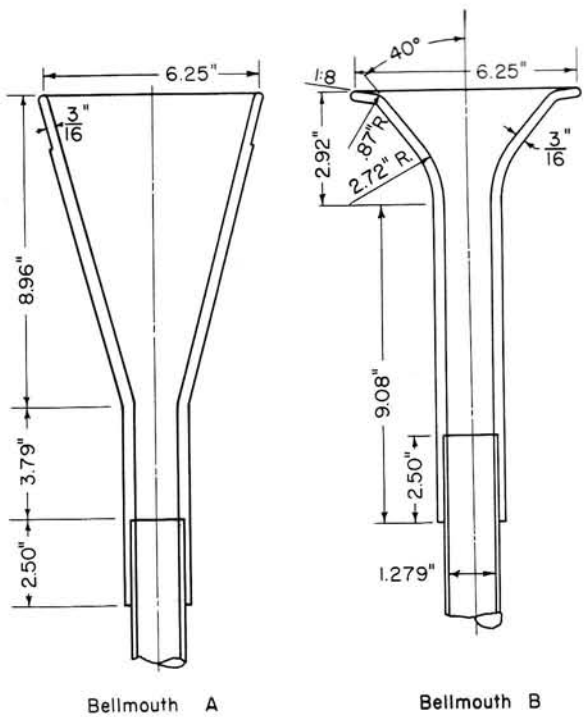


Fig. VII-3 - Vertical Pipe Entrances Tested by Binnie and Hookings.

### Binnie and Hookings

Three different entrances were used by Binnie and Hookings: a plain pipe with its upper end chamfered downwards and outwards at 45 degrees and the two entrances shown in Fig. VII-3. The crests of the entrances were 16D above the bottom of the tank to minimize bottom effects. The overall length was 25.8D. Water was admitted to the tank in which the entrances were located either radially, tangentially, or some combination of radially and tangentially. Two tangential pipes were used to produce the tangential flow. The pipe diameters were 1/2, 1 and 2 in. so that the strength of the vortex could be varied.

The results of the tests on the three entrances are given in Fig. VII-4. The curves shown are for water entering either radially or tangentially. When part of the water entered tangentially and the remainder entered radially, the head-discharge curves fell between those drawn in Fig. VII-4. This indicates that tangential inflow alone, which induces the greatest circulation at any given rate of flow, produces the least outflow discharge. Similarly, tangential flow through

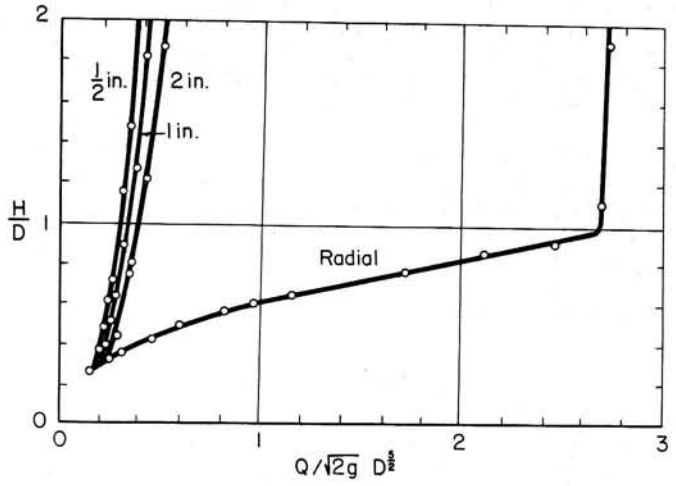


(a) Discharge Tests on the Plain Pipe

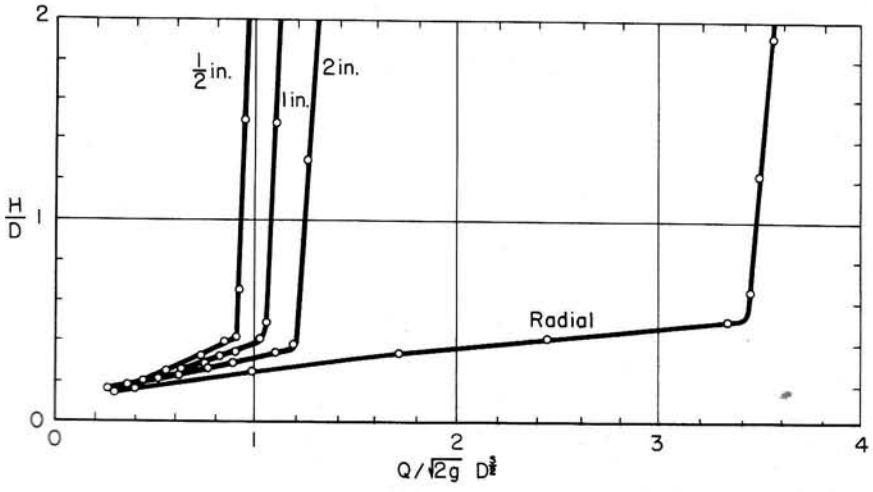


(b) Discharge Tests on Bellmouth A

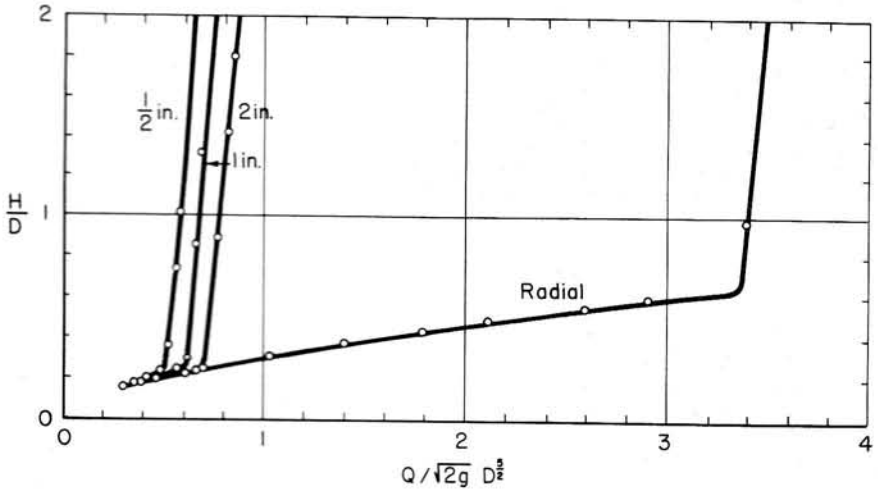


(c) Discharge Tests on Bellmouth B

**Fig. VII-4 - Head-Discharge Curves for Radial and Tangential Flow as Determined by Binnie and Hookings.**

the smallest pipe produces the vortex of greatest strength and, as a result, the outflow is less than when the tangential flow enters through the larger pipes. Binnie and Hookings report that there was an air core down the center of the pipe when the entering flow was solely tangential. The fact that the pipe did not flow full under these conditions, of course, is one reason why the discharge is so much lower for tangential flow than for radial flow.

The results obtained by Binnie and Hookings indicate that vortices can reduce the flow through spillways by as much as 90 per cent in the case of the plain pipe, 74 per cent in the case of Bellmouth A, and 73 per cent in the case of Bellmouth B. When there is weir flow over the crest, the whirling water reduces the flow by as much as 62 per cent in the case of Bellmouth A. Lesser reductions were obtained for the other entrances, but it appears that vortices and circulation must be inhibited for weir flow as well as for full pipe flow to insure the maximum discharge at any given head.

### Rahm

The laboratory tests reported by Rahm were made on five glass pipes varying in diameter and length as shown in Table VII-1. The pipes were installed vertically through the floor 90 cm upstream from the bulkhead at the downstream end of a channel. The resulting tank was 60 cm wide by 120 cm deep by 650 cm long. The ends of the pipes were ground square.

TABLE VII-1

PIPES TESTED BY RAHM

| Pipe No. | D cm | $\frac{\ell}{D}$ | $\frac{t}{D}$ |
|---|---|---|---|
| 1 | 13.3 | 5.04 | 0.0256 |
| 2 | 8.3 | 15.06 | .0193 |
| 3 | 8.3 | 8.07 | .0193 |
| 4 | 8.3 | 4.10 | .0193 |
| 5 | 4.0 | 16.75 | .0325 |

The crests of Pipes 1, 2, 3 and 5 were 60 cm above the floor of the tank. Pipe 4 had its top 20 cm above the floor. The pipes discharged freely. Water entered the channel from one end. No attempt was made to cause vortices or to inhibit their formation. Vortices were observed but they occurred naturally. Rahm presents some excellent pictures, describes the various types of weir, orifice and full pipe flow he observed, and explains the cycling between flow types also reported by the writer in detail in Parts I and II.

For full pipe flow Rahm reports: "Even when the vortexes on the water surface in the test tank were very marked, their effect on the discharge was not noticeable under the test conditions." The effect of vortices on the discharge would not be noticed if their strength is constant. Vortices of varying strength do affect the discharge as reported by Posey and Hsu, Binnie and Hookings, and the writer. It is quite likely that Rahm's "test conditions" were such that relatively stable vortices were obtained.

## SIMILITUDE OF VORTICES

Do vortices which form in the laboratory models also form in the field structure? Can the effect of vortices be predicted quantitatively from laboratory studies on small-sized structures? These questions were raised during the studies. The answer to both questions is yes. Proof has been published by Camichel, Escande and Sabathe [I-13].

The apparatus used in the experiments reported by Camichel, Escande and Sabathe consisted of a vertical casing whose cross section had the form of a logarithmic spiral. Water entered the casing through a vertical opening or nozzle along the entire height of one side, which initiated the vortex, and left through orifices in the bottom of the casing. The orifices had diameters of 30, 20 or 15 cm. Scale models of one-tenth size were constructed also. Both the prototype and the model were tested and the results were compared after multiplying the model heads by 10 and the prototype discharges by $10^{5/2}$. The results of the tests on the

three orifices are compared in Fig. VII-5. There it can be seen that the data obtained from the 1:10 model and the prototype exhibit good agreement.

One point of dissimilarity was noted during these tests, but only one brief paragraph is devoted to it: The jets issuing from the orifices were not similar. The authors offer their statement and a pair of comparative photographs without comment.

As a result of the experiment by Messrs. Camichel, Escande and Sabathe, it is apparent that the quantitative effect of a vortex on the capacity of an orifice--and presumably on a closed

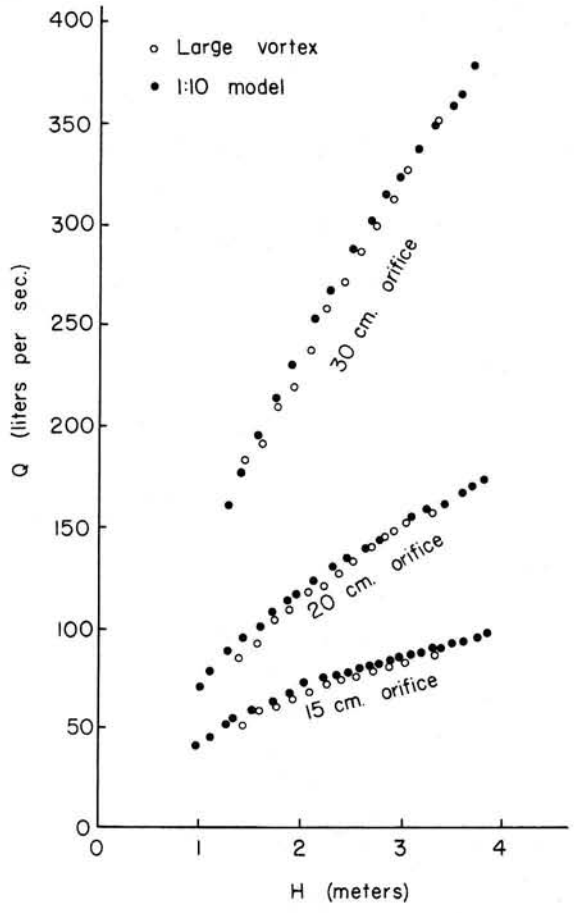


Fig. VII-5 - Comparison of Head-Discharge Relationships with Vortex as Determined by Camichel, Escande and Sabathe.

conduit spillway--can be determined in a model and scaled up to prototype size through the use of a Froude model law.

Although Rahm [I-41] does not report a variation of vortex strength, he does report his discharge coefficients for all pipes. His results verify the similarity relationships. For weir flow Rahm reports a discharge coefficient C in Eq. I-1 of 4.28 for all pipes. For the horizontal orifice at the pipe entrance Rahm reports a discharge coefficient $C_o$ in Eq. I-7 of 4.49 for Pipe 1, 4.57 for Pipes 2, 3 and 4, and 4.65 for Pipe 5. The agreement is very good and well within the limits of experimental precision. For full pipe flow Rahm did not determine $K_e$ in Eq. I-5 but lumped the entrance, exit and friction losses into a single constant that is valid only if his pipe is frictionless.

## HARSPRANGET DIVERSION TUNNEL

Rahm [I-41] reports observations made in 1949 on vortex flow through a drop inlet diversion tunnel. The tunnel is shown in Fig. VII-6. This tunnel was 11 m (36 ft) long. The nearly horizontal tunnel 280 m (918 ft) long had an average cross sectional area of 110 sq m (1184

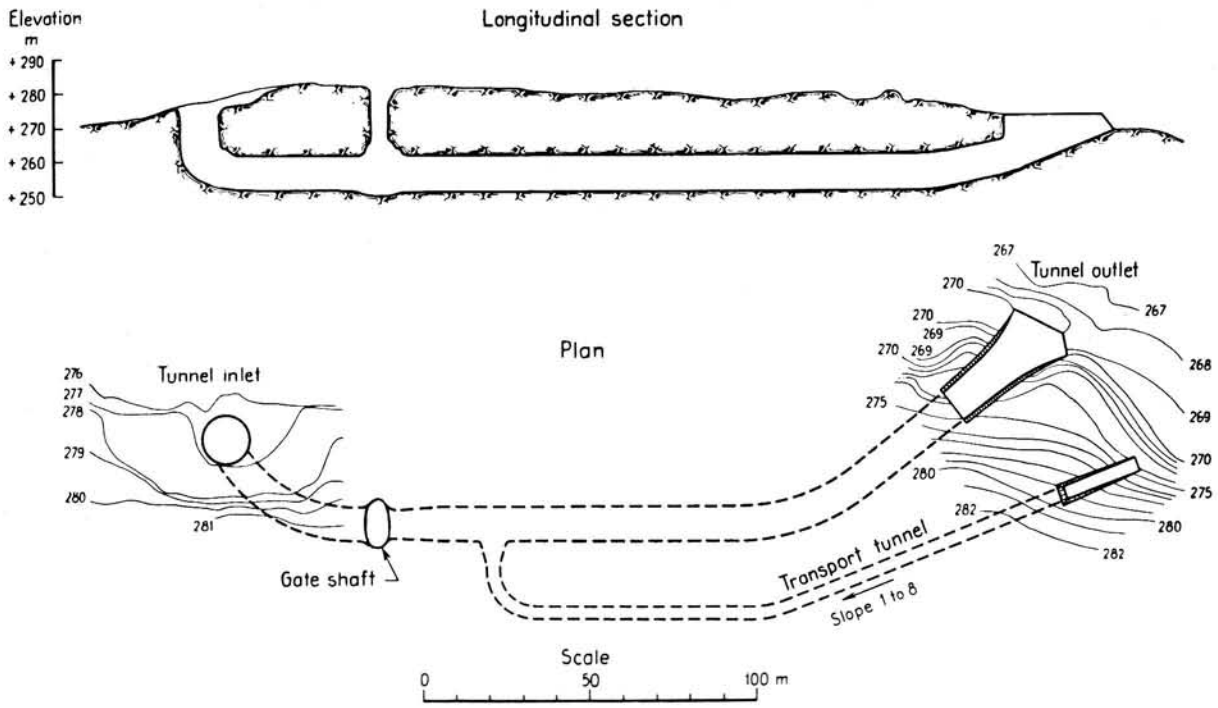


Fig. VII-6 - Harsprånget Diversion Tunnel.

sq ft). The oblique upward tunnel mouth was 50 m (164 ft) long. The gate shaft was to be used for closing off the tunnel. The transport tunnel was used for removal of the excavated rock. Rahm states that full pipe flow through the tunnel begins at 850 $m^3$/sec (30,000 cfs). Mr. Rahm writes:

> As long as the flow did not exceed 850 $m^3$/s, the water level above the tunnel inlet varied continuously and regularly with the fluctuations in discharge. On July 6th [1949], however, the rate of flow increased rapidly from 850 $m^3$/s [30,000 cfs], which rate had been maintained constant for about 24 hours, to slightly above 870 $m^3$/s [30,700 cfs]. This caused a rise in the water level of no less than 2,5 m [8.2 ft], from + 284,8 m to + 287,3 m, in 2 hours.... In order to prevent the site from being flooded, the flow was then reduced...to its initial value of 850 $m^3$/s. Even so, the water level did not fall to its previous position of equilibrium corresponding to this rate of flow, i.e. + 284,8 m, as had been expected. Instead, a stable level was reached at a considerably higher value, + 287,6 m.
>
> When the water level was higher than about + 283 m, the water was discharged both through the tunnel inlet and through the gate shaft, Fig. [VII-7]. At high water levels, this caused the formation of whirlpools at both inlets, a strong one at the tunnel inlet and a weaker one at the gate shaft. The water rotated clockwise above the tunnel inlet and counter-clockwise above the gate shaft....
>
> The high water level observed on July 6th remained unchanged even after the rate of inflow had been reduced to a value that formerly corresponded to a water level 2,7 m lower. This fact is probably due to the topographical configuration of the ground surface around the tunnel inlet. The increase in the rate of flow from 850 $m^3$/s to 870 $m^3$/s caused a rise in water level and an intensification of the vortical motion above the inlet, especially when a vortex was also formed above the gate shaft. Since the inlet is located on the river bank, this rise in water level increased the extent of the body of water between the inlet and the river bank, and hence afforded more favourable conditions for intense vortical motion at the inlet. The vortex strength was therefore maintained at a high value even after the reduction in the rate of flow. This state of flow with strong vortical motion at high water levels was then as stable as the former weak rotation at low water levels.

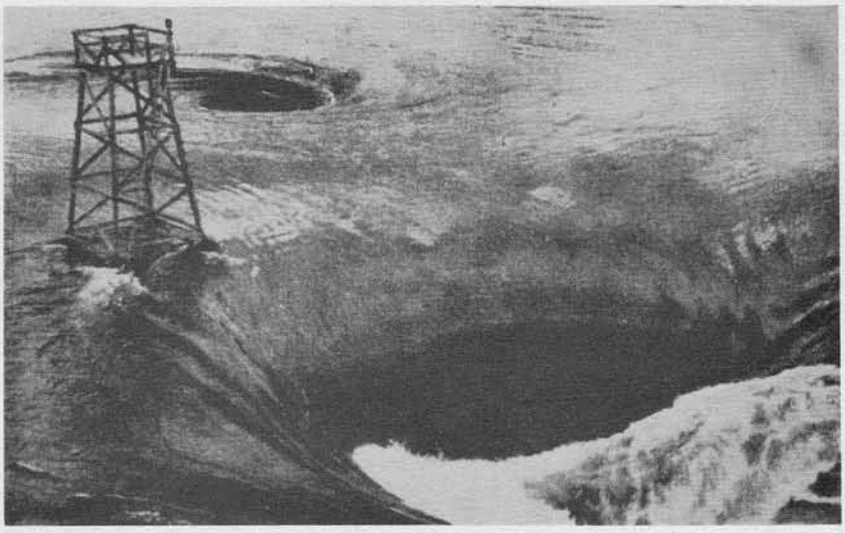

Fig. VII-7 - View of the Flow at Harsprånget when Water Was Discharged Through Both the Tunnel Inlet and the Gate Shaft. The gate shaft is in the foreground.

It is apparent that a vortex developed when the rate of flow was increased and that the vortex caused a reduction in the rate of flow through the tunnel. The increase in head of 2.5 m mentioned by Rahm corresponds to an increase of 21 per cent; the reduction in flow as a result of the vortex is 11 per cent.

It was thought that flow through the gate shaft impeded the outflow, so the water level was lowered and the gate shaft closed. Rahm comments:

> After closing the gate shaft, the discharge was still reduced by about 5 per cent,....This reduction in discharge, which is a minimum value, may then be due to the remaining vortex, which formed a funnel of air above the inlet and was very powerful at high water levels.
>
> According to the measurements made by Hsu, such a reduction in the discharge through a bottom orifice would be obtained if the tangential velocity were about 10 times as high as the radial velocity. Visual observations and film records made at Harsprånget have also demonstrated that the swirl in the inflow to the tunnel inlet was of this order of magnitude. A view of the vortex is shown in Fig. [VII-8].

Fig. VII-8 - View of Tunnel Intake at Harsprånget on August 15, 1949, as Seen from the Dam.

Rahm comments on the air carried through the tunnel as follows:

> At some rates of flow, water spouts could be observed at the tunnel outlet,...water being thrown up 5 to 10 m [16.4 to 32.8 ft] above the water level. These water spouts had no clear periodicity but came at intervals of 1 to 3 seconds. They did not occur at discharges lower than about 200 $m^3/s$ [7060 cfs], but above this value they became stronger and more powerful as the discharge increased. When a discharge of 800 to 850 $m^3/s$ [28,200 to 30,000 cfs] was reached, the spouts disappeared.
>
> These spouts were produced at the outlet by the expanding of large air bubbles formed within the tunnel by air sucked down at the tunnel inlet. ...there was no air, or only a small volume, at low discharges, but as the flow increased and the control section moved downwards in the tunnel inlet, the volume of air increased. At maximum discharge through the tunnel practically no air was entrained.

## CONCLUSIONS AND RECOMMENDATIONS

The following conclusions are derived from the foregoing comments:

1. Circulation or the presence of a vortex reduces the flow through closed conduit spillways and orifices.

2. No reliable prediction of the flow can be made in the presence of circulation or vortices because variations in vortex strength cause changes in the flow rate.

3. For closed conduit spillways where the vortex was not forced but occurred naturally, the maximum effect of the vortex is at intermediate heads with the effect decreasing to small or negligible proportions at high submergences of the spillway crest. However, for the forced vortices of Binnie and Hookings, there was little or no improvement observed at the high submergences.

4. A vortex of any size reduces the capacity of a spillway with the percentage reduction increasing as the strength of the vortex increases.

5. The effect of vortices on the capacity of a closed conduit spillway may be quantitatively predicted from tests on small-sized models.

As a result of the above conclusions, it is recommended that some means be provided to inhibit or, preferably, prevent circulation and the formation of vortices.

## ACKNOWLEDGEMENTS

The results described here are a product of an investigation conducted by the staff of the Agricultural Research Service, U. S. Department of Agriculture, located at the St. Anthony Falls Hydraulic Laboratory, University of Minnesota, Minneapolis. There the Agricultural Research Service, the Minnesota Agricultural Experiment Station, and the St. Anthony Falls Hydraulic Laboratory cooperate in the solution of problems concerning conservation hydraulics. The laboratory experiments and the initial analysis were performed by a number of different persons between 1941 and 1951. All data were reanalyzed by the writer. The analytical methods and the computations have been checked by Robert V. Keppel.